

AN EXAMINATION OF THE SCALED PARTICLE
THEORY OF GAS SOLUBILITIES

by

Bruce A. Cosgrove

B.Sc., Simon Fraser University, 1977

A THESIS SUBMITTED IN PARTIAL FULFILLMENT OF
THE REQUIREMENTS FOR THE DEGREE OF
MASTER OF SCIENCE
in the Department
of
Chemistry



Bruce A. Cosgrove 1980

SIMON FRASER UNIVERSITY

April 1980

All rights reserved. This thesis may not be reproduced in whole or in part, by photocopy or other means, without permission of the author.

APPROVAL

Name Bruce Anthony Cosgrove

Degree Master of Science

Title of Thesis: An Examination of the Scaled Particle
 Theory of Gas Solubilities.

Examining Committee:

Chairperson: T.N. Bell

J. Walkley,
Senior Supervisor

I.D. Gay

J.M. D'Auria

G.L. Malli,
Internal Examiner

Date Approved: 11 April 80.

PARTIAL COPYRIGHT LICENSE

I hereby grant to Simon Fraser University the right to lend my thesis, project or extended essay (the title of which is shown below) to users of the Simon Fraser University Library, and to make partial or single copies only for such users or in response to a request from the library of any other university, or other educational institution, on its own behalf or for one of its users. I further agree that permission for multiple copying of this work for scholarly purposes may be granted by me or the Dean of Graduate Studies. It is understood that copying or publication of this work for financial gain shall not be allowed without my written permission.

Title of Thesis/Project/Extended Essay

"An Examination of the Scaled Particle Theory of Gas

Solubilities"

Author: _____

(signature)

Bruce A. COSGROVE

(name)

April 14, 1980

(date)

ABSTRACT

The extension of Scaled Particle Theory (S.P.T.) to the predictions of the thermodynamic properties of dissolved gases was first demonstrated in 1963. Over the intervening years this theory has been extensively used and has always been shown to provide excellent agreement with experimental data. No modifications of the original theory have been made despite the fact that, since its conception, progress in other theoretical studies has indicated basic inconsistencies in its formulation.

The purpose of this research was twofold, to test the theory against experimentally determined solubility data for a range of gases in H_2O and D_2O solvents, and to incorporate certain improvements into the structure of the theory itself and predict thermodynamic properties of dissolved gases in various organic solvents.

Much data already exists for the solubility of gases in H_2O . Surprisingly enough, the S.P.T. is able to predict quite accurately this data. It is known that H_2O exhibits properties that are unlike those of simple organic solvents and this difference is reflected in gas solubility data. No adequate theory for the description of the properties of pure H_2O exists and yet it would appear that the S.P.T., despite its simplicity, can predict the properties of gases dissolved in this solvent. D_2O is a solvent matching the complexity of H_2O and yet known to show a 5 to 10% difference in its gas solubility behaviour. No application of the S.P.T. to gases dissolved in D_2O has been made, primarily due to insufficient data. Such a comparison was considered a good test of the S.P.T., so solubility data was obtained for a range of gases over a 40 °C temperature range in this latter solvent.

The technique developed for these measurements is novel in that it

allows direct determination of a gas dissolved in a 1/2 cc sample of D_2O and simultaneous determination of the same dissolved gas in a 1/2 cc sample of H_2O , the latter providing an internal reference. The gas chromatographic method developed compared directly the stripped gas from the 1/2 cc solvent sample to a pure gas calibration curve obtained under identical conditions, hence eliminating the need for relative measurements by comparison to known amounts of 'another' dissolved gas in the same solvent.

The Scaled Particle Theory of gas solubilities is rigorously developed incorporating certain features only appreciated as necessary to the theory from theoretical studies performed since its original formulation. From this development the approximations intrinsic to the original theory are seen and their validity is tested. Consideration of the limiting (hard sphere) conditions of the theory show the original development to be inconsistent. It is found that the more rigorous theory cannot predict the properties of gases dissolved in H_2O and D_2O solvents and has only limited success in the common organic solvents. The reason for the predictive success of the original Scaled Particle Theory is revealed by the subsequent examination of a hard sphere version of the S.P.T. It is shown to be rather fortuitous.

DEDICATION

To Katherine Cosgrove

ACKNOWLEDGMENTS

I would like to express my sincere thanks to Dr. John Walkley for his intellectual leadership, interest and more importantly his approachability during the author's graduate career.

I would also like to thank Dr. Ian Gay for the discussions and ideas regarding the experimental solubility apparatus.

Thanks are also due to Mr. Peter Hatch and his associates in the glassblowing shop for the many ideas in the design of the solubility apparatus and the skillful construction.

Thanks are due to Mr. Bob Lyall for the design of the computer program used in the S.P.T. calculations. I wish to thank Daniel Say of the S.F.U. science library for his assistance in locating many of the required parameters used in the S.P.T. calculations.

Last, but not least, I would like to thank Margaret Fankboner for typing this thesis which, I'm sure, at times appeared to be a formidable task.

Bruce A. Cosgrove

Simon Fraser University

Burnaby, B.C., CANADA

April 1980

TABLE OF CONTENTS

	Page
Title Page	i
Approval	ii
Abstract	iii
Dedication	v
Acknowledgments	vi
Table of Contents	vii
List of Tables	viii
List of Figures	x
 <u>Section I</u> 	
Introduction	3
CHAPTER I: Solubility of Gases in H ₂ O and D ₂ O	5
Experimental	6
Results and Discussion	14
References	29
Appendix I	21
 <u>Section II</u> 	
Introduction	32
CHAPTER II: Scaled Particle Theory of Gas Solubilities	35
Theory and Development	36
Hard Sphere Limits	53
Scaled Particle Theory	65
CHAPTER III	83
Discussion	84
Conclusions	102
References	106
Appendix I	108

LIST OF TABLES

Table N ^o	Page
<u>Section I</u>	
I: MOLE FRACTION X_2 OF GASES DISSOLVED IN H_2O AND D_2O	15
II: COEFFICIENTS IN THE EQUATION $R \ln \chi_2 = A + B/T + C \ln(T/^\circ K)$	19
III: ENTHALPY OF SOLUTION OF GASES IN H_2O AND D_2O	21
IV: ENTHALPY OF SOLUTION OF GASES IN H_2O AND D_2O (REF. 1)	22
V: THERMODYNAMIC PROPERTIES IN D_2O AT $298.15^\circ K$	24
VI: THERMODYNAMIC PROPERTIES IN H_2O AT $298.15^\circ K$	24
VII: ΔH_{tr}° (CAL MOLE ⁻¹) At $298.15^\circ K$	26
<u>Section II</u>	
I: COEFFICIENTS IN THE EQUATION $\ln K_H = A + B\alpha + C\alpha^2 + D\alpha^3$	59
II: SOLVENT EFFECTIVE HARD SPHERE DIAMETERS	60
III: EXTRAPOLATED SOLVENT DIAMETER TEMPERATURE DEPENDENCE	62
IV: EXTRAPOLATED THERMODYNAMIC HARD SPHERE DATA AT $298.15^\circ K$	64
V: PROPERTIES OF THE SOLUTES AT $298.15^\circ K$	67
VI: PROPERTIES OF THE SOLVENTS AT $298.15^\circ K$	68
<u>THERMODYNAMIC DATA CASE I</u>	
VII: H_2O CASE I	69
VIII: C_6H_6 CASE I	70
IX: c- C_6H_{12} CASE I	71
X: n- C_6H_{14} CASE I	72
XI: $\Delta S H_2O$ CASE I	73
XII: $\Delta S C_6H_6$ CASE I	73
XIII: ΔS c- C_6H_{12} CASE I	74
XIV: ΔS n- C_6H_{14} CASE I	74

THERMODYNAMIC DATA CASE II

XV: H ₂ O CASE II	75
XVI: C ₆ H ₆ CASE II	75
XVII: c-C ₆ H ₁₂ CASE II	76
XVIII: n-C ₆ H ₁₄ CASE II	76
XIX: HARD SPHERE PROPERTIES AT 298.15 °K	79

THERMODYNAMIC DATA CASE III AND IV

XX: H ₂ O CASE III AND IV	80
XXI: C ₆ H ₆ CASE III AND IV	80
XXII: c-C ₆ H ₁₂ CASE III AND IV	81
XXIII: n-C ₆ H ₁₄ CASE III AND IV	81
XXIV: SOLVENT EFFECTIVE HARD SPHERE DIAMETERS AT 298.15 °K	98
XXV: H ₂ O AT 298.15 °K INTERACTION TERMS FOR CASE I AND II	99
XXVI: C ₆ H ₆ AT 298.15 °K INTERACTION TERMS FOR CASE I AND II	100
XXVII: H ₂ O AT 298.15 °K INTERACTION TERMS FOR CASE III AND IV	100
XXVIII: C ₆ H ₆ AT 298.15 °K INTERACTION TERMS FOR CASE III AND IV	101

LIST OF FIGURES

Page

Section I

FIGURE 1	GAS STRIPPING LINE	8
FIGURE 2	STRIPPING CELL	9
FIGURE 3	$\ln X_2$ VS $1/T$ ($^{\circ}K^{-1}$) ARGON IN H_2O AND D_2O	18

Section II

FIGURE 1	INERT GASES HARDCSPHERE DIAMETER (\AA) VS POLARIZABILITY ($CM^3/MOLECULE$)	55
FIGURE 2	$\ln K_H$ VS α (POLARIZABILITY) GASES IN H_2O AT T_H 10, 20, 30 AND $45^{\circ}C$	57
FIGURE 3	$\ln K_H$ VS α (POLARIZABILITY) GASES IN D_2O AT 10, 25, 35 AND $45^{\circ}C$	58
FIGURE 4	ΔS FOR INERT GASES IN C_6H_6 VS GAS POLARIZABILITY	78
FIGURE 5	ΔS FOR INERT GASES IN H_2O VS GAS POLARIZABILITY	85
FIGURE 6	$\ln K_H - \bar{G}_i / RT$ FOR INERT GASES IN BENZENE VS SOLUTE EFFECTIVE HARD SPHERE DIAMETER (\AA)	87
FIGURE 7	$\ln K_H - \bar{G}_i / RT$ FOR INERT GASES IN H_2O VS SOLUTE EFFECTIVE HARD SPHERE DIAMETER	88
FIGURE 8	$\Delta H - \bar{H}_i$ FOR INERT GASES IN H_2O VS. SOLUTE EFFECTIVE HARD SPHERE DIAMETER	90
FIGURE 9	$\Delta H - \bar{H}_i$ FOR INERT GASES IN C_6H_6 VS SOLUTE EFFECTIVE HARD SPHERE DIAMETER	91
FIGURE 10	$\Delta H - \bar{H}_i$ FOR HARD SPHERE (2.55\AA) IN BENZENE AT $298.15^{\circ}K$ VS. BENZENE HARD SPHERE DIAMETER	92
FIGURE 11	$\Delta H - \bar{H}_i$ FOR HARD SPHERE IN BENZENE AT $298.15^{\circ}K$ VS BENZENE SOLVENT HARD SPHERE DIAMETER	94
FIGURE 12	THERMAL EXPANSION COEFFICIENT AS A FUNCTION OF a_1 VS BENZENE SOLVENT HARD SPHERE DIAMETER	96
FIGURE 13	INERT GASES IN BENZENE $\Delta H^{CALC} - \Delta H^{EXP}$ VS SOLUTE H.S. DIAMETER	105.

INTRODUCTION

This thesis is divided into two separate sections. The following outline summarizes the topics covered in each section.

Section I details the experimental gas chromatographic system which was designed for the determination of gas solubilities in H_2O and D_2O . From the solubility values so obtained the enthalpies associated with the dissolution process were calculated for both H_2O and D_2O and compared to other experimental data where available. The data for gases dissolved in D_2O were used to test the Scaled Particle Theory (S.P.T.) which had been previously shown to give good agreement for gases dissolved in H_2O . Further examination of the S.P.T. using transfer coefficients revealed that the enthalpy expression was a strong function of the solvent experimental thermal expansion coefficient and represented a rather simplistic approach for the calculation of the enthalpy.

In section II the S.P.T. for gas solubility is rigorously developed. It was noticed that in the original theory the temperature dependence of the effective hard sphere diameter of the solute and solvent molecules had been ignored. Use was made of the (extrapolated) properties of a solute molecule of zero polarizability to determine the need for inclusion of such a temperature dependence. It was unambiguously shown that the dependence must be included in the theory. Rederiving the theory to include the temperature dependence, it was shown that agreement between theory and experiment (for a wide range of solvents) was now very poor and, in an attempt to further understand the theory, the theory was now derived in a purely hard sphere formulation.

The approximations necessary to produce the equations of the original S.P.T. were then examined. This showed that the originally observed

agreement between theory and experiment was purely fortuitous. Indeed it is shown that the theory can only be applied to systems wherein the behaviour of the solute molecules is sufficiently similar to that of a hard sphere.

The theory is thus shown to be a very simple model of a perturbation theory in which the reference system is that of a system of hard spheres.

Section I - Introduction

The thermodynamic properties of solutions of gases in water display anomalies in contrast to the properties observed in organic solvents. These are revealed in the unusually low molar entropies of solution and large negative molar heats of solution. Correlations of gas solubilities have been attempted using such properties as partial vapour pressures, surface tension and partial molar volumes in an attempt to formulate a theory for dissolved gases, but lack of reliable solubility data has hindered these attempts.

Battino⁽¹⁾ has tabulated and curved fitted solubility values for dissolved gases in water to obtain the temperature dependence of the solubility according to the equation

$$\ln X_2 = A + BT^{-1} + C \ln(T^{\circ}K^{-1}) \quad (1)$$

where A, B and C are coefficients and T is Temperature ($^{\circ}K$). The criteria for selecting the solubility data were based on the reliability of the experimental method employed, the reproducibility of the worker's own data and from comparison with data from other sources. Consequently data for many of the temperature dependent studies consists of data obtained by various workers using many different techniques⁽²⁾.

This research has developed a gas chromatographic technique which, unlike other techniques, allows an absolute measurement of a dissolved gas in a solvent. The use of a gas chromatographic technique to determine the amount of a gas dissolved in a known

4

volume of solvent is widely reported^(3,4,5). With appropriate chromatographic conditions, small solvent samples can be analysed and amounts of dissolved gas down to 10^{-8} moles can be accurately measured. Most workers have used the so-called 'stripping' technique wherein the chromatograph carrier gas is bubbled rapidly through the sample under investigation, the gas is then dried of solvent by passage through an appropriate absorbent, and finally the amount of solute gas stripped from solution is measured using a gas chromatograph^(6,7). The stripping technique has caused most workers to adopt a relative rather than an absolute measurement of gas solubility^(6,8). Thus, the amount of gas dissolved in a solvent is measured relative to the amount of 'another' gas dissolved in the same solvent under conditions wherein the saturation solubility is well established.

In this research we report a gas chromatographic method which allows a dissolved gas sample to be measured against a calibration response curve obtained using pure gas samples, yet allowing the calibration curve to be obtained under conditions matching those used in stripping the dissolved gas.

Solubility of Gases in H_2O and D_2O

CHAPTER I

"Let us learn to dream, gentlemen, then perhaps we shall find the truth. But let us beware of publishing our dreams till they have been tested by the waking understanding."

Friedrich August Kekulé
Translated by F.R. Japp
Journal of Chemical Education
35, 21 (1958)

EXPERIMENTAL

Distilled H_2O or D_2O (99.8% Stohler Isotope Chemicals) is degassed by a sublimation technique. Twenty mls of the solvent is introduced into a degassing cell through a Rotaflo valve. Liquid nitrogen is placed in the cold finger above the degassing cell and the system is evacuated to 10^{-4} torr causing the solvent to freeze. Sublimation is achieved by placing a heating mantle around the solvent container and subliming the frozen solvent onto the cold finger. Once degassing is completed the saturation cell which is connected to the degassing cell is evacuated (10^{-4} torr) and the frozen solvent is allowed to melt under vacuum. Approximately 20 mls of the solvent is then transferred to the saturation cell under an atmosphere of the gas under study.

Teflon stopcocks are used to prevent grease contamination. No detectable amounts of gas have been observed in a G.C. analysis (on maximum sensitivity) upon analysis of the degassed solvent.

Saturation Cell

The saturation cell is maintained in an insulated water bath at $T^{\circ}C \pm .01^{\circ}C$. Upon transfer of the solvent from the degassing cell to the saturation cell the gas under study is dispersed through the solvent using a fritted disk⁽³⁾. At the same time the solution is constantly stirred by a magnetic stirrer (controlled from outside the water bath). The gas pressure above the sample is maintained at atmospheric pressure, thus preventing supersaturation. Complete saturation is normally achieved within 2.5 hrs. This was determined by monitoring gas uptake as a function of time for several gases. Before samples are withdrawn the bubbling of the gas through the solvent is halted and the

7

solution is left stirring for 1 h under one atmosphere of gas to ensure equilibrium.

Sample Transfer

The saturated sample is transferred to the gas stripping line using a greaseless gas tight $2.5000 \pm .0001$ ml Gilmont micrometer syringe. The syringe is initially flushed with the gas under study to prevent air contamination of the sample. The saturated sample is withdrawn from the saturation cell by inserting the needle of the syringe through a rubber serum cap fitted on the saturation cell. The syringe is designed such that the barrel can be filled with 2.5 mls. of solvent extremely slowly, thus preventing the sample from being placed under a reduced pressure. The syringe is then withdrawn from the saturation cell, containing approximately 2.5 ml of the saturated solvent.

Gas Stripping Line

The gas stripping line shown diagrammatically in FIG. 1 is constructed of 4mm I.D. Duran 50 glass.

The line is previously evacuated (10^{-6} torr) through stopcocks 12 and 13 and then permanently maintained under Helium carrier gas pressure.

Initially, .25 mls of the sample are injected into the gas stripping cell (Fig. 2) to "wet" the frit since it would appear that some absorption of dissolved gas occurs on the frit. Then four .500 ml samples are injected sequentially (allowing the previous sample sufficient time to be stripped) and the stripped gas analysed on the G.C. These samples are injected without the syringe being withdrawn from the stripping cell, ensuring that no leaks or air contamination occurs. For

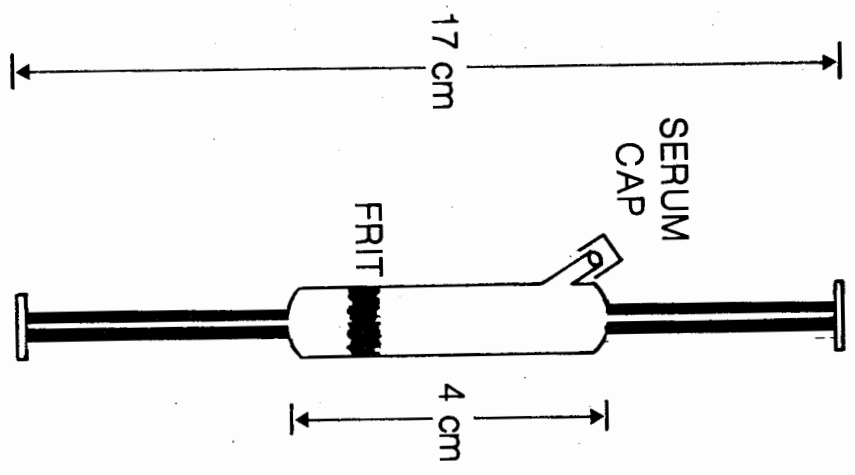


FIG 2
STRIPPING
CELL

each injection the dissolved gas is rapidly stripped from the solution by Helium carrier gas dispersed through the sample by a #2 porosity glass frit placed at the base of the stripping cell⁽⁹⁾.

The Helium carrier gas flow can be preferentially directed into stripping cell #1 or cell #2 using stopcock 7 (3-way). Closing stopcocks 9 and 10 or stopcocks 8 and 11 allows each stripping cell to be used individually. The stripping cells were initially evacuated (10^{-6} torr) through stopcocks 12 and 13, and the line purged with Helium through stopcock 16.

The stripped gas is dried by passage through a 50% CaCl_2 and 50% CaSO_4 drying tube before entering the chromatographic column; appropriate columns are used for each gas (see APPENDIX I). The stripped gas is then analysed in a Varian (Model 90P) dual filament thermal conductivity detector. The signal from the detector is integrated on a C.M.C. digital readout (Model 707 BN) frequency counter and the response is compared directly to a calibration plot. The variation in response being no more than 1.0% amongst the four injected samples.

GAS CALIBRATION

The solubility value is obtained by a direct comparison with a calibration plot of moles of gas vs. chromatographic response as recorded by an on line integrator. The calibration curve is obtained by observing the chromatogram's response to a known number of moles of gas contained in the gas sampling loop⁽¹⁰⁾ (Fig. 1).

The gas sampling loop (Volume $.7076 \pm .0001$ mls) and line are evacuated (10^{-6} torr) through stopcock 1 while stopcocks 3, 4, 5 and 6 are open. The line is then isolated from the rest of the vacuum

system by shutting stopcock 1. Shutting stopcock 5 enables one to utilize the U-tube as a closed end manometer. The gas is introduced into the sampling loop at room temperature from one of the gas bulbs. After attaining equilibrium, the temperature of the gas is read and the pressure accurately measured on the Hg-manometer. The number of moles of gas in the sampling loop is then obtained using the ideal gas law. To transfer the gas to the detector for analysis the sampling loop stopcock is rotated 90° . The carrier gas transfers the sample via line A through a stripping cell, drying tube, and chromatographic column to the detector. The loop stopcock is then rotated back 90° to the original position. Stopcocks 1 and 5 are opened and the system is then evacuated to 10^{-6} torr. The process is repeated for various gas pressures until the desired number of calibration points are obtained.

GAS DETECTION

The gas is detected by a dual filament thermal conductivity detector with one filament being used as a reference and the other filament as the gas detector. A flow rate of 75 mls/min for both reference line and sample line is maintained. A current of 175 mA is used for detection and the detector block maintained at 110°C .

The signal from the detector is recorded on a 1 mV full scale Varian chart recorder (Model 9176) and the signal is integrated by an electronic C.M.C. (Model 707BN) digital readout frequency counter. Using this method, a complete calibration curve can be obtained for the gas under study from 10^{-8} moles.

The gas flow into the detector is divided into an internal reference flow and an external carrier flow both maintained at the same flow rate. The carrier gas always flows through the line and then to the detector via line B with stopcocks 18, 19 and 16 closed and stopcock 17 open.

Before the sample is injected into the stripping cell that part of the vacuum line is evacuated (10^{-6} torr) through stopcocks 12 and 13. Stopcocks 7, 8, 9, 10, 11, 14 and 15 are open, this enables the stripping line and the sampling loop to be completely evacuated. Stopcocks 12 and 13 are shut off and the line is thoroughly purged with Helium through stopcock 16. This process is repeated and the line is maintained under He carrier gas pressure by opening stopcock 18 while stopcocks 17 and 19 are closed. Stopcock 16 is closed (to the Helium tank) and directs the He carrier gas through the chromatographic column to the detector. Stopcocks 8 and 9 are then closed, while stopcock 7 (3-way) remains open. This enables the carrier gas to flow through the gas sampling loop, and through each of the two stripping cells. The gas flow is then directed through the drying column by adjusting stopcocks 14 and 15, and subsequently through the chromatographic column to the detector. Each stripping cell may be used independently by directing the carrier gas with stopcock 7.

Stripping cell #1 can be used by directing the He carrier gas through stopcock 7 in the direction of cell #1 with stopcock 10 open and shutting stopcock 11, thus isolating cell #2. Similarly cell #2 can be used by turning stopcock 7 180° and closing stopcock 10 while stopcock 11 is open, thus isolating cell #1 and maintaining the carrier gas flow through cell #2. By preferentially isolating each

cell one can rapidly perform sample analysis on two different solvents. In practice, two saturation cells are used simultaneously thus allowing one gas to be studied in two different solvents (eg. H_2O and D_2O) at identical temperatures and pressures. One can thus determine the amount of gas dissolved in H_2O in cell #1 and the same gas dissolved in D_2O in cell #2. The gas calibration curve is obtained as previously described.

In practice a calibration response curve is obtained prior to the analysis of the dissolved gas samples ('dry' calibration) and then repeated after the analysis. These calibration points obtained after the 'stripping' of the dissolved gas samples requires the dry gas to be passed (with Helium carrier gas) through the 2.5 mls of solvent remaining in the stripping cells. We call these 'wet' calibration points, serving both to show that no instrumental factors have altered during the time taken for sample analysis and that the presence of the solvent on top of the fitted disks in the stripping cells has not caused changes in chromatographic response through a change in carrier gas flow rate.

Our experiments show that the calibration plot is independent of the cell used. Our experiments have also shown that the introduction of approximately 2.5 mls of sample into the stripping cell is not sufficient to retard the carrier gas flow rate, and hence change the response of the detector. Consequently "dry calibration" is identical to the "wet calibration". By direct comparison of the integrator response of the four stripped samples to the calibration curve, one obtains the number of moles of dissolved gas. For low solubility gases the injected sample size can be increased from 1/2 cc to 1 cc and the amount of gas can be accurately determined.

Again, no change in detector response is observed for the 1 cc injections. This experimental technique has been applied to various dissolved gases in H₂O and D₂O with an estimated accuracy of 1% for most gases and 2% for the least soluble gases.

RESULTS AND DISCUSSION

The saturation of the gas into each solvent was carried out simultaneously and the analysis of the amount of gas dissolved was made using one sample cell for H₂O and one sample cell for D₂O. Two sets of 'four 0.5 ml injections' were performed on each solvent. A comparison of the data obtained with that reported in the literature is made in Table 1. The comparison is seen to be excellent.

There is little data reported for gases dissolved in D₂O, perhaps due to the quantities of solvent required for experiments. One of the advantages of our technique is that less than 20 mls of solvent is required for saturation and less than .5 mls is required for analysis for any one temperature, all of which is recovered.

Using the solubility data in Table I, the gas solubility values were fitted to equation (1) with a standard deviation reported as a % difference in the $\ln X_2$ fit compared to the experimental $\ln X_2$ at 298.15 °K. Table II summarizes these results and Figure 3 is a typical plot of Argon gas solubility in H₂O and D₂O expressed as $\ln X_2$ versus $1/T(^{\circ}\text{K}^{-1})$.

Using the coefficients so obtained from the curve fit, the enthalpies associated with the dissolution process in H₂O and D₂O were computed from equation (1) using the following expression:

$$\Delta H = RT^2 \frac{\partial \ln X_2}{\partial T} = -B + CT \quad (2)$$

Table I

Mole Fraction X_2 of Gases Dissolved in H_2O and D_2O Argon ($X \cdot 10^4$)

T° (K)/Ref.	H_2O			D_2O			
	(11)	(12)	(13)	(1)	Present Study	Present Study	(1)
278.15	.3769	.3788	—	.3787	.3785	.4271	.4270
283.15	.3360	.3364	.3352	.3367	.3333	.3731	.3750
288.15	.3019	.3026	.2953	.3025	.2988	.3333	.3341
293.15	.2742	.2756	.2697	.2746	.2722	.3048	.3003
298.15	.2517	.2530	.2482	.2516	.2520	.2680	.2724
303.15	.2332	—	.2284	.2326	.2316	.2497	—

Krypton ($X \cdot 10^4$)

T° (K)/Ref.	H_2O			D_2O			
	(14)	(13)	(1)	Present Study	Present Study	Present Study	(1)
278.15	.7533	—	.7526	.7533	.8624	.7264	.7264
283.15	.6576	.5989	.6498	.6577	.6472	.6472	.6472
288.15	.5688	.5317	.5680	.5740	.5544	.5544	.5544
293.15	.5026	.4799	.5025	.5113	.4803	.4803	.4803
298.15	.4512	.4305	.4494	.4526	.4451	.4451	.4451
303.15	.4069	.3955	.4062	.4180	.3809	.3809	.3809
308.15	.3723	.3606	.3708	—	—	—	—
313.15	.3362	.3345	.3417	.3469	—	—	—

Xenon ($X \cdot 10^4$)

T° (K)/Ref.	H_2O			D_2O			
	(13)	(14)	(1)	Present Study	Present Study	Present Study	(1)
278.15	—	1.466	1.404	—	—	—	—
283.15	—	1.223	1.188	—	—	—	—
288.15	.9991	1.039	1.019	—	—	—	—
293.15	.8857	.8937	.8840	.8843	.9058	.9058	.9058
298.15	.7835	.7785	.7761	—	—	—	—
303.15	.6878	.6887	.6889	.6847	.7090	.7090	.7090
308.15	.6193	.6163	.6177	—	—	—	—
313.15	.5613	.5558	.5592	.5652	.5605	.5605	.5605

Table I (continued)

Nitrogen ($\times 10^4$)

T° (K)/Ref.	H ₂ O		Present Study		D ₂ O
	(12)	(11)	(1)		Present Study
278.15	.1702	.1680	.1695	.1692	.1862
283.15	.1527	.1507	.1519	.1513	.1691
288.15	.1387	.1371	.1379	.1372*	.1561
293.15	.1275	.1254	.1265	.1275	.1467
298.15	.1182	.1162	.1173	.1175	.1335
303.15	————	.1086	.1098	.1116	.1249
308.15	————	————	.1038	.1062	.1170*
313.15	————	————	.0989 ⁴	.09986	.1069

Oxygen

	H ₂ O		Present Study		D ₂ O
	(11)	(15)	(1)		Present Study
278.15	————	.3416	.3458	.3446	.3729
283.15	.3053	.3025	.3071	.2963	.3332
288.15	.2738	.2708	.2759	.2678	.2950
293.15	.2492	.2445	.2505	.2496	.2673
298.15	.2281	.2221	.2298	.2264	.2459
303.15	.2115	.2035	.2127	.2081	.2263*
308.15	————	————	.1988	.1985	.2101
313.15	————	————	.1873	.1853	.2000

CH₄

	H ₂ O		Present Study		D ₂ O	
	(16)	(17)	(1)		Present Study	(1)
278.15	————	.3977	.3979	.3978	.4371	.4349
283.15	.3360	.3457	.3483	.3467	.3732	.3782
288.15	.2968	.3096	.3086	.2940	(.3187)*	.3328
293.15	.2681	.2754	.2767	.2720	.3006	.2962
298.15	.2426	.2527	.2507	.2485	.2655	.2664
303.15	.2221	.2341	.2295	.2278	.2382	————
308.15	.2049	.2143	.2121	.2140*	.2176	————
313.15	————	————	.1978	.1943	.2080	————
318.15	.1936	————	.1860	.1899	.1854	————

T° (K)/Ref.	<u>C₂H₆</u>				<u>D₂O</u>	
	H ₂ O		(1)	Present Study	Present Study	(1)
	(16)	(17)				
278.15	—	.6445	.6488	.6483	.7010	.6983
283.15	—	.5226	.5359	.5226	.5775	.5748
288.15	.3966	.4469	.4506	.4438	.4869	.4808
293.15	.3482	.3849	.3852	.3832	.4121	.4082
298.15	.3079	.3321	.3345	.3330	.3520	.3514
303.15	.2753	.2922	.2948	.2916	.3024	—
308.15	.2498	.2609	.2633	—	—	—
313.15	.2313	—	.2384	—	—	—

	<u>SF₆</u>				<u>D₂O</u>	
	H ₂ O		(1)	Present Study	Present Study	
	(18)	(19)				
278.15	.09393*	.09123	.09164	.09164	.1106	
283.15	.07368*	.07340	.07335	.07340	.07812	
288.15	.05780	.06041	.06032	.06035	.06505	
293.15	.04801*	.05056	.05088	.05143	.05465	
298.15	.04047	.04393	.04394	.04426	.04829	
303.15	—	.03842	.03881	.03486	.04280	
308.15	—	.03469	.03499	.03786	.03960	
313.15	—	.03232	.03218	.03226	.03584	
323.15	—	—	—	—	.03311	

	<u>CF₄</u>			
	H ₂ O		D ₂ O	
	(1)	Present Study	Present Study	Present Study
293.15	.04265	.04349		.04874
298.15	.03819	.03750		.04063
303.15	.03477	.03492		.03719

* interpolated value

() omitted value, clearly in error

FIG. 3
 $\ln x_2$ vs $1/T$ ($^{\circ}\text{K}^{-1}$) ARGON in H_2O and D_2O

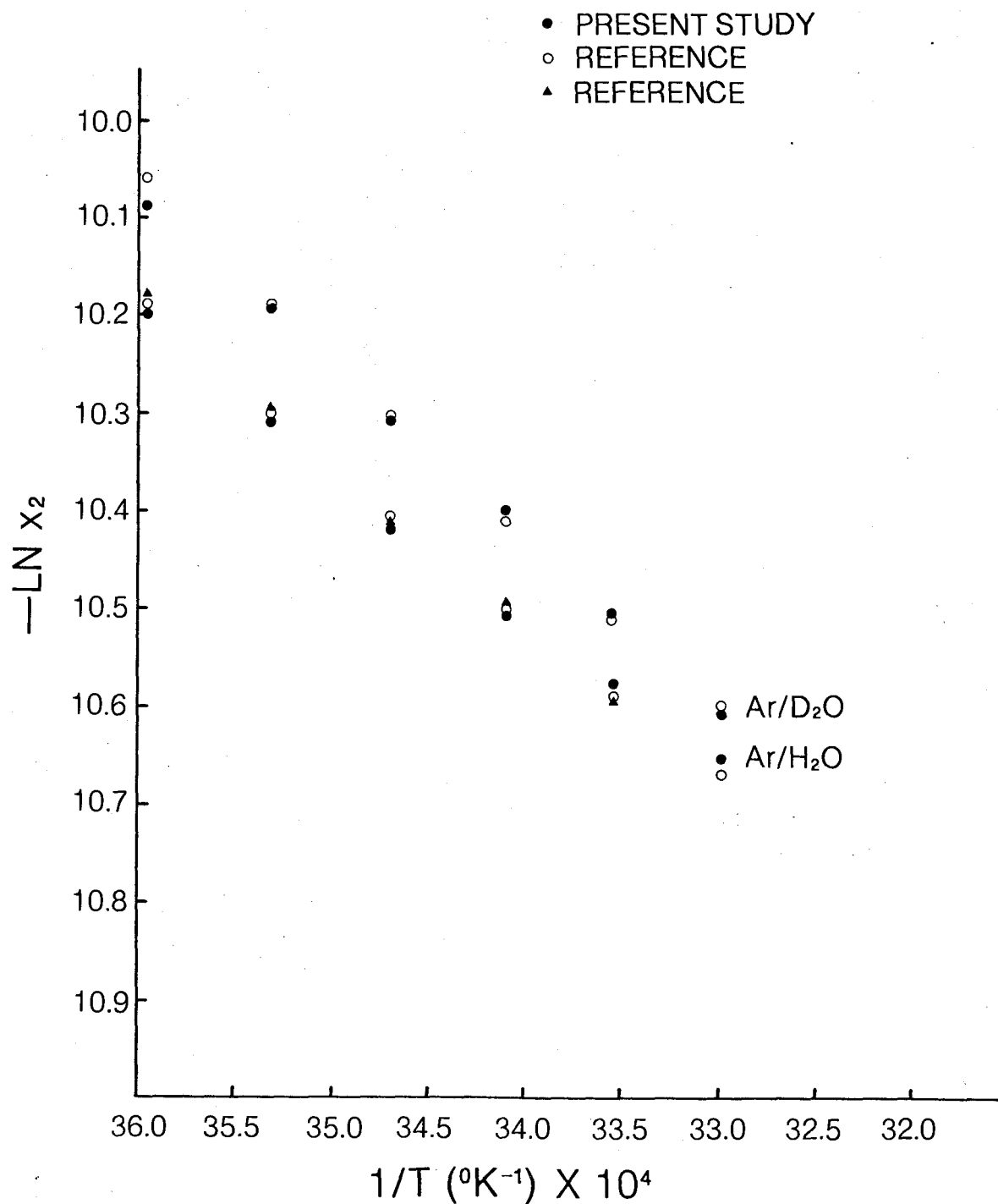


Table II

Gas/Solvent	Coefficients in the Equation $R \ln x_2 = A + B/T + C \ln (T/K^\circ)$			%O*
	A Cal Mole ⁻¹ °K ⁻¹	B Cal Mole ⁻¹	C Cal Mole ⁻¹ °K ⁻¹	
Ar/H ₂ O	-336.5	16452.2	45.7	.51
Ar/D ₂ O	-279.1	14317.4	36.9	.40
Kr/H ₂ O	-308.7	16005.4	41.3	1.0
Kr/D ₂ O	-583.5	28350.6	82.3	1.31
O ₂ /H ₂ O	-418.5	20059.8	57.9	.40
O ₂ /D ₂ O	-385.9	18752.4	53.0	.30
N ₂ /H ₂ O	-393.6	18544.7	54.2	.15
N ₂ /D ₂ O	10.2	846.8	-6.2	.18
CH ₄ /H ₂ O	-507.5	24361.5	71.0	.92
CH ₄ /D ₂ O	-286.3	14919.8	37.8	.22
C ₂ H ₆ /H ₂ O	-554.5	27749.5	77.4	.26
C ₂ H ₆ /D ₂ O	-201.7	12680.5	24.4	1.2
SF ₆ /H ₂ O	-742.6	36142.5	104.8	.93
SF ₆ /D ₂ O	-1196.6	56244.3	172.6	.94

* Standard Deviation of Fit $\ln X_2$ as a percentage at 298.15 °K

Tables III and IV summarize these results for various gases in both H_2O and D_2O . The experimental enthalpies of solution compare quite favorably with those from Reference (1). One must remember that the experimental values of the Henry's law constants from this reference were fitted to equation (1) using data from many workers incorporating different techniques.

These data can be considered ideal since any values which deviated from the fit by greater than one standard deviation were rejected; hence only data conforming to the curve fit of equation (1) were used. From the above Tables of enthalpy values, one can see distinct trends for both H_2O and D_2O : as the temperature increases the enthalpy decreases. Also one observes a greater enthalpy of solution for the dissolved gases in D_2O than in H_2O . To draw comparison to the experimentally determined solubility thermodynamic properties, the generally accepted practice has been to use the Scaled Particle Theory (S.P.T.) of gas solubilities, although to date no such comparison for the solubility of the inert gases in D_2O has been made. The next section of this thesis deals in great depth with the S.P.T. of gas solubility. To present the predicted gas solubility data for D_2O one must introduce the required equations of the theory. Here, only a brief description of the theory will be presented to introduce the equations whilst the reader is referred to the following section for a detailed discussion.

The dissolution of a gas into a liquid is considered as a two step process. The first being the creation of a cavity of suitable size to accommodate the solute molecule. The second step is the introduction of the solute into the cavity created. The thermodynamic functions

Table III
Enthalpy of Solution of Gases in H₂O and D₂O

T° (K)	H ₂ O ΔH (Cal Mol ⁻¹)*									
	Ar ±1%	Kr ±5%	Xe ±6%	O ₂ ±13%	N ₂ ±1%	CH ₄ ±2%	C ₂ H ₆ ±3%	SF ₆ ±3%	CF ₄	
283.15	-3512	-4311	—	-3665	-3198	-4258	-5834	-6468	—	
298.15	-2827	-3692	-4257	-2797	-2385	-3193	-4673	-4896	-3877	
313.15	-2141	-3072	—	-1928	-1572	-2128	-3512	-3324	—	
	<u>D₂O ΔH (Cal Mol⁻¹)*</u>									
	±6%	±2%	±2%	±1%	±5%	±10%	±2%	±10%		
283.15	-3869	-5047	—	-3745	-2808	-4217	-5772	-7373	—	
298.15	-3316	-3813	-4327	-2950	-2695	-3650	-5405	-4784	-4777	
313.15	-2762	-2578	—	-2155	-2788	-3083	-5039	-3488	—	

* Error expressed as a function of ΔH from the derivative of ln x₂ at 298.15 °K

associated with these steps are the reversible work or the Gibbs free energy in creating a hard sphere cavity and, after insertion of the solute, the Gibbs free energy of solute-solvent interaction. These steps were described in a series of papers by Reiss et al. (20,21) for a system of hard spheres, and later extended by Pierotti for the solubility of a gas in a real solvent. (22,23,24) The standard Gibbs free energy for the process is given by

$$\Delta \bar{G} = \bar{G}_c + \bar{G}_i + RT \ln (RT/V_1) \quad (3)$$

where \bar{G}_c and \bar{G}_i describe the above two step dissolution process and are defined in equations (7) and (17) respectively in the following section, V_1 is the solvent molar volume. The Henry's law constant K_H is given by

$$\ln K_H = \bar{G}_i/RT + \bar{G}_c/RT + \ln (RT/V_1) \quad (4)$$

The corresponding enthalpy of solution is written as

$$\Delta H = -RT^2 \left(\frac{\partial \ln K_H}{\partial T} \right)_P = \bar{H}_c + \bar{H}_i - RT + \alpha_P RT^2 \quad (5)$$

where R is the universal gas constant, T is the temperature and α_P is the thermal expansion coefficient of the solvent. \bar{H}_c and \bar{H}_i are the enthalpies associated with cavity formation and interaction respectively.

Tables V and VI give the predicted Henry's law constant ($\ln K_H$) and the enthalpy associated with the dissolution of selected gases in both H_2O and D_2O and compares them to my experimentally obtained values.

Table V

Thermodynamic Properties in D₂O at 298.15 °K

Gas	ln K _H exp.	ln K _H S.P.T.	ΔH (cal Mole ⁻¹) exp.	ΔH (cal Mole ⁻¹) S.P.T.
Ar	10.53	10.39	-3316	-2612
Kr	9.94	9.76	-3813	-3364
Xe	—	9.34	-4327	-4545
CH ₄	10.64	10.08	-3650	-3372
C ₂ H ₆	10.10	9.50	-5405	-5151
SF ₆	12.24	11.86	-4784	-6586

Table VI

Thermodynamic Properties in H₂O at 298.15 °K

Gas	ln K _H exp.	ln K _H S.P.T.	ΔH (cal Mole ⁻¹) exp.	ΔH (cal Mole ⁻¹) S.P.T.
Ar	10.59	10.44	-2827	-2425
Kr	10.00	9.80	-3692	-3161
Xe	—	9.39	-4257	-4299
CH ₄	10.60	10.12	-3193	-3159
C ₂ H ₆	10.17	9.55	-4825	-4871
SF ₆	12.33	12.14	-4896	-5802

One is amazed at the predictive abilities of the Scaled Particle Theory: not only does it predict reasonably good ΔH values, but it also predicts a higher enthalpy of solution ($\approx 6\%$) for the gases dissolved in D_2O , which compares favorably with the experimental difference. One notes that the Henry's law constants (expressed as $\ln K_H$) are predicted well for both H_2O and D_2O , but one recognizes that these predictions could be rather fortuitous since there is little difference in the H_2O and D_2O $\ln K_H$ values.

Of interest are the values of the enthalpy 'transfer' coefficients for the inert gases from H_2O to D_2O , that is the enthalpy associated with the transfer of one mole of solute from H_2O to D_2O . These are of particular interest since the values of the hard sphere diameter, the dipole moment and the polarizability of H_2O and D_2O are the same. This effectively allows the cancellation of the interaction term in the enthalpy expression (eqn. (5)) shown above for the dissolution process. The enthalpy change accompanying the transfer of a solute from H_2O to D_2O is

$$\Delta H_{tr}^O = \Delta H_{gas}(D_2O) - \Delta H_{gas}(H_2O) \quad (6)$$

which, with the cancellation of like terms in equation (5), gives

$$\Delta H_{tr}^O = (\alpha_P^{D_2O} - \alpha_P^{H_2O}) [yRT^2(1-y)^{-3} \{3(1+2y)A^2 + 3(1-y)A + (1-y)^2\} + RT^2] \quad (7)$$

where α_P is the experimental thermal expansion coefficient of the solvent and y is the 'compactness' factor (a function of the molar volume of the solvent). Table VII summarizes the experimental enthalpy transfer coefficients for selected gases and compares these to the values predicted by the S.P.T.

Table VII

$$\Delta H_{tr}^{\circ} \text{ (cal Mole}^{-1}\text{) at } 298.15 \text{ }^{\circ}\text{K}$$

Gas	ΔH_{tr}° Present Study	ΔH_{tr}° Ref. 1	ΔH_{tr}° S.P.T.
Ar	-489 \pm 30	-338	-187
Kr	-121 \pm 7	—	-203
Xe	- 70 \pm 5	—	-246
CH ₄	-457 \pm 47	-268(a)	-222
C ₂ H ₆	-580 \pm 21	-328(a)	-285

(a) Reference (25)

One observes from Table VII that the experimental enthalpy transfer coefficients decrease for the noble gases from Argon to Xenon, whilst the S.P.T. predicts an increase. Generally poor agreement is obtained for the experimental transfer coefficients when compared to the Scaled Particle Theory prediction.

One notes that a small difference in either the H₂O or D₂O enthalpy values for the gases contributes to a very large difference in the experimental transfer coefficients. It is also interesting to note that the transfer enthalpies predicted by the S.P.T. at other temperatures actually increase with increasing temperature while the experimental values decrease with increasing temperature. One is surprised at the predicted enthalpies of solution using the S.P.T. considering the simplicity of equation (7).

The transfer enthalpy coefficients actually give one an insight into the Scaled Particle Theory's method of differentiating between H₂O and D₂O, as shown in equation (7). Upon examination of the bracketed term in equation (7), one sees that, for the gas Argon, this term represents approximately a 1% difference, while the difference in the solvent thermal expansion coefficients represents approximately 25% ($\alpha_P^{H_2O} = 2.57 \times 10^{-4} \text{ } ^\circ\text{K}^{-1}$; $\alpha_P^{D_2O} = 1.918 \times 10^{-4} \text{ } ^\circ\text{K}^{-1}$) at 298.15 °K. From Tables V and VI one can see approximately a 6% difference in the predicted enthalpies for the various gases in H₂O and D₂O. This difference in predicted enthalpies appears to be a reflection of the differences in the experimental thermal expansion coefficients of H₂O and D₂O, which also suggests why there is no apparent difference in the predicted $\ln K_H$ values, since \bar{G}_c is not a function of the expansion coefficients of the solvents. This then appears to be a rather simplistic approach to the prediction of the thermodynamic

properties associated with the dissolution process for these two complex systems. It suggests that this theory is in fact overspecified since both γ (compactness factor) and α_p are functions of solvent molar volume, and also since the temperature and pressure of the system is specified. At this point it is interesting to examine the S.P.T. in depth to determine what in fact allows one to predict with such apparent success the thermodynamic properties associated with the dissolution of a gas into a liquid.

- (1) E. Wilhelm, R. Battino and R.J. Wilcock.
Chem. Reviews 77: 219 (1977).
- (2) R. Battino and H.L. Clever.
Chem. Reviews 66: 395 (1966).
- (3) S.K. Shoor, R.D. Walker, Jr. and K.E. Gubbins.
J. Phys. Chem. 73: 312 (1969).
- (4) H.P. Kollig, J.W. Falco and F.E. Stancil, Jr.
Environmental Science and Technology 9: 957 (1975).
- (5) R.F. Weiss and H. Craig.
Deep Sea Research 20: 291 (1973).
- (6) J.W. Swinnerton and V.J. Linnenbom.
J. of Gas Chromatography 5: 570 (1967).
- (7) K.E. Gubbins, S.N. Carden and R.D. Walker, Jr.
J. of Gas Chromatography Oct.: 330 (1965).
- (8) K.E. Gubbins, S.N. Carden and R.D. Walker, Jr.
J. of Gas Chromatography March: 98 (1965).
- (9) J.W. Swinnerton, V.J. Linnenbom and C.H. Cheek.
Anal. Chem. 34: 483 (1962).
- (10) B.A. Cosgrove and I.D. Gay.
J. of Chromatography 136: 306 (1977).
- (11) E. Douglas.
J. Phys. Chem. 68: 169 (1964).
- (12) C.E. Klots and B.B. Benson.
J. of Marine Research 21: 48 (1963).
- (13) T.J. Morrison and N.B. Johnstone.
J. Chem. Soc. 3441 (1954).
- (14) A. Lannung.
J. Am. Chem. Soc. 52: 68 (1930).
- (15) C.N. Murray and J.P. Riley.
Deep Sea Research 16: 311 (1969).
- (16) T.J. Morrison and F. Billett. .
J. Chem. Soc. 3819 (1952).
- (17) W.-Y. Wen and J.H. Hung.
J. Phys. Chem. 74: 170 (1970).

- (18) H.L. Friedman.
J. Am. Chem. Soc. 76: 3294 (1954).
- (19) J.T. Ashton, R.A. Dawe, K.W. Miller, E.B. Smith and B.J. Stickings.
J. Chem. Soc. A 1793 (1968).
- (20) H. Reiss, H.L. Frisch and J.L. Lebowitz.
J. Chem. Phys. 31: 369 (1959).
- (21) H. Reiss, H.L. Frisch, E. Helfand and J.L. Lebowitz.
J. Chem. Phys. 32: 119 (1960).
- (22) R.A. Pierotti.
J. Chem. Phys. 67: 1840 (1963).
- (23) R.A. Pierotti.
J. Chem. Phys. 69: 281 (1965).
- (24) R.A. Pierotti.
Chem. Revs. 76: 717 (1976).
- (25) W.-Y. Wen and J.A. Muccitelli.
J. Sol. Chem. 8: 225 (1979).

APPENDIX I

Gas	Column	Temperature
Ar	6'x1/4" Silical Gel 30/60 Mesh	0°C
CH ₄	5'x1/4" Silical Gel 30/60 Mesh	0°C
N ₂	6'x1/4" Molecular Sieve 5A 40/60 Mesh	0°C
O ₂ , Kr	6'x1/4" Molecular Sieve 5A 40/60 Mesh	0°C
SF ₆	5'x1/4" Silical Gel 40/60 Mesh	120°C
C ₂ H ₆	6'x1/4" Silical Gel 30/60 Mesh	120°C
N ₂ +O ₂	8'x1/4" Molecular Sieve 5A 30/60 Mesh	-28°C
Xe	30"x1/4" Molecular Sieve 5 A 30/60 Mesh	R.T.

Over the years much work has been done to develop a theory in an attempt to predict gas solubility data. Sisskind and Kasarnowsky⁽¹⁾, studying Argon solubility in various solvents, showed that the energy of solution consisted of two terms. The first term was described by the increase in surface area of the cavity created (upon insertion of the solute) times the surface tension of the solvent. The second term being the molecular solute-solvent interaction.

Uhlig⁽²⁾ derived thermodynamic equations which expressed the solubility of a gas as a function of its molecular radius and the surface tension of the solvent. Unfortunately, solute-solvent interactions are rather complex and at that time not well understood, hence only a qualitative representation could be made. Also, the concept of using macroscopic parameters to describe microscopic phenomena is a poor assumption. Uhlig had the right idea in considering the dissolution process as a two step process: the energy of cavity formation and the complex interaction energy. Lack of accurate solubility data and of an understanding of solute-solvent interactions made the development of a theory a formidable task. Even so, these calculations yielded an insight into the anomolous behaviour of water when compared to organic solvents.

Eley⁽³⁾ considered a model in which the number of gas molecules dissolved was interchangeable with the same number of water molecules in a quasi-lattice. Eley concluded that this was energetically unfavourable and that the available points must in fact be cavities which could easily be enlarged to accomodate a gas molecule. An approximate partition function was constructed which took into account the effect of the gas upon dissolution. Again, gross approximations were made

regarding solute-solvent interactions.

In a series of papers, Reiss, Frisch, Lebowitz⁽⁴⁾ and Helfand⁽⁵⁾ developed a statistical mechanical theory of rigid spheres, based upon an exact radial distribution function, which could be applied to real fluids. From this theory it emerged that, for hard sphere particles, the only part of the radial distribution function which contributed to the chemical potential of the fluid was the part which determined the number density of particles in contact with the hard sphere particle. Hence, the calculation of the entire radial distribution function was not required. The theory yields an approximate expression for the reversible work required to introduce a spherical particle into a fluid of spherical particles. The particles in solution obey a pairwise additive potential and, upon addition of another particle to this system, the particle obeys the same potential by a procedure of distance scaling. A necessary condition for this Scaled Particle Theory (S.P.T.) is that the solvent molecules be approximately spherical with effectively rigid cores for both the solvent and solute. Assuming the solvent-solute interactions are described by a Lennard-Jones 6-12 potential, Reiss et al.⁽⁴⁾ calculated Henry's law constants for systems which satisfied the above criteria for the theory. Satisfactory agreement was found for Helium in Benzene and Helium in Argon.

The development of this theory provided the foundation for Pierotti to formulate a theory of gas solubility using the soft potential as a perturbation to the treatment of hard spheres. Using the expressions of Reiss et al. for the reversible work required to introduce a spherical particle into a fluid of spherical particles and by a method of extrapolation using experimental data, Pierotti was able to predict

thermodynamic properties for the dissolution of gases in organic solvents⁽⁶⁾ and water^(7,8). The major drawbacks in Pierotti's Scaled Particle Theory are the basic assumptions inherent in the treatment, which will be discussed later. In light of the assumptions made, it seemed appropriate to redo the Scaled Particle Theory extending the hard sphere treatment as was originally developed by Reiss et al.^(4,5) incorporating the concept of temperature dependent hard sphere diameters. An extension of the Scaled Particle Theory is presented incorporating a more comprehensive hard sphere treatment for the dissolution of a gas into a liquid.

CHAPTER II

Scaled Particle Theory of Gas

Solubilities

Theory and Development

If one considers a system of N spherically symmetrical molecules possessing an effective rigid core of diameter σ_1 with the necessary pressure to maintain the system at a constant volume and, if one excludes the centres of all N molecules from a spherical region of space of radius r in the volume, then one has created a cavity in the fluid. It is convenient to consider the process of introducing the solute molecule into the real solvent as consisting of two steps. The first step being the creation of a cavity in the solvent of suitable size to accommodate the solute molecule, assuming the reversible work or partial molecular Gibb's free energy \bar{g}_c is identical with that of charging the hard sphere of the same radius as the cavity into the solution.

The second step is the introduction into the cavity of a solute molecule which interacts with the solvent according to some potential law. The reversible work \bar{g}_i is identical with that of charging the hard sphere or cavity introduced in step one to the required potential. If the cavity size chosen in step one was suitable, there should be no change in size upon charging.

The standard equation for the chemical potential of a nondissociative solute in a very dilute solution is given by⁽⁴⁾

$$U_2^l = -\chi_2 + P\bar{v}_2 - K T \ln \lambda_{2,2}^3 + K T \ln(N_2/V) \quad (1)$$

$-\chi_2$ is the potential of the solute molecules in the solution relative to infinite separation, P is the pressure, \bar{v}_2 the partial molecular volume

of the solute, λ_2^3 and J_2 are the partition functions per molecule for the translational and internal degrees of freedom for the solute, N_2 is the number of solute molecules in solution, and V is the volume of solution. The sum of the first two terms on the right represents the reversible work required to introduce a solute molecule into a solution of volume N_2/V . These terms can be replaced by $(\bar{g}_i + \bar{g}_c)$ for the two step process, assuming that the solution is sufficiently dilute to ignore solute-solute interactions. Replacing N_2/V by x_2/v_1 yields the chemical potential of the solute in the liquid phase

$$U_2^l = \bar{g}_i + \bar{g}_c - KT \ln \lambda_2^3 J_2 + KT \ln (x_2/v_1) \quad (2)$$

The chemical potential of the solute in the gas phase (assumed ideal) is given by

$$U_2^g = -KT \ln (\lambda_2^3 J_2) + KT \ln (P_2/KT) \quad (3)$$

Assuming the internal degrees of freedom of the solute are not affected by the solution process, equating equations (2) and (3) one obtains

$$\ln P_2 = \bar{g}_i/KT + \bar{g}_c/KT + \ln(KT/v_1) + \ln X_2 \quad (4)$$

Using Henry's law (defined as $P_2 = K_H X_2$, where K_H is the Henry's law constant), equation (4) becomes, for partial molar quantities,

$$\ln K_H = \bar{G}_i/RT + \bar{G}_c/RT + \ln(RT/v_1) \quad (5)$$

The molar heat of solution is

$$\Delta H_S = \left(\frac{\partial \ln K_H}{\partial (1/RT)} \right)_P = \bar{H}_i + \bar{H}_c - RT + \alpha_p RT^2 \quad (6)$$

where α_p is the thermal expansion coefficient.

The Partial Molar Gibbs free energy of cavity creation was derived by Reiss et al. ⁽⁴⁾ for a system of hard spheres. They obtained

$$\bar{G}_c = K_0 + K_1 a_{12} + K_2 a_{12}^2 + K_3 a_{12}^3 \quad (7)$$

where the K's were evaluated to be

$$K_0 = RT\{-\ln(1-y) + 9/2[y/(1-y)]^2\} - N\pi Pa_1^3/6 \quad (7a)$$

$$K_1 = -(RT/a_1)\{[6y/(1-y)] + 18[y/(1-y)]^2\} + N\pi Pa_1^2 \quad (7b)$$

$$K_2 = (RT/a_1^2)\{[12y/(1-y)] + 18[y/(1-y)]^2\} - 2N\pi Pa_1 \quad (7c)$$

$$K_3 = (4/3)\pi PN \quad (7d)$$

The K's are functions of density, molar volume and diameter of the solvent through the compactness factor y , where $y = \frac{\pi a_1^3 N}{6V}$. The radius of the cavity created is equivalent to inserting a hard sphere of radius $a_{12} = (a_1 + a_2)/2$ (excluding the centers of solvent molecules), where a_2 is the diameter of the cavity to be created.

The Gibbs Free Energy of interaction (\bar{G}_i) was derived by Pierotti ⁽⁶⁾ in the following fashion. The reversible work for the charging process is

$$\bar{g}_i = \bar{e}_i + P\bar{v}_i - T\bar{S}_i = \bar{h}_i - T\bar{S}_i \quad (8)$$

where \bar{e}_i is the molecular energy and \bar{v}_i, \bar{S}_i are the partial molecular volume and entropy. The $P\bar{v}_i$ term for the change of state of the solute at normal pressures is considered negligible compared to the energy of the system and the entropy will be small and negative in the charging process. This term will then be assumed small, hence

$$\bar{G}_i = \bar{H}_i \quad (9)$$

If the interaction energy of a solute molecule with a given solvent molecule is $e_i(r)$, then the interaction per mole of solute will be E_i . Since E_i is approximately H_i from equation 8, hence one can determine \bar{G}_i .

Approximating the repulsive and dispersive interactions by a Lennard-Jones 6-12 pairwise additive potential⁽⁹⁾ $U(r)_{\text{dis}} = -4\epsilon_{12} \left[\left(\frac{\sigma_{12}}{r} \right)^6 - \left(\frac{\sigma_{12}}{r} \right)^{12} \right]$ and the inductive interaction for a nonpolar solute in a polar solvent by $U(r)_{\text{ind}} = U_1^2 \alpha_2 / r^6$, the interaction energy per solute molecule described by inductive, dispersive and repulsive forces is given by

$$e_i = -c_{\text{dis}} \sum_p (r_p^{-6} - \sigma_{12}^6 r_p^{-12}) - c_{\text{ind}} \sum_p r_p^{-6} \quad (10)$$

where r_p is the distance from the center of the solute molecule to the center of the p^{th} solvent molecule and σ_{12} is the distance of closest approach of the solute and solvent molecule hard sphere diameters. The Lennard-Jones force constant is approximated for the interaction of two molecules, viz $\epsilon_{12} = (\epsilon_1 \epsilon_2)^{1/2}$. U_1 is the dipole moment of the solvent and α_2 the polarizability of the solute. Evaluation of equation (10) requires that the solute molecule be immersed in the solvent and completely surrounded by the solvent which is assumed to be infinite in extent.

The number of solvent molecules in a spherical shell between r and $(r + dr)$ is equal to $g(r)4\pi r^2 \rho dr$, where $g(r)$ is the radial distribution function and ρ is the number density of the solvent. Replacing the summation with an integration in (10), the total interaction energy yields

$$E_i(r) = \left[-C_{\text{dis}} \int_{\text{vol}} (r_p^{-6} - \sigma_{12}^6 r_p^{-12}) - C_{\text{ind}} \int_{\text{vol}} r_p^{-6} \right] 4\pi r^2 \rho g(r) dr \quad (11)$$

The integration of this energy requires information regarding the radial distribution function, which is generally not known. A reasonable value can be approximated from x-ray studies on liquids. Generally one assumes that $g(r) = 1$ outside the radius r , recognizing that common solvents behave as Van der Waals type fluids. Substitution for the various constants yields

$$E_i(R) = -4C_{\text{dis}} \pi \rho \int_R^{\infty} r_p^{-4} + \sigma_{12}^6 r_p^{-10} dr - C_{\text{ind}} 4\pi \rho \int_R^{\infty} r_p^{-4} dr \quad (12)$$

where R is the distance from the center of the solute molecule to the centre of the nearest solvent molecule, the integration yields

$$E_i(R) = -4/3\pi\rho(C_{\text{dis}} + C_{\text{ind}})r^{-3} + 4/9\pi\rho C_{\text{dis}}\sigma_{12}^6 r^{-9} \quad (13)$$

Introducing $\epsilon_i^* = C_i \pi \rho / 6\sigma_{12}^3$ and $R' = R/\sigma_{12}$

$$E_i(R') = -8(\epsilon_{\text{dis}}^* + \epsilon_{\text{ind}}^*)R'^{-3} + 8/3\epsilon_{\text{dis}}^*R'^{-9} \quad (14)$$

where R' is found by differentiating equation (14) and equating to zero to obtain the minimum value of E_i with variation of R' . The result being

$$\epsilon_{\text{dis}}^* + \epsilon_{\text{ind}}^* = \epsilon_{\text{dis}}^* R'^{-6} \quad (15)$$

Since ϵ_{ind}^* is small compared to ϵ_{dis}^* , then R' is approximately unity. Substitution for R' into equation (14) and noting from equation (8) that $\bar{G}_i \approx E_i$ yields the required equation

$$\bar{G}_i/RT = -16/3(\epsilon_{\text{dis}}^*/KT) - 8\epsilon_{\text{ind}}^*/KT \quad (16)$$

This equation is in exact agreement with that of Pierotti⁽⁸⁾, noting that the dipolar interactions have been omitted since they are not required in this thesis. Also, $C_{\text{ind}} = U_1^2 \alpha_2$ for a nonpolar solute and a polar solvent and $C_{\text{dis}} = 4\epsilon_{12} \sigma_{12}^6$ where σ_1 and σ_2 are the solute and solvent Lennard-Jones parameters and $\sigma_{12} = \frac{(\sigma_1 + \sigma_2)}{2}$. These values are defined when the L.J. 6-12 potential is zero. One then assumes that σ_1 and σ_2 can be replaced by a_1 and a_2 .

The enthalpy of interaction defined in equation (16) can be further reduced by direct substitution of the appropriate constants, hence

$$\bar{E}_i = \bar{H}_i = \bar{G}_i = -3.555R\pi\rho\sigma_{12}^3(\epsilon_{12}/K) - 1.333R\pi\rho U_1^2 \alpha_2 / K \sigma_{12}^3 \quad (17)$$

where K is the Boltzman constant = 1.3805×10^{-16} erg $^{\circ}\text{K}^{-1}$, R is the gas constant = 1.987 cal mole $^{-1}$ $^{\circ}\text{K}^{-1}$ and ρ is the number density of the solvent which is the only term that implicitly accounts for different solvent structures. U_1 is the dipole moment of the solvent in esu $\cdot\text{cm}$, σ_{12} as previously defined has units of cm, the polarizability of the solvent α has units cm^3 molecule $^{-1}$, and ϵ_{12}/K , as previously defined, has units $^{\circ}\text{K}$.

The enthalpy of solution was defined in equation (6) as the derivative of $\ln K_H$, which entails the derivatives of \bar{G}_i and \bar{G}_c ; the Gibbs free energy of interaction and cavity formation. It was assumed in equation (9) that $\bar{G}_i = \bar{H}_i$, hence only the temperature derivative of \bar{G}_c , as defined by equation (7) is required. In this present derivation, the hard sphere diameter of the solvent is assumed to be temperature dependent. As the temperature of the solvent molecules increases the root mean square (r.m.s.) kinetic energy increases, which allows the molecules to penetrate. It will be shown later that obtaining the solvent hard sphere diameter a_1 from Henry's law coefficient shows a_1 to decrease with increasing temperature.

An effective hard sphere or rigid sphere is defined by the potential energy of interaction with another molecule.

$$\begin{aligned}
 U(r) &= \infty & r \leq \frac{1}{2}(a_1 + a_2) \\
 U(r) &= 0 & r > \frac{1}{2}(a_1 + a_2)
 \end{aligned}
 \tag{18}$$

where r is the separation between the centers of a solute and solvent molecule of diameter a_1 and a_2 .

To obtain \bar{H}_c , the derivative of \bar{G}_c is required, $\frac{\partial \bar{G}_c / RT}{\partial (1/RT)} = \bar{H}_c$, which entails differentiating all the K's, equations (7a-7d). One can simplify the problem with the following procedures. The substitution of $-dT/RT^2$ for $\partial(1/RT)$. Hence

$$\frac{\partial \bar{G}_c / RT}{\partial (1/RT)} = -RT^2 \frac{d\bar{G}_c / RT}{dT} = H_c \quad (19)$$

Next divide \bar{G}_c by RT and group the first set of terms in K_0 , K_1 and K_2 together, then group the last term in K_0 , K_1 and K_2 with K_3 and evaluate these groups separately.

Hence

$$\bar{G}_c / RT = K_0 / RT + a_{12} K_1 / RT + a_{12}^2 K_2 / RT + a_{12}^3 K_3 / RT \quad (20)$$

$$\begin{aligned} 1^{\text{st}} \text{ Term} &\equiv -\ln(1-y) + \frac{9}{2} [y/(1-y)]^2 - \frac{a_{12}}{a_1} \{ [6y/(1-y)] + 18[y(1-y)]^2 \} \\ &\quad + \frac{a_{12}^2}{a_1^2} \{ [12y/(1-y)] + 18[y(1-y)]^2 \} \end{aligned} \quad (21)$$

$$2^{\text{nd}} \text{ Term} \equiv \frac{4}{3} \frac{\pi P N a_{12}^3}{RT} - \frac{N \pi P a_1^3}{6RT} + \frac{a_{12} a_1^2 P \pi N}{RT} - \frac{2N P a_1 a_{12}^2}{RT} \quad (22)$$

Then let $Z = [6y/(1-y)] + 18[y/(1-y)]^2$ and $a_{12} = \frac{a_1 + a_2}{2}$,

$A = \frac{a_2}{a_1}$. The first and second term reduce to

$$1^{\text{st}} \text{ Term} = -\ln(1-y) + \frac{9}{2}[y/(1-y)]^2 - \frac{1}{2}(1+A)Z + \frac{1}{4}(1+2A+A^2)(Z + 6y/(1-y)) \quad (23)$$

$$2^{\text{nd}} \text{ Term} = \frac{N\pi Pa_2^3}{6RT} \quad (24)$$

The expression for the first term can now be further simplified

$$\begin{aligned} 1^{\text{st}} \text{ Term} &= -\ln(1-y) + \frac{9}{2} \left[\frac{y}{1-y} \right]^2 - \frac{Z}{2} - \frac{ZA}{2} + \frac{Z}{4} + \frac{2ZA^2}{4} + \frac{1}{4} \left(\frac{6y}{1-y} \right) (1+2A+A^2) \\ &= -\frac{Z}{4} + A^2 \left[\frac{Z}{4} + \frac{6y}{4(1-y)} \right] + \frac{6y}{4(1-y)} + \frac{12yA}{4(1-y)} - \ln(1-y) + \frac{9}{2} [y/(1-y)]^2 \quad (25) \end{aligned}$$

Resubstitution for Z yields

$$\begin{aligned} &= A^2 \left\{ \frac{9}{2} [y/(1-y)]^2 + 3y/(1-y) \right\} - \frac{9}{2} [y/(1-y)]^2 - \ln(1-y) + \frac{9}{2} [y/(1-y)]^2 \\ &\quad + \frac{3yA}{(1-y)} \\ &= A^2 \left\{ \frac{9}{2} [y/(1-y)]^2 + 3y/(1-y) \right\} + \frac{3yA}{(1-y)} - \ln(1-y) \quad (26) \end{aligned}$$

Inclusion of the second term yields the simplified expression for \bar{G}_c/RT

$$\bar{G}_c/RT = A^2 \left\{ \frac{9}{2} [y/(1-y)]^2 + \frac{3y}{(1-y)} \right\} + \frac{3yA}{(1-y)} - \ln(1-y) + \frac{N\pi Pa_2^3}{6RT} \quad (27)$$

The derivative of \bar{G}_c involves the derivative of A and since both a_1 and a_2 are assumed to be temperature dependent and the derivative of A yields $A(\ell_2 - \ell_1)$, where ℓ_i is introduced as the hard sphere temperature dependence $1/a_i \left(\frac{da_i}{dT} \right)_P$, then the following assumption

is made: $\frac{dA}{dT} = 0$. Typical values of $-\ell_1$ for organic solvents are ⁽¹⁰⁾ .13 to $.16 \times 10^{-3} \text{ } ^\circ\text{K}^{-1}$ and a typical value for $-\ell_2$ for Argon ⁽¹¹⁾ is $.16 \times 10^{-3} \text{ } ^\circ\text{K}^{-1}$ so, using the above values, the assumption is valid.

Hence

$$\begin{aligned} \frac{d\bar{G}_c/RT}{dT} &= A^2 \left\{ \frac{9}{2} \frac{d}{dT} [y/(1-y)]^2 + \frac{3d(y/1-y)}{dT} \right\} + 3A \frac{d(y/1-y)}{dT} - \frac{d}{dT} \ln(1-y) + \frac{N\pi P}{6R} \frac{d}{dT} \frac{a_2^3}{T} \\ &= A^2 \left\{ \left(\frac{dy}{dT} \right) \left(\frac{9y}{1-y} \right) \left[\frac{y}{(1-y)^2} + \frac{1}{(1-y)} \right] + \left(\frac{dy}{dT} \right) \left(\frac{3y}{(1-y)^2} + \frac{3}{(1-y)} \right) \right\} \\ &\quad + \frac{dy}{dT} A \left\{ \frac{3y}{(1-y)^2} + \frac{3}{(1-y)} \right\} + \frac{1}{1-y} \frac{dy}{dT} + \frac{N\pi P}{6R} \left\{ \frac{3a_2^2}{T} \frac{da_2}{dT} - \frac{a_2^3}{T^2} \right\} \end{aligned}$$

Further simplification yields

$$\frac{d\bar{G}_c/RT}{dT} = \frac{dy}{dT} (1-y)^{-3} \{ 6yA^2 - 3yA + 3A^2 + 3A + (1-y)^2 \} + \frac{N\pi P a_2^3}{6RT^2} \left\{ \frac{3T}{a_2} \frac{da_2}{dT} - 1 \right\} \quad (28)$$

$$\text{Since } y = \frac{\pi a_1^3 N}{6V}$$

$$\text{Then, } \frac{dy}{dT} = - \frac{\pi a_1^3 N}{6V^2} \frac{dV}{dT} + 3a_1^2 \frac{da_1}{dT} \frac{\pi N}{6V} \quad (29)$$

The thermal expansion coefficient α_p is defined as $\frac{1}{V} \left(\frac{dV}{dT} \right)_P$. Since one is dealing with a hard sphere system, it seems appropriate to

introduce α_p as a hard sphere (H.S.) expansion coefficient ($\alpha_p^{\text{H.S.}}$). Substituting both the hard sphere temperature dependence coefficient ℓ_1 and the H.S. thermal expansion coefficient yields

$$\frac{dy}{dT} = y(3\ell_1 - \alpha_p^{\text{H.S.}}) \quad (30)$$

Substitution for $\frac{dy}{dT}$ into equation (28) yields

$$\frac{d\bar{G}_c/RT}{dT} = y(3\ell_1 - \alpha_p^{\text{H.S.}})(1-y)^{-3} \{3(1+2y)A^2 + 3(1-y)A + (1-y)^2\} + \frac{N\pi Pa_2^3}{6RT^2} (3T\ell_2 - 1)$$

Since $\bar{H}_c = -RT^2 \frac{d\bar{G}_c/RT}{dT}$, one obtains the enthalpy of cavity formation as

$$\bar{H}_c = yRT^2(\alpha_p^{\text{H.S.}} - 3\ell_1)(1-y)^{-3} \{3(1+2y)A^2 + 3(1-y)A + (1-y)^2\} - \frac{N\pi Pa_2^3}{6} (3T\ell_2 - 1) \quad (31)$$

The thermal expansion coefficient substituted in the equation for the enthalpy of cavity formation, \bar{H}_c , was previously defined as a hard sphere term and, hence, should be derived from an equation of state for a system of hard spheres. The equation of state for a hard sphere system derived by Carnahan and Starling^(12,13) serves as a starting point

$$\frac{PV}{RT} = \frac{1+y+y^2-y^3}{(1-y)^3} \quad (32)$$

Differentiating equation (32) for V yields

$$\begin{aligned} \left(\frac{dV}{dT}\right)_P = \frac{R}{P} \left[\frac{1+y+y^2-y^3}{(1-y)^3} \right] + \frac{RT}{P} \left[\left(\frac{dy}{dT} + 2y \frac{dy}{dT} - 3y^2 \frac{dy}{dT} \right) (1-y)^{-3} \right. \\ \left. + (1+y+y^2-y^3) \cdot 3 \frac{dy}{dT} (1-y)^{-4} \right] \end{aligned} \quad (33)$$

Substitution of equation (32) for $\frac{R}{P}$ and $\frac{RT}{P}$ followed by division with V yields

$$\alpha_P^{\text{H.S.}} = \frac{1}{V} \left(\frac{dV}{dT}\right)_P = \frac{1}{T} + \frac{dy}{dT} \frac{(1+2y-3y^2)}{(1+y+y^2-y^3)} + 3 \frac{dy}{dT} (1-y)^{-1} \quad (34)$$

Further simplification yields

$$\alpha_P^{\text{H.S.}} = \frac{1}{T} + \frac{dy}{dT} \frac{(4 + 4y - 2y^2)}{(1-y)(1+y+y^2-y^3)} \quad (35)$$

Substitution of equation (30) for $\frac{dy}{dT}$ followed by suitable rearrangement yields

$$\alpha_P^{\text{H.S.}} + \frac{\alpha_P^{\text{H.S.}}(4y + 4y^2 - 2y^3)}{(1-y)(1+y+y^2-y^3)} = \frac{1}{T} + \frac{3\lambda_1(4y + 4y^2 - 2y^3)}{(1-y)(1+y+y^2-y^3)} \quad (36)$$

With sufficient manipulation, one obtains an expression for the thermal expansion coefficient for a system of hard spheres

$$\alpha_P^{\text{H.S.}} = \frac{1}{T} \frac{(1 - 2y^3 + y^4)}{(1 + 4y + 4y^2 - 4y^3 + y^4)} + 6\lambda_1 \frac{(2y + 2y^2 - y^3)}{(1 + 4y + 4y^2 - 4y^3 + y^4)} \quad (37)$$

This is similar to the expression obtained by Wilhelm⁽¹⁴⁾ presuming that a typographic error exists in the latter half of equation (17) in Wilhelm's⁽¹⁴⁾ paper.

A good test for any theory is the ability to predict the partial molar volumes of the solute⁽¹⁵⁾, which is defined as

$$\bar{V}_2 = \left(\frac{\partial U_2^{\text{SOL } n}}{\partial P} \right)_{T, N} \quad (38)$$

Hence, from (2)

$$\bar{v}_2 = \left(\frac{\partial \bar{G}_i}{\partial P} \right)_{T,N} + \left(\frac{\partial \bar{G}_c}{\partial P} \right)_{T,N} - \frac{\partial RT}{\partial P} \ln(\lambda_{2,2}^3) \Big|_{T,N} + \frac{\partial}{\partial P} RT \ln(x_2/v_1) \Big|_{T,N} \quad (39)$$

therefore,
$$\bar{v}_2 = \bar{v}_i + \bar{v}_c + RT \left(-\frac{1}{V} \frac{dV}{dP} \right)_T \quad (40)$$

where the isothermal compressibility is defined as $B_T = -\frac{1}{V} \left(\frac{dV}{dP} \right)_T$;

substitution for this term yields

$$\bar{v}_2 = \bar{v}_i + \bar{v}_c + B_T RT \quad (41)$$

This equation clearly shows that the partial molar volume of the solute is both a function of the cavity formation and solute solvent interaction upon charging. Using equation (17), one can deduce quite readily the \bar{v}_i term, $\left(\frac{\partial \bar{G}_i}{\partial P} \right)_{T,N}$. Since \bar{G}_i is a function of the density or the partial molar volume of the solute in both terms of the equation, then

$$\bar{G}_i = \frac{1}{V} (\text{constants A} - \text{constants B}) \quad \text{and}$$

$$\bar{v}_i = \left(\frac{\partial \bar{G}_i}{\partial P} \right)_{T,N} = -\frac{1}{V^2} \left(\frac{dV}{dP} \right)_T (\text{const. A} - \text{const. B}) \quad (42)$$

Substitution for B_T yields for a system of hard spheres

$$\bar{v}_i = \left(\frac{\partial \bar{G}_i}{\partial P} \right)_{T,N} = B_T \bar{G}_i \quad (43)$$

The determination of \bar{v}_c involves the derivative of the more complex function \bar{G}_c . A good starting point is the simplified version of \bar{G}_c/RT

from equation (27) where \bar{G}_c is defined as

$$\bar{G}_c = RTA^2 \left\{ \frac{9}{2} \left[\frac{y}{(1-y)} \right]^2 + \frac{3y}{(1-y)} \right\} + \frac{3RTYA}{(1-y)} - RT \ln(1-y) + \frac{N\pi a_2^3}{6} \quad (44)$$

Hence

$$\begin{aligned} \bar{v}_c = \left(\frac{\partial \bar{G}_c}{\partial P} \right)_{T,N} &= \frac{9}{2} RT A^2 \left\{ 2 \left(\frac{y}{1-y} \right) \cdot \left[\frac{dy}{dP} \frac{1}{1-y} + \frac{y}{(1-y)^2} \frac{dy}{dP} \right] + \right. \\ &\quad \left. 3 \frac{dy}{dP} \frac{1}{(1-y)} + \frac{3y}{(1-y)^2} \frac{dy}{dP} \right\} + 3RTA \left[\frac{dy}{dP} \frac{1}{1-y} + \frac{y}{(1-y)^2} \frac{dy}{dP} \right] \\ &\quad + \frac{RT}{1-y} \frac{dy}{dP} + \frac{N\pi a_2^3}{6} \end{aligned} \quad (45)$$

Substituting for $\left(\frac{dy}{dP} \right)_T = y(B_T + 3Q_1)$ and introducing Q_1 as $\frac{1}{a_1} \frac{da_1}{dP}$, the solvent effective H.S. diameter pressure dependence, one obtains with suitable manipulation and collection of terms

$$\left(\frac{\partial \bar{G}_c}{\partial P} \right)_{T,N} = yRT(B_T + 3Q_1)(1-y)^{-3} \left\{ 6yA^2 + 3A^2 - 3Ay + (1-y)^2 \right\} + \frac{N\pi a_2^3}{6} \quad (46)$$

Finally,

$$\bar{v}_c = yRT(B_T^{H.S.} + 3Q_1)(1-y)^{-3} \left\{ 3A^2(1+2y) + 3A(1-y) + (1-y)^2 \right\} + \frac{N\pi a_2^3}{6} \quad (47)$$

The isothermal compressibility term is that for a system of hard spheres and as such must be derived from the Carnahan-Starling equation of state⁽¹¹⁾. Using equation (32) as a starting point and the definition of $B_T^{H.S.}$ one obtains

$$-v_{B_T}^{H.S.} = \frac{d}{dP} \left[\frac{RT}{P} \left(\frac{1+y+y^2+y^3}{(1-y)^3} \right) \right] \quad (48)$$

Then

$$\left(\frac{dV}{dP}\right)_T = -\frac{V}{P} + \frac{3V}{1-y} \frac{dy}{dP} + \frac{RT}{P} \left(\frac{1+2y-3y^2}{(1-y)^3}\right) \frac{dy}{dP} \quad (49)$$

Substituting $y(B_T + 3Q_1)$ for $\left(\frac{dy}{dP}\right)_T$ yields

$$-\frac{1}{V} \left(\frac{dV}{dP}\right)_T = \frac{1}{P} - \left(\frac{3y(B_T + 3Q_1)}{(1-y)}\right) - y(B_T + 3Q_1) \frac{(1+2y-3y^2)}{(1+y+y^2-y^3)} \quad (50)$$

Rearrangement yields

$$-\frac{1}{P} = -B_T + (B_T + 3Q_1) \left[\frac{-4y - 4y^2 + 2y^3}{1 - 2y^3 + y^4} \right] \quad (51)$$

$$-\frac{1}{P} = B_T \left(-1 + \left[\frac{-4y - 4y^2 + 2y^3}{1 - 2y^3 + y^4} \right] \right) + 3Q_1 \left[\frac{-4y - 4y^2 + 2y^3}{1 - 2y^3 + y^4} \right] \quad (52)$$

$$\frac{1}{P} + 3Q_1 \left[\frac{-4y - 4y^2 + 2y^3}{1 - 2y^3 + y^4} \right] = B_T \left(\frac{1 + 4y + 4y^2 - 4y^3 + y^4}{1 - 2y^3 + y^4} \right) \quad (53)$$

Finally, the isothermal compressibility is given by

$$B_T^{\text{H.S.}} = \frac{1}{P} \left(\frac{1 - 2y^3 + y^4}{1 + 4y + 4y^2 - 4y^3 + y^4} \right) - 3Q_1 \left(\frac{4y + 4y^2 - 2y^3}{1 + 4y + 4y^2 - 4y^3 + y^4} \right) \quad (54)$$

where one recognizes that the pressure P is now for a system of hard spheres and is calculated from equation (32). Typically for organic solvents the pressure required to maintain the system of hard spheres at a constant

temperature and volume resembling that of the real fluid system is 10^3 atm.

The partial molar volume of the solute for the dissolution process is given by

$$\bar{V}_2 = B_T \bar{G}_i + yRT(B_T + 3Q_1)(1-y)^{-3} \left\{ 3(1+2y)A^2 + 3(1-y)A + (1-y)^2 \right\} + \frac{N\pi a_2^3}{6} + B_T RT \quad (55)$$

One notes the similarity between the equations (47) for \bar{V}_c and equation (31) for \bar{H}_c . Substitution for the bracketed term in \bar{V}_c with the equivalence of that term in \bar{H}_c , yields for \bar{V}_2

$$\bar{V}_2 = B_T \bar{G}_i + \frac{1}{T} \cdot \left(\frac{B_T + 3Q_1}{\alpha_P - 3\ell_1} \right) \left(\bar{H}_c + \frac{N\pi P a_2^3}{6} (3T\ell_2 - 1) \right) + B_T RT + \frac{N\pi a_2^3}{6} \quad (56)$$

Using the original concept of the Scaled Particle Theory, as presented by Reiss.etal. (5), the thermodynamic equations for the dissolution process and the corresponding hard sphere parameters were derived incorporating an equation of state for a system of hard spheres. Using these equations the Pierotti S.P.T. will be examined and a pure hard sphere theory will be presented and considered as an alternate method for the calculation of the thermodynamic properties for the dissolution process.

The dissolution process of a gas into a solvent is now considered as a four step process: (1) the gas solute is discharged to that of a hard sphere with no attractive potential; (2) a hard sphere cavity is then made in the solvent of suitable size to accommodate the solute; (3) the hard sphere solute is placed in the cavity at a constant pressure and temperature; and (4) the solute is then recharged, thus allowing solute-solvent interactions. The thermodynamic steps considered in this model are the reversible work in creating a cavity in a real fluid as given by the S.P.T. \bar{G}_c term. The second is the solute-solvent interaction in the recharging process; this can be written in terms of some potential of interaction and the radial distribution function of the solvent and expressed as \bar{G}_1 .

In this section four cases of the above model for the dissolution of a gas in a liquid will be considered. For Case I, only the solute has been discharged to that of a hard sphere and the solvent always retains its normal potential of interaction, even so the solute-solvent interaction in forming the cavity is still that of a pair of hard spheres. A consequence of letting the solvent retain its real potential of interaction is that the α_p and B_T values are those of the real solvent and a temperature dependence on the solvent effective hard sphere diameter must be incorporated. Case II is as above, but excluding the temperature dependence on the solvent and solute effective hard sphere diameters, as was assumed in the original model used by Pierotti.

For case III not only is the solute discharged to that of a hard sphere, but so is the solvent. A consequence of this is that one must use pressures calculated from an equation of state for a system of hard

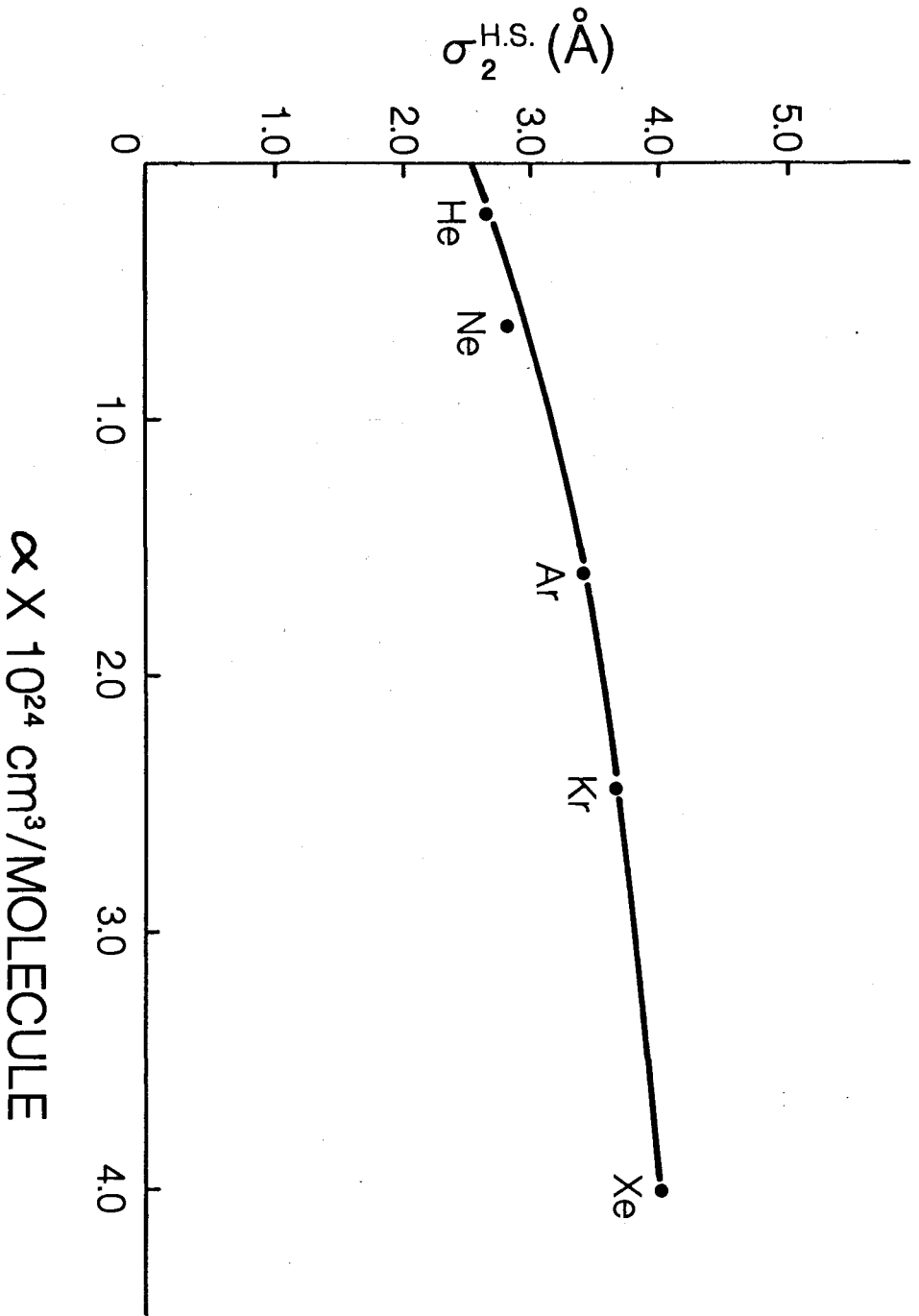
spheres (typically 10^3 atm. for organic solvents) to maintain the system at the volume and temperature of the real system. Hence, the α_p and B_T values will now be those values calculated from an equation of state for a system of hard spheres. In this particular case the temperature dependence of the effective hard sphere diameter of the solvent and solute will be included. Finally, in Case IV, both the solvent and solute temperature dependence of the effective hard sphere diameter will be excluded. Hence, Case IV is the hard sphere equivalence of the original Pierotti Theory.

For the inert gases dissolved in a given solvent, one is able to plot any solubility thermodynamic property as a function of the gas polarizability and obtain a smooth curve. Extrapolation of this curve to zero polarizability yields the value of that thermodynamic property for an inert gas type hard sphere dissolved in that particular solvent. Figure 1 is a plot of the effective hard sphere diameter of the inert gases versus their respective polarizabilities. A smooth extrapolation yields a value of 2.55 \AA for the effective hard sphere diameter of the inert gas type hard sphere having no attraction potential, $E_2/K=0$, which defines the solute hard sphere limiting case.

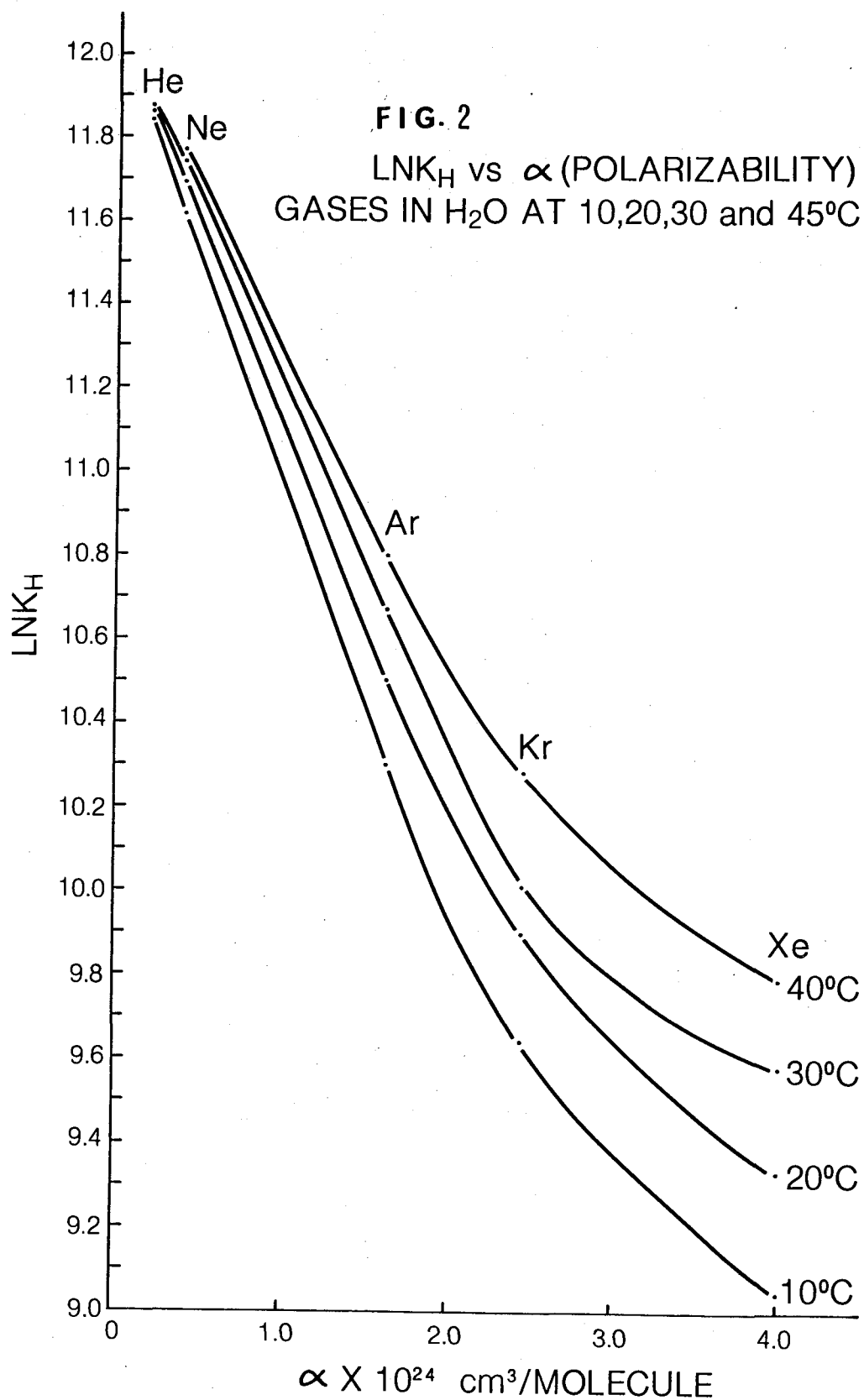
If a similar plot of the Henry's law constant (for the inert gases in a given solvent) against the solute polarizability is extrapolated to zero polarizability, one obtains a value for the Henry's law constant $\ln K_H^0$ of the hard sphere gas ($a_1=2.55 \text{ \AA}$, $E/K=0$) in that solvent. The extrapolated $\ln K_H^0$ value can be equated to equation (5) to obtain

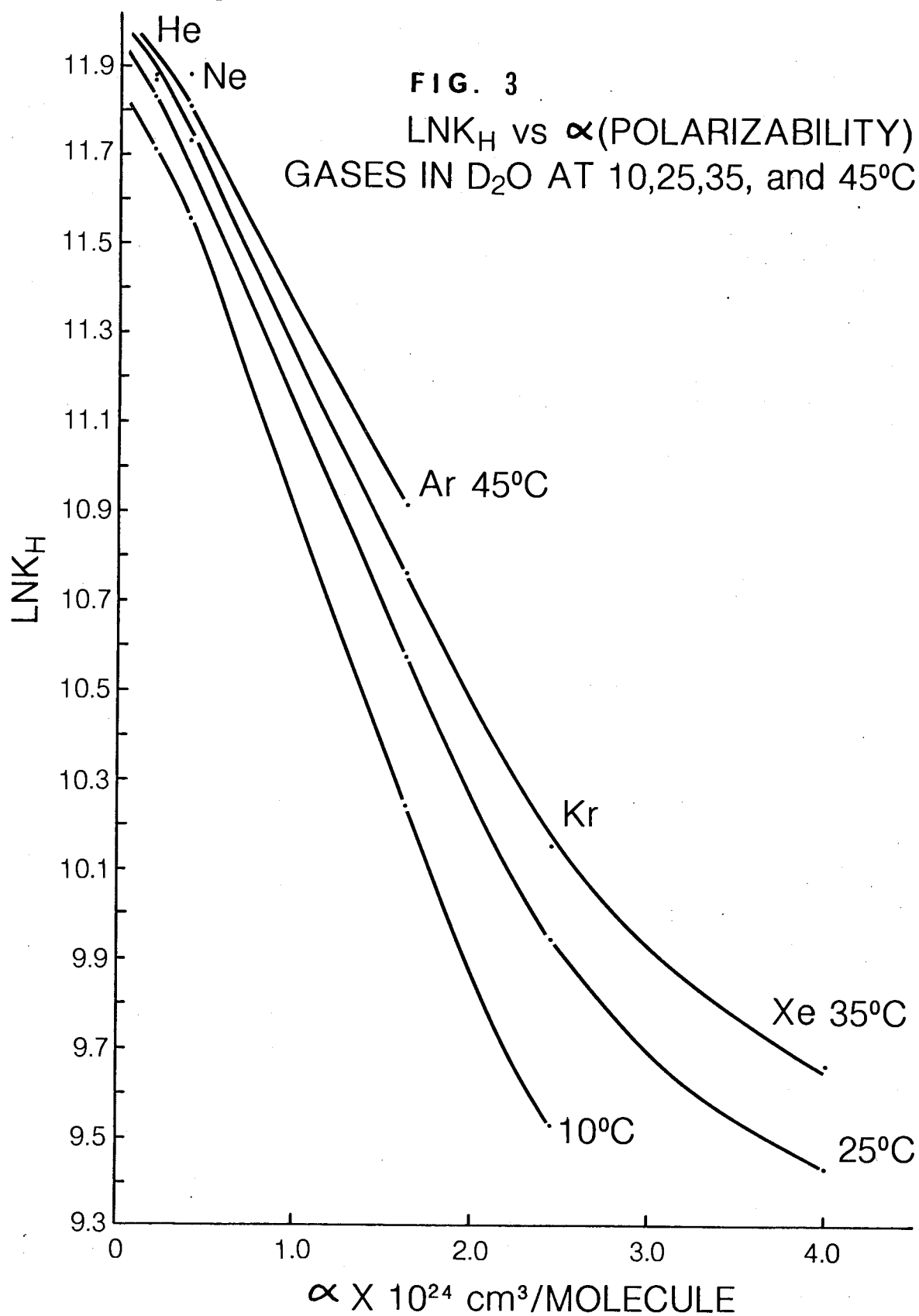
$$\lim_{\alpha \rightarrow 0} \ln K_H = \ln K_H^0 = \bar{G}_c / RT + \ln (RT/V) \quad (57)$$

FIG. 1
INERT GASES
HARDSPHERE DIAMETER (\AA) vs POLARIZABILITY (cm^3/molec)



One notes that \bar{G}_1 becomes zero when $\alpha \approx 0$. This is easily seen since the inductive constant C_{ind} , which is a function of the solute polarizability becomes zero. Also, since the attractive well depth potential for a hard sphere is zero ($E_2/K = 0$), then the dispersive constant C_{dis} is zero. This hard sphere limit value of $\ln K_H$ was originally used by Pierotti to establish the effective hard sphere diameter value for various solvents at 298.15 °K. This concept was later used by Wilhelm⁽¹⁰⁾ at other temperatures, thus establishing a finite temperature dependence for the effective hard sphere diameter of a wide range of solvents. Since the interaction term is zero for a hard sphere, one simply equates equation(57) to the extrapolated $\ln K_H^0$ values obtained for the inert gases in a given solvent over a temperature range, and solves for a_1 at the various temperatures (incorporating the equation for \bar{G}_c). Using our data we illustrate in Figures 2 and 3 for H₂O and D₂O the method of graphical extrapolation to obtain $\ln K_H^0$ values over a temperature range. For these graphs my experimental solubility data was supplemented with Helium and Neon solubility data from Battino⁽¹⁶⁾ in H₂O and Abrosimov⁽¹⁷⁾ in D₂O. The curves were fitted using a cubic polynomial, Table I gives the coefficients.





Coefficients in the equation $\ln K_H = A + B\alpha + C\alpha^2 + D\alpha^3$

T ⁰ _K	H ₂ O				
	A	BX10 ⁻²⁴	CX10 ⁻⁴⁶	DX10 ⁻⁷⁰	σ%(1)
283.15	12.0857	-1.2291	6.889	1.007	.01
293.15	12.0698	-0.9764	-2.767	2.542	-.04
303.15	12.0679	-0.8679	-3.732	2.485	-.11
313.15	12.0319	-0.6917	-8.0515	2.820	-.13

T ⁰ _K	D ₂ O				
	A	BX10 ⁻²⁴	CX10 ⁻⁴⁶	DX10 ⁻⁷⁰	σ%(1)
283.15	12.1084	-1.5184	30.49	4.63	.01
298.15	12.0157	-0.7563	-13.94	4.17	-.06
308.25	11.944	-0.2179	-45.80	9.24	.10

(1) Percentage standard deviation from experimental $\ln K_H$ values for helium.

Setting the polarizability to zero in the cubic polynomial for $\ln K_H$ yields the $\ln K_H^0$ values at a given temperature. Hence

$$\lim_{\alpha \rightarrow 0} A + B\alpha + C\alpha^2 + D\alpha^3 = A = \ln K_H^0 \quad (58)$$

Substituting the $\ln K_H^0$ values in equation (57) one obtains

$$\ln K_H^0 = A^2 \left[\frac{9}{2} \left[\frac{y}{(1-y)} \right]^2 + 3y/(1-y) \right] + 3yA/(1-y)$$

$$-\ln(1-y) + \frac{N\pi Pa_2^3}{6RT} + \ln(RT/V) \quad (59)$$

Recognizing for the Pierotti treatment that $P = 1$ atm and using $a_2 = 2.55 \text{ \AA}$, one is able to solve this equation for a_1 , the solvent effective hard sphere diameter of the solvent.

Table II summarizes the extrapolated $\ln K_H^0$ values for a hard sphere solute of 2.55 \AA , and the respective hard sphere diameters obtained from solving equation (59) for H_2O and D_2O .

Table II

Solvent Effective Hard Sphere Diameters

T ^o K	H ₂ O		D ₂ O	
	lnK _H ^o	a ₁ (Å)	lnK _H ^o	a ₁ (Å)
283.15	12.086	2.785	12.108	2.795
293.15	12.070	2.781	-----	-----
298.15	-----	-----	12.016	2.777
303.15	12.067	2.779	-----	-----
308.15	-----	-----	11.944	2.766
313.15	12.032	2.775	-----	-----

Using this data one obtains a ℓ_1 -value ($\ell_1 = 1/a_1 da_1/dT$) of $-.12 \times 10^{-3} \text{ } ^\circ K^{-1}$ for H_2O and $-.42 \times 10^{-3} \text{ } ^\circ K^{-1}$ for D_2O .

It is difficult to make a quantitative assessment of all the possible sources of error involved with the determination of ℓ -values. Wilhelm estimated the error to be $\pm 30\%$ using the graphical extrapolation method⁽¹⁰⁾. The ℓ -value obtained for H_2O is in good agreement

with that reported by Wilhelm⁽¹⁰⁾ of $-.08 \times 10^{-3} \text{ }^\circ\text{K}^{-1}$. The ℓ -value obtained for D_2O appears unusually high with respect to water and other solvents. This is directly attributable to the $\ln K_{\text{H}}$ values of Helium and Neon suggesting that the data of Abrosimov (Ref. 17) is unreliable. As can be seen from Figure 3, these values deviate considerably from the smooth curve which is expected when compared to the H_2O curves. It is interesting to note, however, that this method of extrapolation yields an effective hard sphere diameter for both H_2O and D_2O of 2.78 \AA at $298.15 \text{ }^\circ\text{K}$, which is the average value used by most workers.

If one plots the enthalpies of solution for the inert gases in a given solvent versus the gases' polarizability and extrapolates to the hard sphere limit, one obtains ΔH° for a hard sphere in that solvent. Equating these hard sphere enthalpies and recognizing that the \bar{H}_1 term in equation 6 is zero, one obtains

$$\lim_{\alpha \rightarrow 0} \Delta H = \bar{H}_c - RT + \alpha_p RT^2 \quad (60)$$

where \bar{H}_c is defined in equation (31). Since y is a function of a_1 , which has previously been obtained from the $\ln K_{\text{H}}^\circ$ values, equation (60) can be solved for ℓ_1 at the hard sphere limit. The ℓ -value obtained with the ΔH° extrapolation can be compared to the ℓ -value obtained from the $\ln K_{\text{H}}^\circ$ values, thus producing a self consistent check for ℓ_1 . Using the original concept of the scaled particle theory as in Case I, $\alpha_p^{\text{H.S.}}$ in equation (30) is replaced by the experimental value of α_p for a given solvent, and leaving ℓ_1 as an undetermined variable, equation (60) can be solved to obtain the temperature dependence $1/a \text{ da/dT}$ of the solvent effective hard

sphere diameter. The following table compares for selected solvents the λ_1 values obtained by $\ln K_H^\circ$ and ΔH° extrapolations.

Table III

Extrapolated Solvent Diameter Temperature Dependence

	ΔH° (cal Mol ⁻¹) exp. extrap.	ΔH° (cal Mol ⁻¹) eqn.(60) $\lambda_1=0$	$\lambda_1 \times 10^3$ °K ⁻¹ eqn.(60)	$\lambda_1 \times 10^3$ °K ⁻¹ eqn.(59)
H ₂ O	275	-90	-.08	-.08
C ₆ H ₆	2750	1929	-.15	-.16
C-C ₆ H ₁₂	2550	1807	-.14	-.13
n-C ₆ H ₁₄	2250	1446	-.19	-.13

Included in the above table are the ΔH° values obtained from equation (60) with λ_1 having a value of zero as in the case of the original Pierotti formulation, it is seen that these values are nowhere near the values obtained from the experimental extrapolations. One is amazed at the remarkable agreement between the temperature dependence of the solvent effective hard sphere diameter obtained from the ΔH° and $\ln K_H^\circ$ extrapolations. Whilst there was never any doubt as to the temperature dependence, this points out unambiguously that the original Pierotti formulation should in fact contain a term reflecting the temperature dependence of the solvent effective hard sphere diameter.

An extrapolation of a plot of the entropy of solution for the inert gases in given solvent against the gases' respective polarizability to the hard sphere limit will yield ΔS° values. The values so obtained can be compared to the theoretical entropy given by

$$\Delta S = \frac{\Delta H - \Delta G}{T} = (\Delta S^\circ \text{ for a solute of } 2.55 \text{ \AA}) \quad (61)$$

The method of obtaining ΔS° from equation (61) is rather fortuitous since from the assumptions in the theory itself one is not required to deliberately set the \bar{H}_i and \bar{G}_i terms equal to zero. The enthalpy of solution ΔH is given by equation (6) and the Gibbs free energy of solution ΔG is given by

$$\Delta G = RT \ln K_H = \bar{G}_c + \bar{G}_i + RT \ln (RT/V_1) \quad (62)$$

Hence the entropy of solution is

$$\Delta S = \frac{\bar{H}_i + \bar{H}_c - RT + \alpha_P RT^2 - \bar{G}_c - \bar{G}_i + RT \ln(RT/v_1)}{T} \quad (63)$$

So, using our previous assumption that $\bar{H}_i = \bar{G}_i$, then

$$\Delta S = \frac{\bar{H}_c - RT + \alpha_P RT^2 - \bar{G}_c + RT \ln (RT/V_1)}{T} = \Delta S^\circ \quad (64)$$

Hence

$$\Delta S^\circ = \frac{\Delta H^\circ - RT \ln K_H^\circ}{T} \quad (65)$$

which is identical to equation (61). The ΔS° values obtained from equation (65), when compared to the hard sphere extrapolated values, provide a good self consistent check for both the ℓ_1 and a_1 values used for calculations of the thermodynamic properties of the dissolution process. The following table gives a summary of extrapolated thermodynamic data using the hard sphere solute as the limiting case

Table IV

Extrapolated Thermodynamic Hard Sphere Data at 298.15 °K

SOLVENT	ΔS°	ΔS°	ΔH°	$\ln K_H^\circ$
	(cal Mol ⁻¹ °K ⁻¹) Experimental	(cal Mol ⁻¹ °K ⁻¹) Eqn. (65), Case I	(cal Mol ⁻¹ °K ⁻¹) Experimental	Eqn.(59)
C ₆ H ₆	-10.25	-10.22	2750	9.84
n-C ₆ H ₁₄	- 9.49	- 9.50	2250	---
n-C ₇ H ₁₆	- 9.9	- 9.9	2250	7.44
C-C ₆ H ₁₂	- 9.1	-10.1	2550	8.56
H ₂ O	-23.0	-23.33	275	12.07

The S.P.T., although severely criticised, yields remarkably good Henry's law constants for both organic solvents and water. This is rather unexpected since this theory treats H₂O like any other solvent and does not take into account any fundamental differences (such as those due to H-bonding). The hard sphere equations derived in the theory section above (taking into account temperature and pressure derivatives of the solvent effective diameters) will now be shown equivalent to the equations obtained by Pierotti.

The Henry's law constant for the dissolution process can be calculated via equation (5) with the \bar{G}_1 term given by equation (17). The free energy cavity formation \bar{G}_c was shown to be

$$\bar{G}_c/RT = A^2 \{9/2[y/(1-y)]^2 + 3y/(1-y)\} + 3yA/(1-y) - \ln(1-y) + \frac{N\pi Pa_2^3}{6RT} \quad (27)$$

For Case I and II, where $P = 1$ atm., the last term in the expression is negligible ($\approx 5 \times 10^{-4}$ for a typical gas, Argon, at 298 °K). In calculating the enthalpy of solution, ΔH , equation (31) describes the contribution due to cavity formation as

$$\bar{H}_c = yRT^2(\alpha_P^{\text{H.S.}} - 3\ell_1)(1-y)^{-3}\{3(1+2y)A^2 + 3(1-y)A + (1-y)^2\} - \frac{N\pi Pa_2^3}{6}(3T\ell_2 - 1) \quad (31)$$

Again for Case I and II, the last term is small ($\approx .3$ cal mol⁻¹ for argon at 298 °K) and may be assumed negligible. In order to obtain the expression for \bar{H}_c given by Pierotti, it is necessary to replace α_P hard sphere by the experimental value of α_P . We will write \bar{H}_c as

$$\bar{H}_c = yRT^2(\alpha_P^{\text{EXP}} - 3\ell_1)(1-y)^{-3}\{3(1+2y)A^2 + 3(1-y)A + (1-y)^2\} \quad (66)$$

and regard the original Pierotti formulation of \bar{H}_c to be that case for which $\ell_1=0$ (though, as we have shown above, this is a poor approximation).

The partial molar volume for the dissolved solute is derived in equation (56) using hard sphere diameter temperature and pressure derivatives. For Case I, replacing hard sphere α_P and B_T values with experimental values, \bar{V}_2 at 1 atm. reduces to

$$\bar{V}_2 = B_T \bar{G}_1 + \frac{1}{T} \left(\frac{B_T + 3Q_1}{\alpha_P - 3\ell_1} \right) (\bar{H}_c) + B_T RT + \frac{N\pi a_2^3}{6} \quad (67)$$

where Q_1 was previously introduced as the pressure dependence on the effective hard sphere diameter $Q_1 = 1/a_1 \left(da_1/dP \right)_T$ and has been estimated to be of the order 10^{-4} atm^{-1} , an order of magnitude less than the ℓ_1 -values⁽¹⁸⁾.

In order to assist in the computations of the thermodynamic properties for the dissolution process, a PLI program labeled 'Hard Sphere' (see Appendix I) was developed incorporating all the required equations for Cases I and III where Cases II and IV are obtained by setting $\ell_1 = \ell_2 = 0$. Computer calculations for the systems: inert gases O_2 , N_2 , CH_4 and SF_6 in H_2O , D_2O , C_6H_6 , CCl_4 , $n-C_7H_{16}$, $C-C_6H_{12}$, and $n-C_6H_{14}$ over the temperature range 273.15 °K to 323.15 °K, were carried out to find the thermodynamic properties for the dissolution process. Tables V and VI summarize all solute and solvent parameters at 298.15 °K required for the calculations. For convenience, only the 298.15 °K values are given for α_P , B_T and densities with the appropriate references containing other temperature values.

Table V

Properties of the solutes at 298.15 °K

Gas	H.S.Diameter ^(b)	Polarizability ^(b)	L-J Force Const. ^(a)
	$\sigma_2 \times 10^8$ (cm)	$\alpha \times 10^{24}$ (cm ³ /molecule)	E_2/K (°K)
Hard Sphere	2.55	0	0
He	2.63	.204	6.03
Ne	2.78	.393	34.9
Ar	3.40	1.63	122
Kr	3.60	2.46	171 ^(b)
Xe	4.06 ^(c)	4.00	221 ^(b)
N ₂	3.70	1.74	95
O ₂	3.46	1.57	118
CH ₄	3.70 ^(c)	2.70	157
SF ₆	5.51 ^(c)	4.48	201

(a) Ref. 19, (b) Ref. 7, (c) Ref. 20

The following tables present thermodynamic data at 298.15 °K for the dissolution process incorporating the temperature dependence Case I ($Q_1 = 1/a_1 da_1/dT$) of the solvents as previously determined at the hard sphere limit.

Table VI

Properties of the Solvents at 298.15 °K

Solvents	$\sigma_1 \times 10^8$ (cm)	U_2 (D)	E_1/K (e) (°K)	$da_1/dT \times 10^{11}$ (g) (cm/°K)	$\lambda_1 \times 10^3$ (g) (°K ⁻¹)	$B_T \times 10^4$ (atm ⁻¹)	$\alpha_p \times 10^3$ (°K ⁻¹)	D (gm/cm ³)
H ₂ O	2.76(e)	1.84(b)	85.3(b)	-.22	-.08	.4583(h)	.257(h)	.997075(h)
C ₆ H ₆	5.26(d)	0	531	-.84	-.16	.9808(h)	1.235(l)	.8738(i)
n-C ₇ H ₁₆	6.25(d)	0	573	-.81	-.13	1.443(h)	1.247(r)	.6796(r)
CCl ₄	5.37(a)	0	536	-.75(d)	-.14(d)	1.081(r)	1.231(r)	1.5842(r)
C-C ₆ H ₁₂	5.65(d)	0	589	-.73	-.13	1.125(h)	1.21(r)	.7738(i)
n-C ₆ H ₁₄	5.92	0	517	-.77	-.13	1.627(h)	1.30(r)	.6550(i)
D ₂ O	2.76(e)	1.84	85.3*	-.22*	-.08*	.4709(f)	.1918(c)	1.10445(h)

* Properties assumed to be identical to those of H₂O

(a) Ref. 7, (b) Ref. 8, (c) Ref. 21, (d) Ref. 22, (e) Ref. average values, (f) Ref. 23, (g) Ref. 10,
(h) Ref. 24,25, (i) Ref. 26, (l) Ref. 27, (r) Ref. 9

Table VII

H₂O Case I

$$\epsilon_1 = -.08 \times 10^{-3} \text{ } ^\circ\text{K}^{-1}$$

GAS	ΔH	ΔH	$\ln K_H$	$\ln K_H$
	(cal Mol ⁻¹)	(cal Mol ⁻¹)		
	Calc.	Exp.	Calc.	Exp.
Hard Sphere	284	---	---	---
He	-56	-182	11.64	11.82
Ne	-554	-896	11.10	11.72
Ar	-1764	-2933	10.44	10.59
Kr	-2432	-3752	9.80	10.01
Xe	-3402	-4402	9.39	9.46
O ₂	-1726	-2882	10.65	10.68
N ₂	-1562	-2495	11.53	11.35
CH ₄	-2395	-3297	10.12	10.59
SF ₆	-4618	-4777	11.95	12.35

(a) Reference 16

Table VIII

 C_6H_6 Case I

$$\rho_1 = -.15 \times 10^{-3} \text{ } ^\circ K^{-1}$$

GAS	ΔH	ΔH	$\ln K_H$ Calc.	$\ln K_H$ ^(a) Exp.
	(cal Mol ⁻¹) Calc.	(cal Mol ⁻¹) Exp.		
Hard Sphere	2768	----	----	----
He	2400	2396	9.08	9.47
Ne	1889	1984	8.05	9.09
Ar	1465	297	6.57	7.03
Kr	1119	-431	5.71	5.90
Xe	1048	-1695	4.89	4.45
O ₂	1595	409	6.71	7.11
N ₂	2265	1016	7.50	7.71
CH ₄	1404	-305	6.05	6.18
SF ₆	3177	-778	5.73	5.94

(a) Reference 16

Table IX

c-C₆H₁₂ Case I

$$\epsilon_1 = -.14 \times 10^{-3} \text{ } ^\circ\text{K}^{-1}$$

GAS	ΔH	ΔH	$\ln K_H$	$\ln K_H$
	(cal Mol ⁻¹)	(cal Mol ⁻¹)		
	Calc.	Exp.	Calc.	Exp.
Hard Sphere	2566	---	----	----
He	2186	2421	8.69	9.01
Ne	1655	1461	7.65	8.63
Ar	1161	-218	6.13	6.52
Kr	798	-831	5.27	5.37
Xe	684	---	----	----
O ₂	1282	58	6.26	6.69
N ₂	1915	511	7.03	7.18
CH ₄	1068	---	----	----
SF ₆	2620	-1377	5.23	5.22

$$n\text{-C}_6\text{H}_{14} \text{ Case I}$$

$$\ell_1 = -.19 \times 10^{-3} \text{ }^\circ\text{K}^{-1}$$

GAS	ΔH (cal Mol ⁻¹)	ΔH (cal Mol ⁻¹)	$\ln K_H$	
			Calc.	Exp.
Hard Sphere	2238	-----	-----	-----
He	1913	1920	7.94	8.25
Ne	1461	1348	7.04	7.90
Ar	1052	-646	5.69	5.99
Kr	751	-1130	4.94	4.97
Xe	672	-2556	4.21	3.65
O ₂	1157	-----	-----	-----
N ₂	1698	-----	-----	-----
CH ₄	983	-539	5.21	5.29
SF ₆	2366	-----	-----	-----

One can see from the above tables that the theory predicts quite well the Henry's law constants and relatively poor agreement is obtained for the enthalpies of solution as one deviates further from the inert gas type hard sphere. As previously shown, the entropies of solution provide a good self consistency check for the ℓ_1 -values. The following tables compare calculated entropies for the dissolution process of the inert gases in selected solvents at 298.15 °K.

Table XI

 $\Delta S(\text{cal Mole}^{-1} \text{ } ^\circ\text{K}^{-1})_{\text{H}_2\text{O}}$ Case I

$$\ell_1 = -.08 \times 10^{-3} \text{ } ^\circ\text{K}^{-1}$$

	Calc. Eqn.(65)	Exp.
Hard Sphere	-23.15	----
He	-23.31	-24.2
Ne	-23.92	-26.29
Ar	-26.66	-30.88
Kr	-27.64	-32.48
Xe	-30.06	-33.57

Table XII

 $\Delta S(\text{cal Mole}^{-1} \text{ } ^\circ\text{K}^{-1})_{\text{C}_6\text{H}_6}$ Case I

$$\ell_1 = -.15 \times 10^{-3} \text{ } ^\circ\text{K}^{-1}$$

	Calc. Eqn.(65)	Exp.
Hard Sphere	-10.14	----
He	- 9.98	-10.79
Ne	- 9.66	-11.42
Ar	- 8.14	-12.98
Kr	- 7.59	-13.17
Xe	- 6.20	-14.53

Table XIII

$\Delta S(\text{cal Mole}^{-1} \text{ } ^\circ\text{K}^{-1})$ c-C ₆ H ₁₂ Case I		
$\epsilon_1 = -.14 \times 10^{-3} \text{ } ^\circ\text{K}^{-1}$		
Hard Sphere	Calc. Eqn. (65)	Exp.
	-10.09	----
He	- 9.94	- 9.79
Ne	- 9.65	-12.24
Ar	- 8.29	-13.68
Kr	- 7.79	-13.45
Xe	- 6.53	-14.76

Table XIV

$\Delta S(\text{cal Mole}^{-1} \text{ } ^\circ\text{K}^{-1})$ n-C ₆ H ₁₄ Case I		
$\epsilon_1 = -.19 \times 10^{-3} \text{ } ^\circ\text{K}^{-1}$		
Hard Sphere	Calc. Eqn. (65)	Exp.
	-9.50	----
He	-9.36	- 9.96
Ne	-9.08	-11.18
Ar	-7.78	-14.06
Kr	-7.30	-13.66
Xe	-6.11	-15.84

From the above tables it is clear that the entropies are predicted relatively well for H₂O, whilst the organic solvent entropies are generally low and also decrease in value while the experimental values increase.

It is interesting to note that the hard sphere entropies calculated from equation (65) are in good agreement with the hard sphere (extrapolated)

limit of the experimental entropy values, which again supports the concept of a temperature dependent hard sphere diameter. 75

In light of the rather poor agreement obtained for the enthalpies and entropies of solution, these thermodynamic properties were recalculated excluding the temperature dependence of the effective hard sphere diameters. The following tables summarize these results for the inert gases in the same solvents for Case II.

Table XV

H₂O Case II

	ΔH (cal Mol ⁻¹) Eqn. (6)	ΔH (cal Mol ⁻¹) Exp.	ΔS (cal Mol ⁻¹ °K ⁻¹) Eqn. (61)
Hard Sphere	- 90	----	-24.58
He	-486	- 182	-24.78
Ne	-1026	- 896	-25.49
Ar	-2424	-2933	-28.88
Kr	-3160	-3752	-30.09
Xe	-4299	-4402	-33.07

Table XVI

C₆H₆ Case II

	ΔH (cal Mol ⁻¹) Eqn. (6)	ΔH (cal Mol ⁻¹) Exp.	ΔS (cal Mol ⁻¹ °K ⁻¹) Eqn. (61)
Hard Sphere	1929	----	-13.00
He	1521	2396	-12.94
Ne	931	1984	-12.87
Ar	149	297	-12.55
Kr	- 325	-431	-12.43
Xe	- 716	-1695	-12.11

Table XVII

	c-C ₆ H ₁₂ Case II		
	ΔH	ΔH	ΔS
	(cal Mol ⁻¹) Eqn. (6)	(cal Mol ⁻¹) Exp.	Eqn. (61)
Hard Sphere	1807	----	-12.64
He	1391	2421	-12.60
Ne	791	1461	-12.55
Ar	- 22	-218	-12.26
Kr	-499	-831	-12.14
Xe	-897	----	-11.83

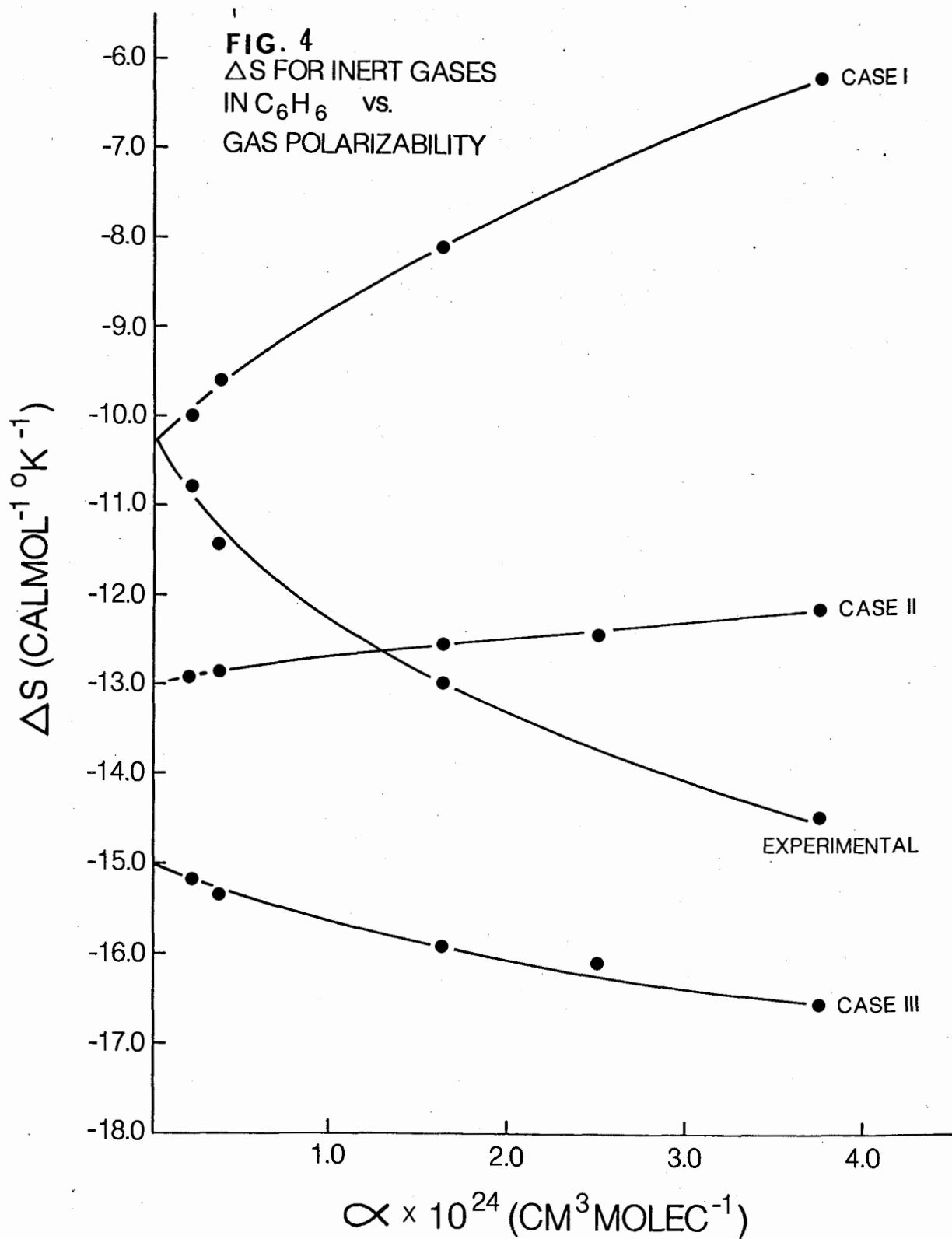
(a) Ref. 7, (b) Ref. 19, (c) Ref. 35, (d) Ref. 36

Table XVIII

	n-C ₆ H ₁₄ Case II		
	ΔH	ΔH	ΔS
	(cal Mol ⁻¹) Eqn. (6)	(cal Mol ⁻¹) Exp.	Eqn. (61)
Hard Sphere	1446	----	-12.16
He	1084	1920	-12.14
Ne	563	1348	-12.09
Ar	- 166	- 646	-11.86
Kr	- 581	-1130	-11.76
Xe	- 944	-2556	-11.53

One can see from the above Tables that, for Case II (excluding a temperature dependence on the solvent effective H.S. diameter), the predicted enthalpies of solution for the organic solvents are generally poor when compared to the appropriate experimental enthalpies. It is not surprising, however, to see good agreement between the predicted and experimental enthalpies for H₂O using this Pierotti formulation. In this formulation the Lennard Jones force constant E_1/K for H₂O was obtained by equating the experimental $\ln K_H$ values for the inert gases to the expression containing \bar{G}_i and solving for the variable parameter E_1/K . Since $\bar{G}_i = \bar{H}_i$ and \bar{H}_i is the dominant term in the enthalpy expression (one notes for He and Ne the $-RT$ term cancels the \bar{H}_c term, leaving \bar{H}_i as the dominant term), one expects good agreement for the predicted enthalpies. For Argon and Krypton the \bar{H}_c values are 707 cal Mole⁻¹ and 797 cal Mole⁻¹ respectively, while the respective \bar{H}_i values are -2585 cal Mole⁻¹ and -3394 cal Mole⁻¹.

Upon examination of the entropies, one observes all the calculated organic entropies to be generally low and have decreasing values from Helium to Xenon, whilst the experimental values actually increase. Figure 4 is a plot of the calculated entropies for Cases I, II and III and the experimental entropies of the noble gases in Benzene solvent versus the gas polarizability. It is clear from this graph that the remarkable difference in the calculated entropies observed for cases I and II is directly attributable to the solvent effective H.S. diameter temperature dependence. One notes, however, that inclusion of an ℓ -value (Case I) enables the calculated entropy to have the same hard sphere limiting case interception point as was obtained with the experimental entropy values.



At this point it is interesting to compare Case I and II with the pure hard sphere treatment which incorporates pure hard sphere pressures and α_P and B_T values calculated from the Carnahan Starling equation of state. Table XIX summarizes the pure hard sphere thermodynamic parameters used in the calculations.

Table XIX

Hard Sphere Properties at 298.15 °K

	H ₂ O	C ₆ H ₆	c-C ₆ H ₁₂	n-C ₆ H ₁₄
$P \times 10^{-3} (\text{atm})$	7.841	3.887	3.426	2.368
$\alpha_P \times 10^3 (^\circ\text{K}^{-1})$ $l=0$	1.085	.737	.717	.770
$\alpha_P \times 10^3 (^\circ\text{K}^{-1})$ $l=l_1$.923	.386	.387	.332
$B_T \times 10^4 (\text{atm}^{-1})$ $l=0$.413	.564	.624	.968
$B_T \times 10^4 (\text{atm}^{-1})$ $l=l_1$.413	.564	.624	.968

Tables XX to XXIV compare the hard sphere treatment using the appropriate calculated values from the equation of state for cases III and IV for the inert gases in H₂O, C₆H₆, C-C₆H₁₂, and n-C₆H₁₄ for the dissolution process at 298.15 °K.

H₂O Case III and IV

	ΔH (cal Mol ⁻¹) $\ell = -.08 \times 10^{-3} \text{ } ^\circ\text{K}^{-1}$	ΔH (cal Mol ⁻¹) $\ell = 0$	ΔS (cal Mol ⁻¹ $^\circ\text{K}^{-1}$) $\ell = -.08 \times 10^{-3} \text{ } ^\circ\text{K}^{-1}$	ΔS (cal Mol ⁻¹ $^\circ\text{K}^{-1}$) $\ell = 0$	$\ln K_H$
He	2429	2088	-18.64	-19.78	13.48
Ne	2263	1885	-18.78	-20.05	13.27
Ar	2756	2206	-19.39	-21.23	14.41
Kr	2757	2144	-19.60	-21.66	14.52
Xe	3572	2802	-20.11	-22.69	16.15

Table XXI

C₆H₆ Case III and IV

	ΔH (cal Mol ⁻¹) $\ell = -.15 \times 10^{-3} \text{ } ^\circ\text{K}^{-1}$	ΔH (cal Mol ⁻¹) $\ell = 0$	ΔS (cal Mol ⁻¹ $^\circ\text{K}^{-1}$) $\ell = -.15 \times 10^{-3} \text{ } ^\circ\text{K}^{-1}$	ΔS (cal Mol ⁻¹ $^\circ\text{K}^{-1}$) $\ell = 0$	$\ln K_H$
He	1382	1088	-15.21	-16.20	9.99
Ne	833	511	-15.35	-16.43	9.13
Ar	319	-138	-15.92	-17.45	8.55
Kr	- 31	-536	-16.10	-17.79	8.05
Xe	- 50	-677	-16.56	-18.66	8.25

Table XXII

c-C₆H₁₂ Case III and IV

	ΔH (cal Mol ⁻¹) $\ell = -.14 \times 10^{-3} \text{ } ^\circ\text{K}^{-1}$	ΔH (cal Mol ⁻¹) $\ell = 0$	ΔS (cal Mol ⁻¹ °K ⁻¹) $\ell = -.14 \times 10^{-3} \text{ } ^\circ\text{K}^{-1}$	ΔS (cal Mol ⁻¹ °K ⁻¹) $\ell = 0$	$\ln K_H$
He	1192	934	-14.88	-15.74	9.50
Ne	622	339	-15.00	-15.95	8.60
Ar	18	-382	-15.58	-16.91	7.87
Kr	-358	-801	-15.77	-17.25	7.33
Xe	-454	-1002	-16.23	-18.06	7.40

Table XXIII

n-C₆H₁₄ Case III and IV

	ΔH (cal Mol ⁻¹) $\ell = -.19 \times 10^{-3} \text{ } ^\circ\text{K}^{-1}$	ΔH (cal Mol ⁻¹) $\ell = 0$	ΔS (cal Mol ⁻¹ °K ⁻¹) $\ell = -.19 \times 10^{-3} \text{ } ^\circ\text{K}^{-1}$	ΔS (cal Mol ⁻¹ °K ⁻¹) $\ell = 0$	$\ln K_H$
He	896	644	-13.86	-14.71	8.49
Ne	393	118	-13.96	-14.88	7.69
Ar	-203	-585	-14.37	-15.65	6.89
Kr	-552	-973	-14.51	-15.92	6.37
Xe	-715	-1231	-14.84	-16.57	6.26

Examination of the enthalpies for the dissolution process using the hard sphere theory reveals that the expected trend, when compared to experimental values, exists. For organic solvents, although the enthalpies are generally low, the values decrease from Helium to Xenon, which is the experimental trend. The effect of including a solvent effective hard sphere diameter temperature dependence for the pure hard sphere theory is not as pronounced. One notes that the enthalpies for H_2O are predicted all positive, which is due in part to the large pressure term in \bar{H}_c . Subsequently with the inclusion of the pressure term the value of \bar{H}_c is positive and approximately twice as large as the \bar{H}_1 term. (For Argon, \bar{H}_c is $6697 \text{ cal mole}^{-1}$ and \bar{H}_1 is $-3394 \text{ cal mole}^{-1}$.) One further notes that the predicted $\ln K_H$ values for H_2O increase from Helium to Xenon while the experimental values decrease, whilst the $\ln K_H$ values for organic solvents, although high, display the correct trend. Examination of the entropies reveals that these values are predicted high for organic solvents and low for H_2O but, unlike the previous cases, they increase in value from Helium to Xenon like the experimental values. Although generally poor agreement is obtained using the hard sphere theory, it is interesting to see that this theory treats H_2O like organic solvents but, unlike the original formulation, has no predictive success.

CHAPTER III

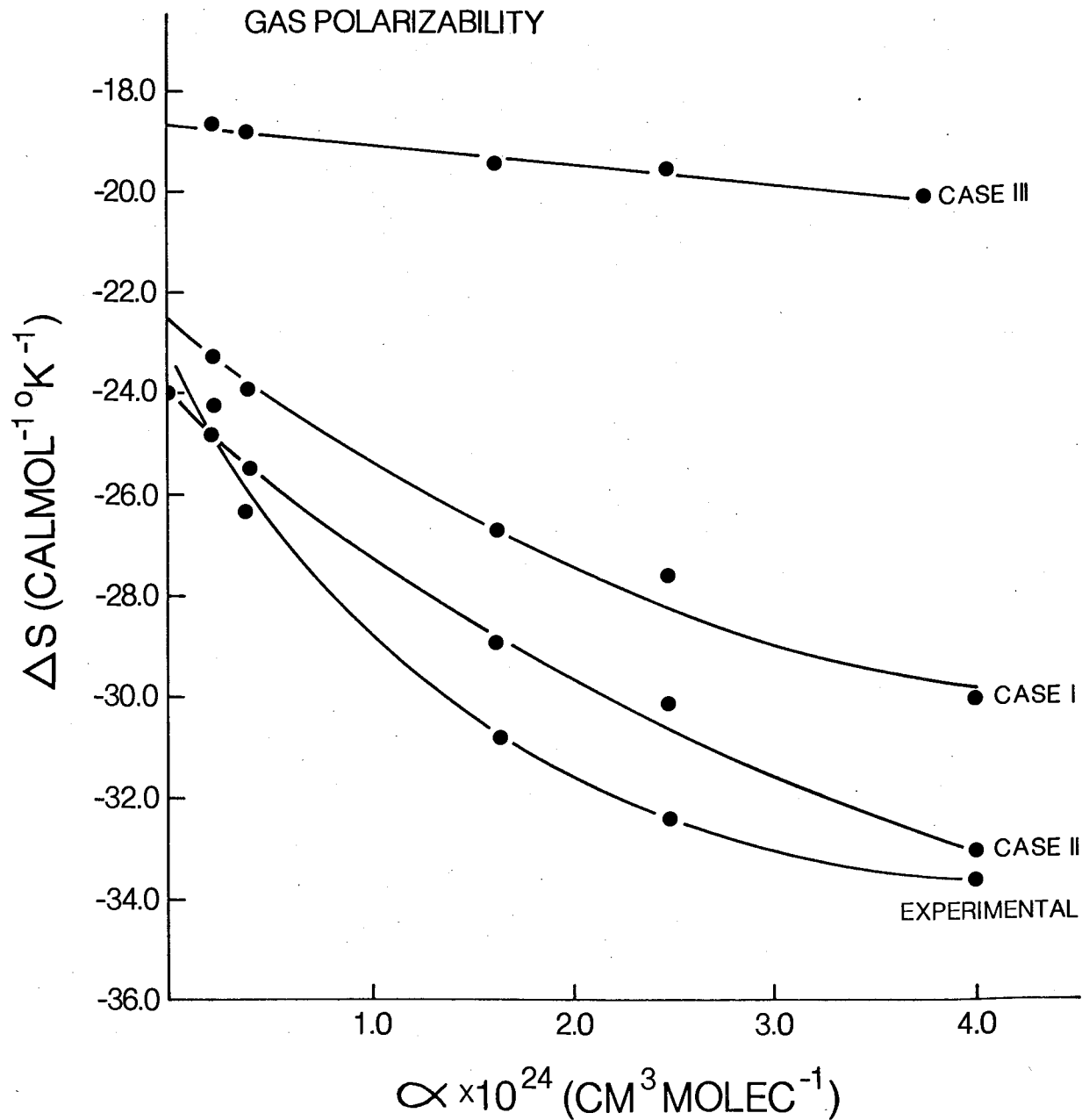
DISCUSSION

Plots of the experimental entropy and calculated entropy for the inert gases in H_2O and C_6H_6 versus the gas polarizability for Cases I, II and III are shown in Figures 4 and 5. One notes that the experimental entropy curve and the Case I entropy curve (with an ϵ_1 value) intersect at the hard sphere limit. As one deviates from the hard sphere limit, it becomes apparent that a rather large entropy associated with the charging process is required to bring agreement between the entropies from Case I and the experimental entropies.

As previously mentioned, one of the inherent assumptions of the S.P.T. is that \bar{H}_i was assumed to be \bar{G}_i , a consequence of this being that the calculated entropy is in fact not a function of the interaction term. Examination of equation (64) reveals that the major contributors to the entropy are the \bar{G}_c and \bar{H}_c terms. For Xe in Benzene Case II, $\bar{H}_c \approx 4800$ cal Mole $^{-1}$, inclusion of a temperature dependence as in Case I yields a value for \bar{H}_c of 9400 cal Mole $^{-1}$, hence contributing an extra 15 cal Mole $^{-1}$ $^{\circ}K^{-1}$ to the entropy, which creates the large difference in the calculated entropy curves for the inert gases in Benzene (Figure 4) for Cases I and II.

It is interesting to note that, for the original Pierotti formulation, in Case II that the \bar{H}_c term is almost identical to the \bar{G}_c term for the inert gases in organic solvents. Typically, for Argon in Benzene, \bar{H}_c and \bar{G}_c , have values of 3612 and 3659 cal Mole $^{-1}$ respectively. Remembering that \bar{H}_i equals \bar{G}_i , then the entropy term for the Pierotti formulation is essentially a function of constants with the major contribution being $R \ln(RT/V_1)$. As a result the calculated entropies when plotted against the inert gases' polarizability are almost a straight line for organic solvents. For H_2O , though, the \bar{H}_c values are much

FIG. 5
 ΔS FOR INERT GASES
IN H_2O vs.
GAS POLARIZABILITY



less that the \bar{G}_c values, and hence one obtains a large negative contribution to the entropy term through \bar{G}_c resulting in a curve which looks similar to the experimental plot shown in Figure 5.

For Case III (with l_1 and l_2 values), typically for Argon in Benzene the \bar{H}_c and \bar{G}_c terms have values of 3281 and 4828 cal Mole⁻¹ respectively; thus the major contribution to the entropy is from these terms. This is typical for all organic solvents and presents a more realistic method for calculating the entropy associated with the dissolution process. From these graphs it is also clear that a large entropy (\bar{S}_i) contribution is required to bring agreement between the calculated and experimental entropy values.

At this point it is instructive to examine the magnitude of the interaction term for the dissolution process. Plots of the experimental $\ln K_H$ values for the inert gases in a solvent, with calculated ($\ln K_H - \bar{G}_i/RT$) values, versus the inert gas polarizability yield insight into the magnitude of the \bar{G}_i term. Exclusion of the \bar{G}_i/RT term from $\ln K_H$ for the inert gases presents a "pure hard sphere" theory, a theory whereby one can include solute and solvent values in the \bar{G}_c term, which allows one to examine the interaction term for the real system by comparison with experimental $\ln K_H$ values for the dissolution process. Figures 6 and 7 are such plots for the inert gases in Benzene and H₂O respectively. One notes that the experimental $\ln K_H$ values are identical to the $\ln K_H - \bar{G}_i/RT$ values at the hard sphere solute value of 2.5 Å. As one deviates from the hard sphere limit, clearly the interaction term becomes increasingly more significant. Typically for Argon in Benzene the \bar{G}_i value required is approximately -3970 cal Mole⁻¹ as compared to a calculated value of -3088 cal Mole⁻¹ to bring agreement between the hard sphere theory and experimental values.

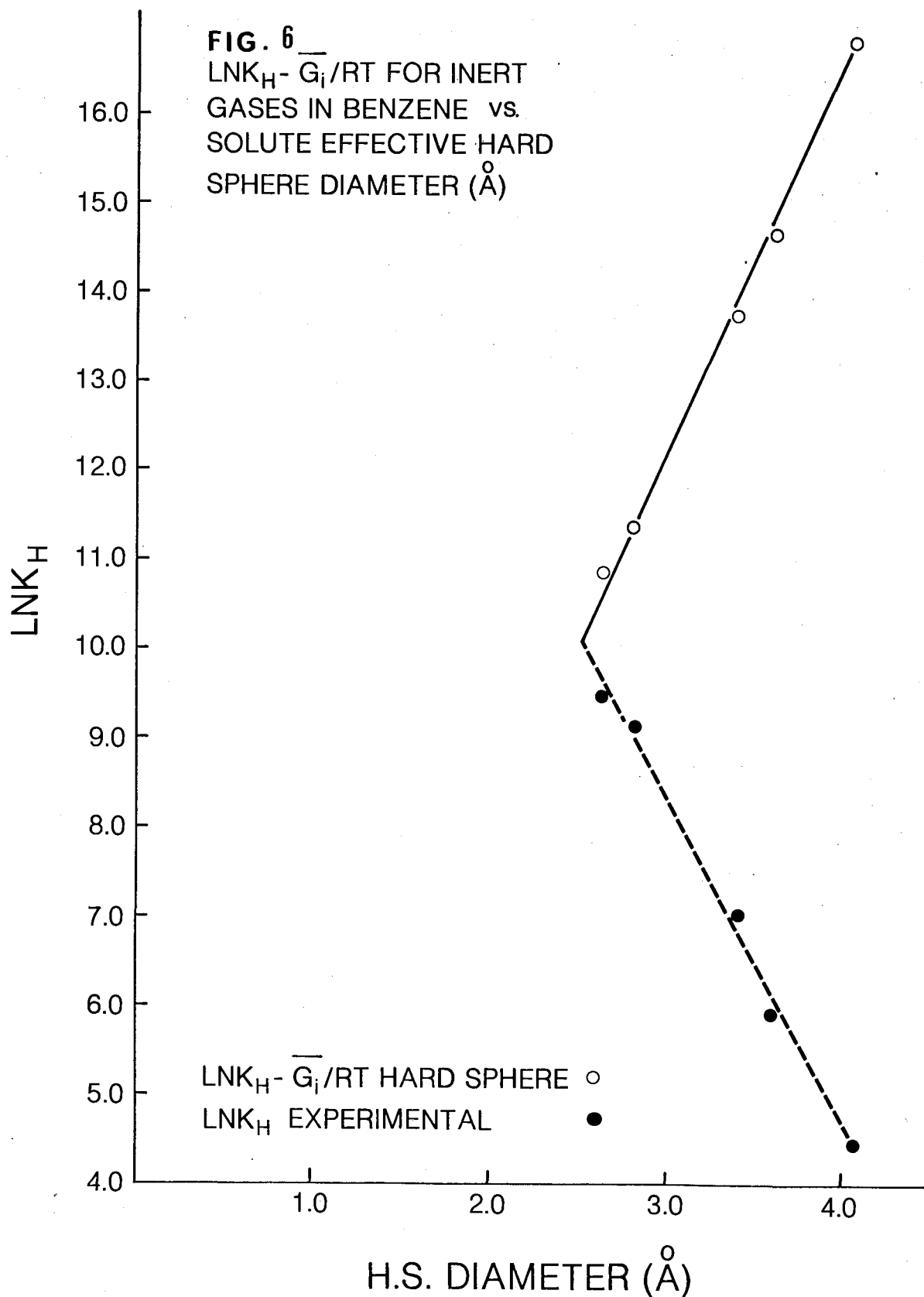
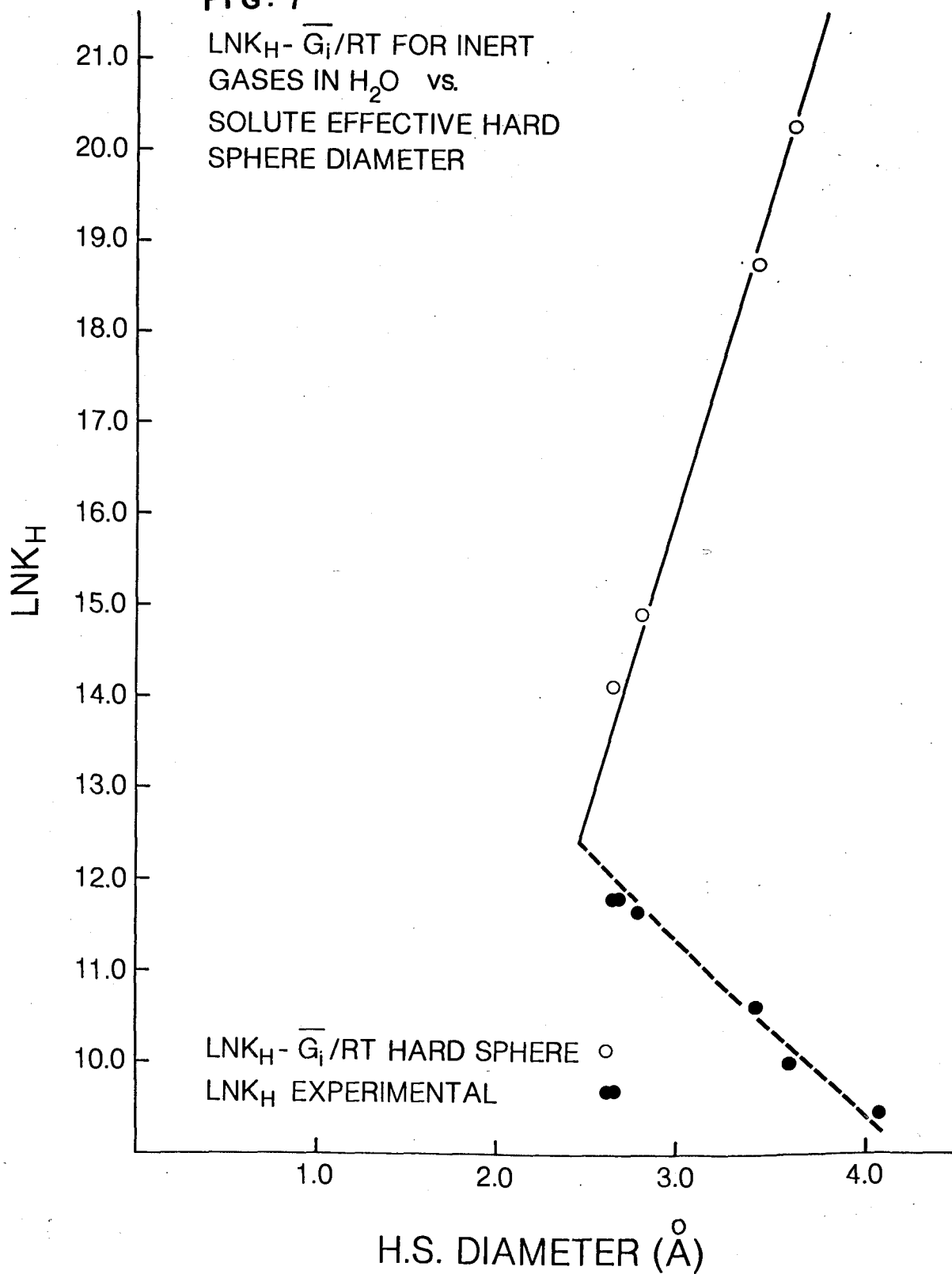


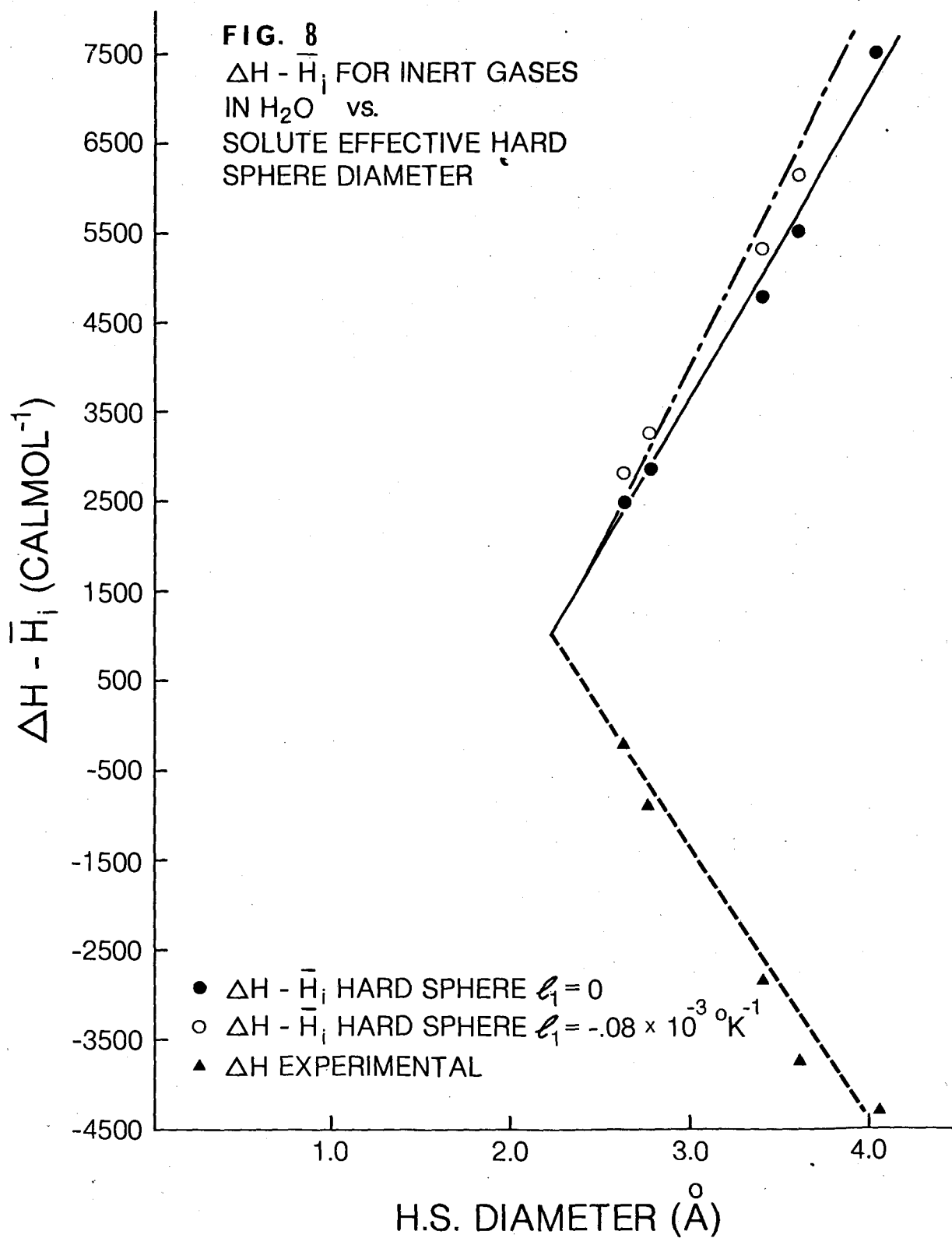
FIG. 7

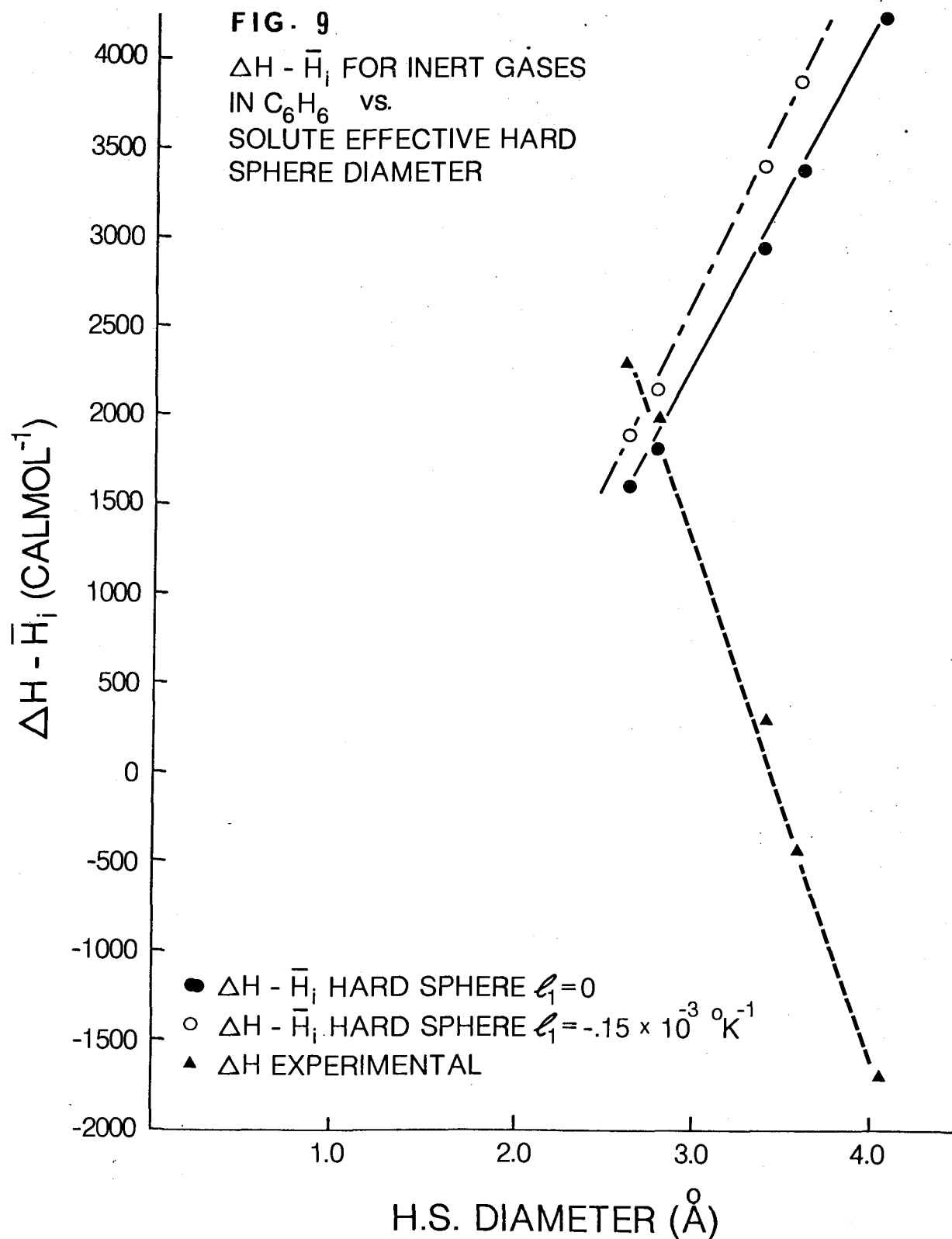
$\text{LNK}_H - \bar{G}_i/RT$ FOR INERT
GASES IN H_2O vs.
SOLUTE EFFECTIVE HARD
SPHERE DIAMETER

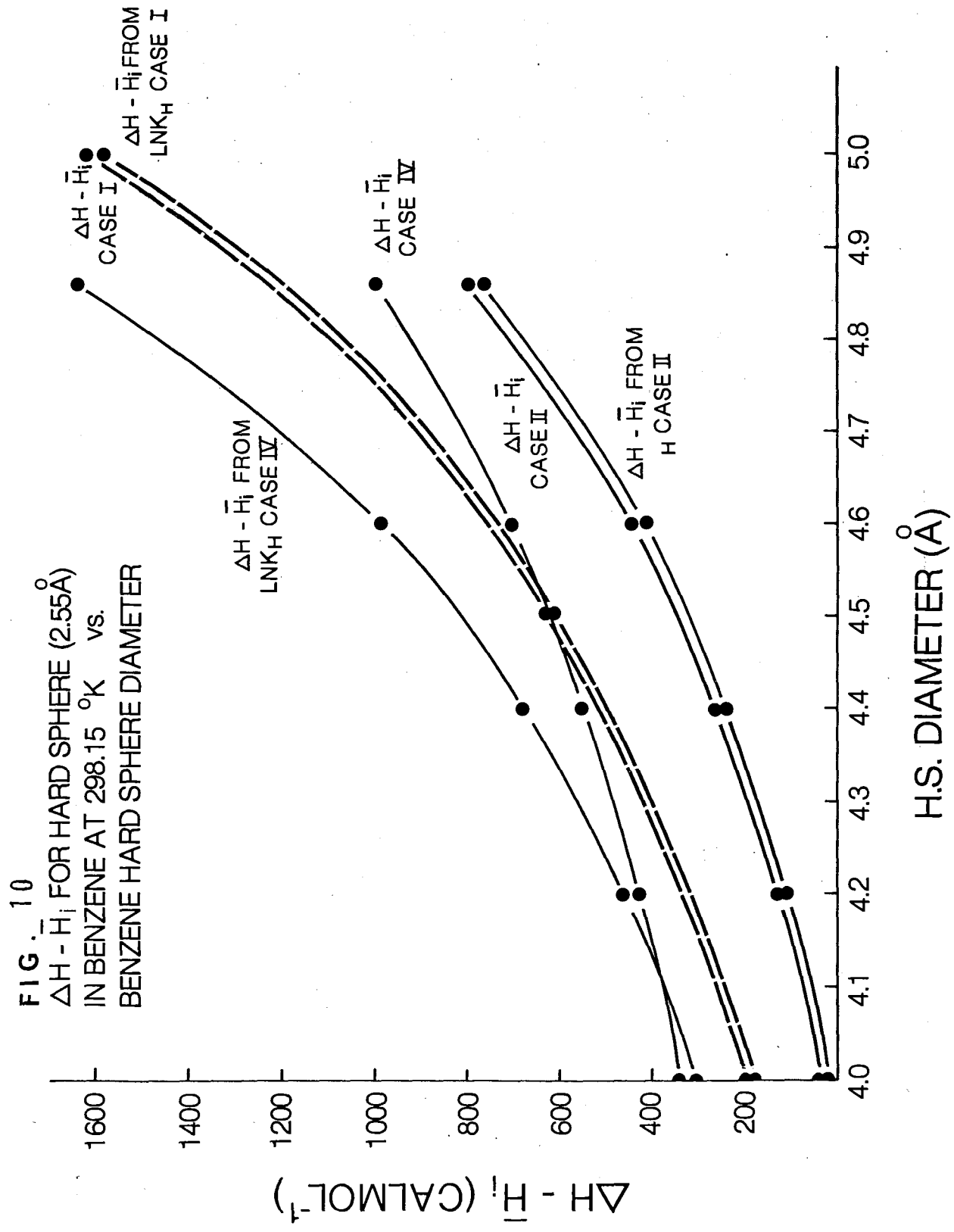


If one plots $\Delta H - \bar{H}_i$ and ΔH experimental for the inert gases in a given solvent versus the solute effective hard sphere diameter, one can clearly see the magnitude of the enthalpy of interaction required to bring agreement between the calculated hard sphere enthalpies and the experimental enthalpies. Figures 8 and 9 are plots of the calculated and experimental enthalpies for the inert gases in H_2O and Benzene respectively. It is clear from these graphs that inclusion of a solvent effective hard sphere diameter temperature dependence does not produce as pronounced an effect as it did for the case of the original Pierotti formulation (Tables VII and VIII), although a large interaction enthalpy is required to bring agreement with the experimentally observed values. It is interesting, however, to note that there are no parameters in the \bar{H}_i term which account for this difference.

Another method for the examination of the interaction term entails varying the solvent effective hard sphere diameter and using a hard sphere solute value of 2.55 \AA , thus eliminating the \bar{H}_i term. One notes that, in the expression for $\ln K_H$, the partial molar volume \bar{V}_2 of the solvent carries the solvent temperature dependence through \bar{G}_c to \bar{H}_c when one differentiates $\ln K_H$ to obtain ΔH . As a result an interesting observation is made when one plots $\Delta H - \bar{H}_i$ for a hard sphere solute of 2.55 \AA , calculated from the expression for ΔH , and ΔH obtained from the derivative of $\ln K_H$ ($\Delta H = -RT^2 \frac{d \ln K_H}{dT}$ equation (6)), as a function of the solvent effective hard sphere diameter. Figure 10 clearly shows for this plot of ΔH values for the hard sphere solute in Benzene an intersection point exists for the two curves at a solvent diameter of 4.13 \AA when $\ell_1 = \ell_2 = 0$ (Case IV). Also included on this graph is the same plot for ΔH values obtained by the two methods of calculation using







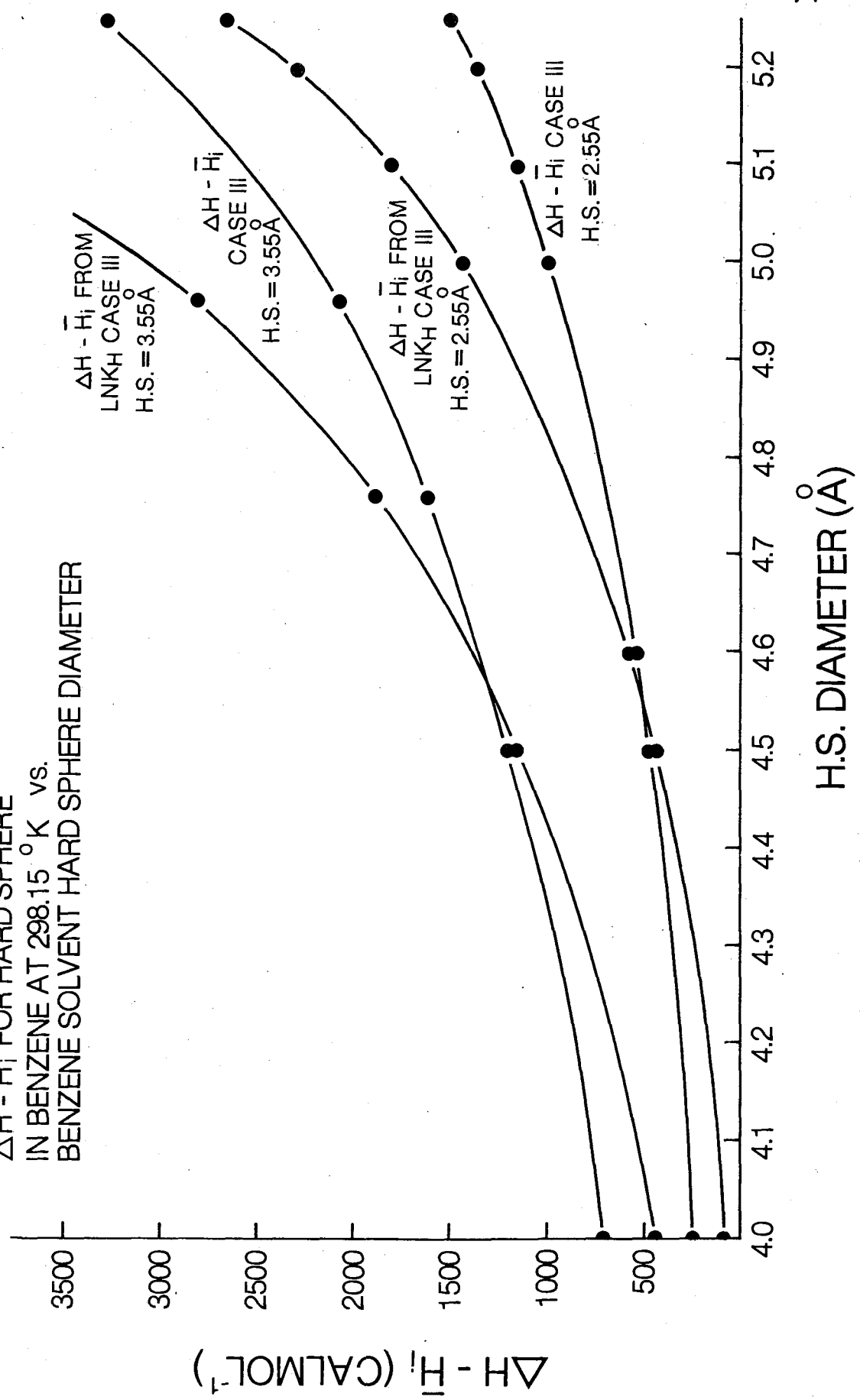
H.S. DIAMETER (Å)

Case I (ρ -values) and the original Pierotti formulation, Case II. Remembering at the hard sphere limit with $a_1^{298} = 5.26 \text{ \AA}$ the extrapolated experimental ΔH° value was only obtained for Case I (see Table III). It is also seen that in the calculation of ΔH° from the $\ln K_H$ values, the extrapolated experimental ΔH° value is only obtained if the $\ln K_H$ values are calculated recognizing that a_1 is a function of temperature. Clearly, this temperature dependence is required to raise the $\Delta H - \bar{H}_1$ curves of Case II to those of Case I (as shown in Figure 10) to obtain the correct values. One observes that these sets of curves for both cases are almost identical and never intersect; this could in fact be due to the experimental error associated with Benzene solvent α_p values. A change in the α_p value of approximately 3 to 5% will bring agreement between these two curves. This agreement does not eliminate the possibility of a solvent effective hard sphere temperature dependence, nor does it affect the extrapolated ΔH° values used in the determination of a solvent H.S. temperature dependence.

Both of the preceding trends are also observed for all organic solvents. Figure 11 is the same plot of the ΔH values calculated by the two methods, but this time for Case III, with the inclusion of a hard sphere solute and Benzene solvent effective hard sphere diameter temperature dependence. Also included on this graph are the same plots, but this time with a different solute effective hard sphere diameter, 3.55 \AA . Clearly comparison of these two plots shows that the solute size has no effect on the intersection value of 4.55 \AA obtained using the two methods of calculating ΔH values. One notes that this Benzene solvent effective hard sphere diameter of 4.55 \AA is different from the value of 4.13 \AA obtained without a solvent hard sphere diameter temperature dependence (Figure 10).

FIG. 11

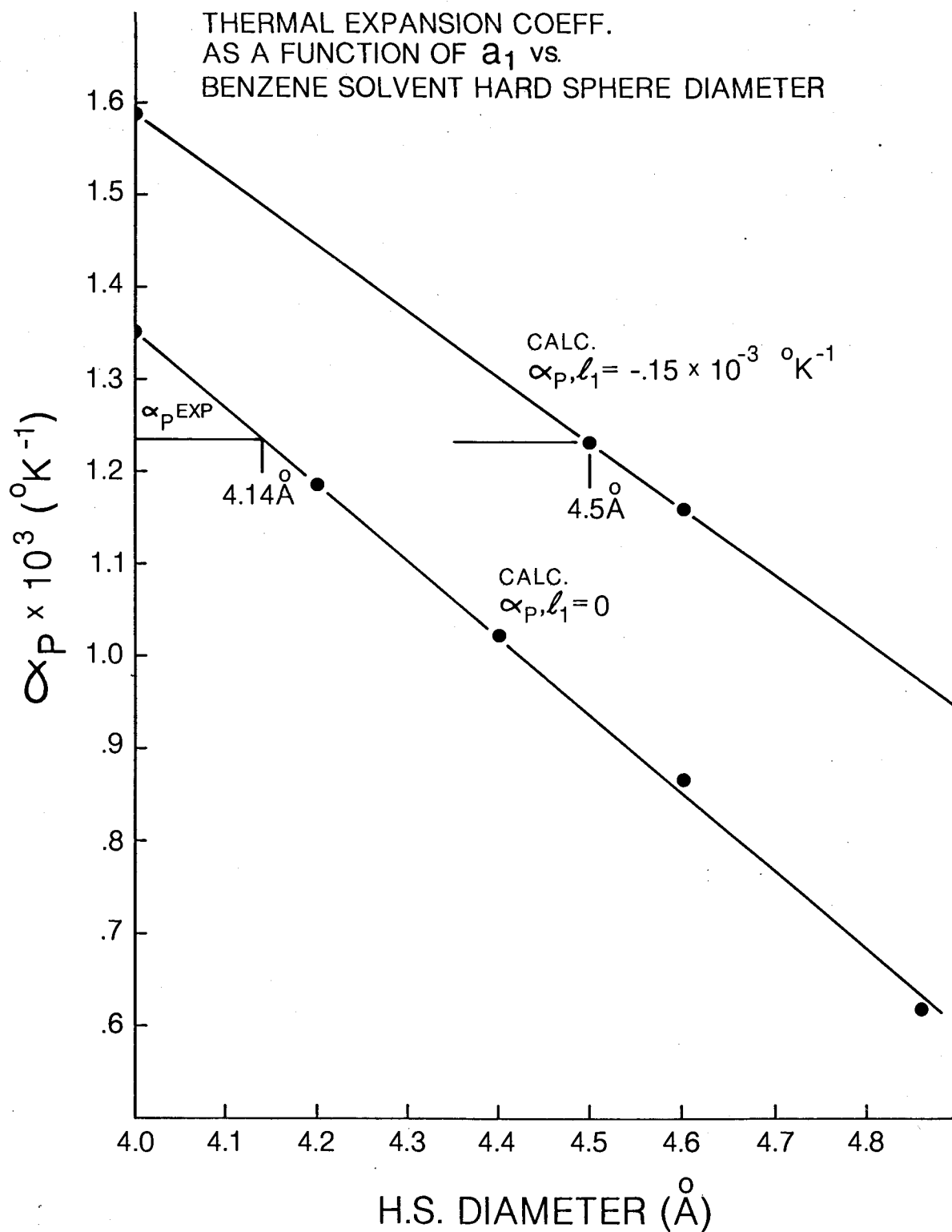
$\Delta H - \bar{H}_i$ FOR HARD SPHERE
IN BENZENE AT 298.15 °K vs.
BENZENE SOLVENT HARD SPHERE DIAMETER



The significance of these hard sphere diameter values is shown by examining plots of the calculated thermal expansion coefficient (with $\ell_1=0$ and $\ell_1 = -.15 \times 10^{-3} \text{ }^\circ\text{K}^{-1}$, eqn. (37)) as a function of solvent effective H.S. diameter. It can be seen from Figure 12 that a solvent hard sphere value of 4.13 \AA (obtained from the intersection of the two ΔH curves) calculated for the case when $\ell_1=\ell_2=0$, gives an α_p value of $1.23 \times 10^{-3} \text{ }^\circ\text{K}^{-1}$ for Benzene. This value is identical to the experimental thermal expansion coefficient for Benzene at $298.15 \text{ }^\circ\text{K}$. For a hard sphere value of 4.5 \AA (obtained from the ΔH curves using the appropriate ℓ_1 values), the α_p curve calculated with $\ell_1 = -.15 \times 10^{-3} \text{ }^\circ\text{K}^{-1}$, again gives an α_p value equal to the Benzene experimental thermal expansion coefficient. Obtaining the experimental value of α_p for Benzene clearly suggests that the experimental thermal expansion coefficient values are required to obtain self consistency between ΔH and $\ln K_H$. This trend is observed for all organic solvents and, as shown in Figure 11, the a_1 value obtained from the intersection of the two ΔH curves is independent of the solute hard sphere diameter. In calculating $\ln K_H$, experimental values of solvent molar volumes at a given temperature are used. Hence, one must input these same experimental values in the expression for the ΔH term which includes the expansion coefficient. This explains why in the original Pierotti formulation (Case II) that comparison of the ΔH values calculated from both the $\ln K_H$ and the ΔH expression yielded similar values. This is the case for all solvents considered and is directly attributable to the use of the experimental expansion coefficient. For Cases III and IV, however, the calculated hard sphere ΔH values for H_2O using the two methods never intersect at a realistic a_1 value.

FIG. 12

THERMAL EXPANSION COEFF.
AS A FUNCTION OF a_1 vs.
BENZENE SOLVENT HARD SPHERE DIAMETER



Typically for the hard sphere solute in H_2O , as one decreases the a_1 value from 2.78 Å to 2.38 Å, the $\Delta H - \bar{H}_1$ values decrease from 2400 to 1100 cal Mole⁻¹, whilst the ΔH values calculated from $\ln K_H$ decrease from 150 to -270 cal Mole⁻¹ and one never obtains the experimental α_p value. Hence, the hard sphere will never work for H_2O since one cannot obtain self consistency through the thermal expansion coefficients and, as such, H_2O cannot be treated like a typical organic solvent; thus the theory has no predictive success with H_2O . This is how the hard sphere theory differentiates organic solvents from H_2O , since self consistency can be obtained for organic solvents. The net result of this being that a smaller solvent effective hard sphere diameter is required for organic solvents effectively to make the α_p value calculated from the equation of state to be equal to the experimental value. The following table summarizes solvent effective hard sphere diameter values required to bring agreement between the calculated and experimental thermal expansion coefficients for selected solvents obtained by the calculation of ΔH by the two methods previously described.

Table XXIV

Solvent Effective Hard Sphere Diameters at 298.15 °K.

Solvent	Pure Hard Sphere calculated (Å)	Experimental (Å)
n-C ₇ H ₁₆	5.31	6.25
C-C ₆ H ₁₂	4.88	5.65
n-C ₆ H ₁₄	4.98	5.92
CCl ₄	4.68	5.37
C ₆ H ₆	4.54	5.26

Since exact agreement between ΔH calculated by the two methods is obtained for a hard sphere solute in H₂O for Case II, it is surprising that, upon inclusion of the interaction term and real solute values, better agreement is not obtained for both the ΔH values and $\ln K_H$ values when compared to experimental values. Also inclusion of the interaction term generally gives poor agreement for the inert gases in organic solvents. One must remember that the only other variable in these calculations of both the $\ln K_H$ and ΔH values is the interaction term, which affects both of these calculations identically. At this point it is instructive to examine actual values of this interaction term and to check the validity of the assumption that $\bar{H}_i = \bar{G}_i$.

It was previously shown that the entropy expression was a good test for both the ℓ_1 and a_1 values used. This same expression was derived with the assumption that \bar{G}_i was equal to \bar{H}_i , but subsequent plots for the entropy (Figures 4 and 5) revealed that a large interaction term \bar{S}_i was required to bring agreement between the calculated and

experimental entropies. It appears that, for some of the cases considered, the assumption regarding \bar{H}_i and \bar{G}_i might be incorrect. The validity of this assumption can be determined by a series of self consistency checks incorporating experimental values and the derived equations of $\ln K_H$ and ΔH for the dissolution process. These values thus obtained for the \bar{H}_i and \bar{G}_i terms can be compared to the original expression for \bar{E}_i .

Using the inert gases in a given solvent, the experimental $\ln K_H$ values can be equated to equation (5) to obtain \bar{G}_i for these gases. These values can be compared to the \bar{H}_i values obtained by equating the experimental enthalpies of the inert gases to equation (6) for the same solvent. These values can then be compared to the values obtained from the expression for E_i (equation(17)), thus determining the validity of the original assumption that $\bar{E}_i = \bar{H}_i = \bar{G}_i$. The following tables summarize these results for the inert gases in H_2O and C_6H_6 calculated for all four cases considered.

Table XXV

	H ₂ O at 298.15 °K Interaction Terms for Case I and II			
	\bar{G}_i (cal Mol ⁻¹) Eqn. (5)	\bar{H}_i (cal Mol ⁻¹) Eqn. (6)	\bar{H}_i (cal Mol ⁻¹) Eqn. (6)	\bar{E}_i (cal mol ⁻¹) Eqn. (17)
		$\lambda_1 = 0$	$\lambda_1 = -.08 \times 10^{-3}$	
He	- 294	- 96	- 526	- 399
Ne	- 617	- 854	-1326	- 984
Ar	-2497	-3093	-3753	-2585
Kr	-3272	-3985	-4713	-3394
Xe	-4670	-4816	-5713	-4713

Table XXVI

C_6H_6 at 298.15 °K Interaction terms for Case I and Case II

	\bar{G}_i (cal Mol ⁻¹)	\bar{H}_i (cal Mol ⁻¹)	\bar{H}_i (cal Mol ⁻¹)	\bar{E}_i (cal Mol ⁻¹)
	Eqn. (5)	Eqn. (6)	Eqn. (6)	Eqn. (17)
		$\lambda_1=0$	$\lambda_1=-.15 \times 10^{-3}$	
He	- 288	+ 356	- 524	- 519
Ne	- 708	- 270	-1228	-1322
Ar	-2819	-2941	-4250	-3088
Kr	-3805	-4021	-5465	-3916
Xe	-5444	-6161	-7925	-5181

Table XXVII

H_2O at 298.15 °K Interaction terms for Case III and Case IV

	\bar{G}_i (cal Mol ⁻¹)	\bar{H}_i (cal Mol ⁻¹)	\bar{H}_i (cal Mol ⁻¹)	\bar{E}_i (cal Mol ⁻¹)
	Eqn. (5)	Eqn. (6)	Eqn. (6)	Eqn. (17)
		$\lambda_1=0$	$\lambda_1=-.08 \times 10^{-3}$	
He	-1383	-2669	-3010	- 399
Ne	-1903	-3765	-4143	- 984
Ar	-4849	-7723	-8274	-2585
Kr	-6065	-9290	-9902	-3394
Xe	-8675	-11917	-12688	-4713

C_6H_6 at 298.15 °K Interaction terms for Case III and Case IV

	\bar{G}_i (cal Mol ⁻¹)	\bar{H}_i (cal Mol ⁻¹)	\bar{H}_i (cal Mol ⁻¹)	\bar{E}_i (cal Mol ⁻¹)
	Eqn. (5)	Eqn. (6)	Eqn. (6)	Eqn. (17)
He	- 829	$\ell_1=0$ + 788	$\ell_1=-.15 \times 10^{-3}$ + 495	- 519
Ne	-1347	+ 151	- 171	-1322
Ar	-3989	-2654	-3110	-3088
Kr	-5192	-3811	-4316	-3916
Xe	-7434	-6200	-6826	-5181

Examination of Tables XXV through XXVIII reveals why the hard sphere theory does not work, the assumption that $\bar{E}_i = \bar{H}_i = \bar{G}_i$ does not hold true. The effect of including an ℓ_1 value on the \bar{H}_i term ($\approx 10\%$) is negligible when compared to the large difference in the \bar{E}_i and \bar{G}_i terms. For Cases I and II, inclusion of an ℓ -value creates approximately a 30% difference in the \bar{H}_i term, which generally invalidates the assumption. Clearly for the original Pierotti formulation, Case II, the assumption is also not valid, although the differences in the interaction terms are much less than the hard sphere treatment differences. It is interesting to note that the agreement between \bar{E}_i and \bar{G}_i for the inert gases in H_2O is just an inherent artifact of the method employed, as previously outlined, for obtaining E/K.

A novel approach for the treatment of gases dissolved in liquids, utilizing the concepts of a pure hard sphere treatment has been examined. The hard sphere treatment results suggested that this theory is in fact a perturbation theory in which the real system is approximated by a hard sphere equivalence. This entailed the use of the Carnahan Starling equation of state to obtain the necessary hard sphere values for the thermodynamic properties. The recharging term appears as the real part correction and the calculated thermodynamic properties were shown to deviate from experimental thermodynamic properties as one increased the magnitude of the interaction term. The hard sphere theory was shown to have no predictive success for the treatment of gases dissolved in H_2O . The theory effectively treated H_2O as a typical organic solvent but, due to fundamental differences in the molecular properties (small E/K , a_1) and calculated hard sphere properties (small α_p and large P), and effects due to hydrogen bonding, the theory was not capable of making valid thermodynamic predictions for the dissolution process. For the treatment of gases dissolved in organic solvents, a remarkable parallel was shown to exist between the predicted enthalpies and those predicted by the original Pierotti formulation. The Henry's law constants for organic solvents typically gave agreement for Helium and Neon solutes, whilst deviating substantially as one increased the solute value of E/K . Using the hard sphere treatment the calculated entropies were shown to parallel the experimental values, unlike the original Pierotti formulation. Since no interaction term exists in this calculation and the pressure terms from both the \bar{G}_c and \bar{H}_c terms effectively cancelled, this suggested that the \bar{H}_c term was in fact a valid approximation for the enthalpy of cavity formation. The disparity observed in the numerical predictions of the entropies is a reflection

of the poor choice of thermal expansion coefficients and was exemplified 103
by observing the differences in $\Delta H - \bar{H}_1$ calculated from both the derivative
of $\ln K_H$ and the expression for ΔH for the inert gases.

The original Pierotti formulation appeared to predict with limited
success the thermodynamic properties for the dissolution of a gas in
 H_2O and organic solvents, which is due in part to the use of the
experimental thermal expansion coefficient. It was also shown unambiguously
that the assumption $\ell_1=0$ was in fact wrong. As was shown in the
Experimental section (eqn. (7)), the thermal expansion coefficients
accounted for the transfer coefficients of a solute from H_2O to
 D_2O , which further substantiates the choice of the experimental thermal
expansion coefficients used in the calculation of the enthalpies. One
also notes that inclusion of a solvent effective hard sphere diameter
temperature dependence does not affect the calculation of the transfer
coefficients. The predictive success of this theory in H_2O was due
to the fitting procedure used to obtain the low value of E/K for H_2O ,
effectively fixing the interaction term. Agreement in organic solvents
(typically Benzene) was shown to be fortuitous in the original Pierotti
formulation predictions, as in the case of the entropies, where the calcu-
lated entropies only crossed over the experimental entropy curve for the
inert gases for a solute with molecular properties typical of Argon gas.
A good test of this theory was the predictions of limiting case at hard
sphere limit. The theory was shown to be inconsistent.

The solvent effective hard sphere diameter temperature dependence
was obtained at the hard sphere limit and compared extremely favourably
with the value obtained using extrapolated enthalpy and $\ln K_H$ values.

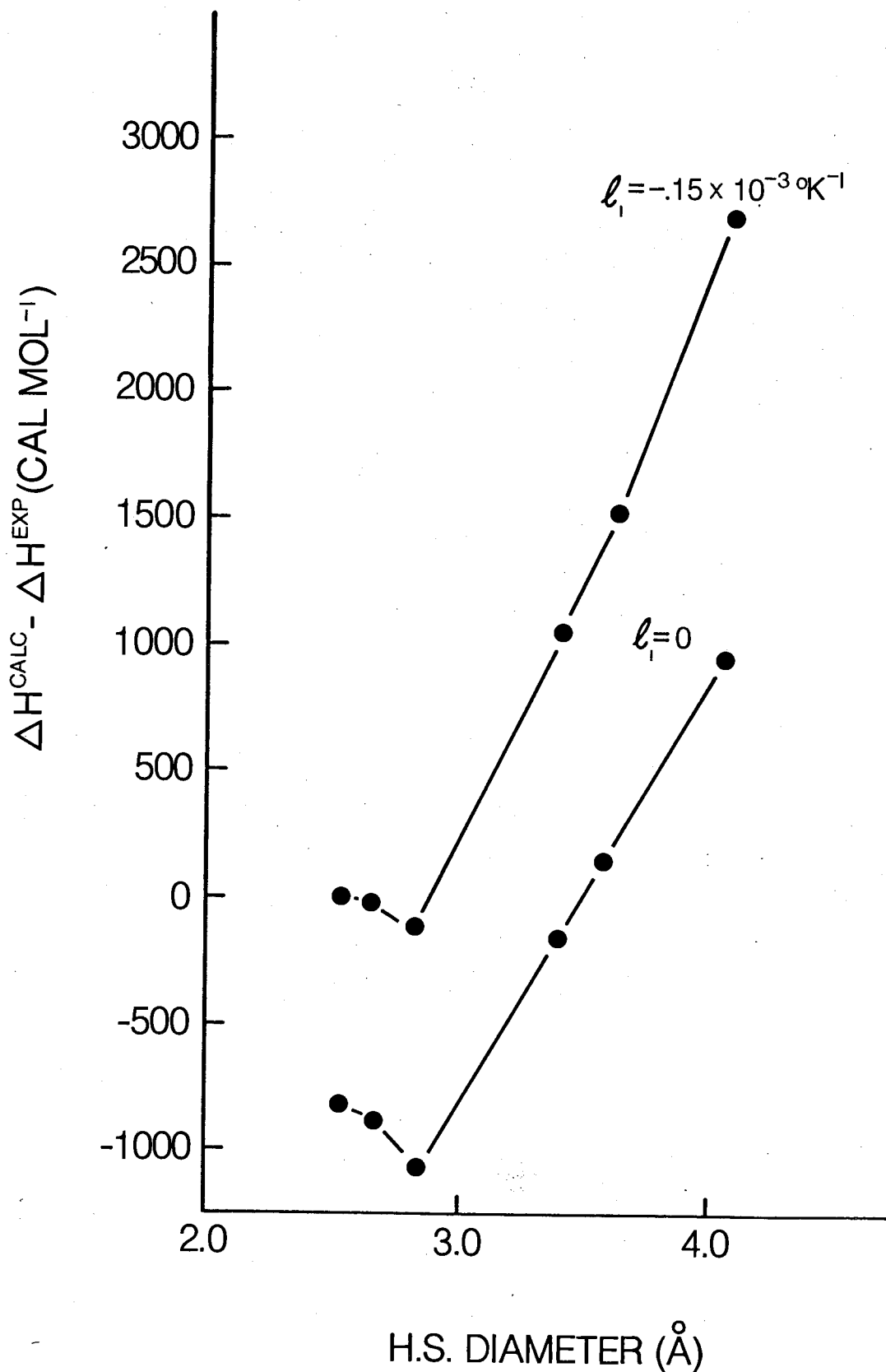
Although generally poor thermodynamic agreement was obtained upon inclusion of this ℓ -value, it suggested that the \bar{H}_c term was correct and that the assumption $\bar{E}_i = \bar{H}_i = \bar{G}_i$ was invalid. Figure 13 is a plot of the difference in the experimental enthalpies of the inert gas in Benzene calculated from the original Pierotti formulation and Case I (inclusion of an ℓ -value) versus the solute effective hard sphere diameter. Clearly, inclusion of the ℓ -value gives better agreement for the small solutes and deviates about the same as does the original Pierotti formulation for the larger solutes.

One would not expect a theory of gas solubilities to predict the thermodynamic properties associated with the dissolution of a gas in both H_2O and organic solvents that does not take into account fundamental differences. At this point the hard sphere treatment yields encouraging results for the treatment of organic solvents.

A novel gas chromatographic technique was developed which allowed direct determination of gases dissolved in H_2O and D_2O by comparison of the stripped gas with a gas calibration curve obtained under conditions matching those of the stripped gas. This technique is rapid and efficient, requiring minimum amounts of solvent, of which all is recovered. The system also has a built in standard, thus allowing for the determination of the solubility of a gas in both H_2O and D_2O simultaneously under identical conditions.

INERT GASES IN BENZENE

$\Delta H^{CALC} - \Delta H^{EXP}$ vs SOLUTE H.S. DIAMETER



SECTION II REFERENCES

- (1) B. Sisskind and I. Kasarnowsky.
Z. Anorg. Allgem Chem. 214: 385 (1933).
- (2) H.H. Uhlig.
J. Phys. Chem. 41: 1215 (1937).
- (3) D.D. Eley.
Trans. Farad. Soc. 35: 1281 (1939).
- (4) H. Reiss, H.L. Frisch and J.L. Lebowitz.
J. Chem. Phys. 31: 369 (1959).
- (5) H. Reiss, H.L. Frisch, E. Helfand and J.L. Lebowitz.
J. Chem. Phys. 32: 119 (1960).
- (6) R.A. Pierotti.
J. Chem. Phys. 67: 1840 (1963).
- (7) R.A. Pierotti.
J. Chem. Phys. 69: 281 (1965).
- (8) R.A. Pierotti.
Chem. Revs. 76: 717 (1976).
- (9) J.S. Rowlinson.
Liquids and Liquid Mixtures. Butterworths Scientific Publications. 1959.
- (10) E. Wilhelm.
J. Chem. Phys. 58: 3558 (1973).
- (11) J.H. Dymond and B.J. Alder.
J. Chem. Phys. 45: 2061 (1966).
- (12) N.F. Carnahan and K.E. Starling.
J. Chem. Phys. 51: 635 (1969).
- (13) N.F. Carnahan and K.E. Starling.
J. Chem. Phys. 53: 600 (1970).
- (14) E. Wilhelm.
J. Chem. Phys. 60: 3896 (1974).
- (15) E.W. Toppel and K.E. Gubbins.
J. Phys. Chem. 76: 3044 (1972).
- (16) E. Wilhelm, R. Battino and R.J. Wilcock.
Chem. Revs. 77: 219 (1977).

- (17) Izvestiia Vysshikh Uchebnykh Zavedenii
V.K. Abrosimov, A.N. Straklov, et al.
Khimia i Khimicheskaya Tekhnologiya Ivanova,
USSR 17: 10 (1974).
- (18) L.R. Pratt and D. Chandler.
J. Chem. Phys. 67: 3683 (1977).
- (19) E. Wilhelm and R. Battino.
Chem. Revs. 73: 1 (1973).
- (20) E. Wilhelm and R. Battino.
J. Chem. Thermo. 3: 379 (1971).
- (21) R.T. Emmet and F.J. Millero.
J. Chem. and Eng. Data 20: 351 (1975).
- (22) E. Wilhelm and R. Battino.
J. Chem. Phys. 58: 3561 (1973).
- (23) R.A. Fini and F.J. Millero.
J. Chem. Phys. 63: 89 (1975).
- (24) Handbook of Chemistry and Physics.
CRC Press, 55th Edition, 1974-1975.
- (25) M. Diaz Pena, G. Tardajos, C. Menduina and R.L. Arenosa.
J. Chem. Therm. 11: 67 (1979).
- (26) Timmermans.
J. Physico-Chemical Constants of Pure Organic Compds. Vol. I
Elsevier New York, N.Y., 1965.
- (27) Landolt-Bornstein.
IV Band Technik
4 Teil Wärmetechnik

APPENDIX I

'HARDSPHERE PROGRAM'

```
//CAB      JOB (0022,U5013), '733-01-4039', TIME=0001
/*JOBPARM PSWD=COS
// EXEC PLIXCG,CPARM='NA,NX,NAG,NOP',REGION=180K
//SYSIN DD *
```

```
HARDSP:PROC OPTIONS(MAIN):
```

```

/*****
/*
/*                                DECLARATIONS                                */
/*
/* 'HCT' : ENTHALPY OF CAVITY FORMATION.                                     */
/* 'HI'  : ENTHALPY OF INTERACTION BETWEEN THE SOLVENT AND THE SOLUTE.     */
/* 'GI'  : GIBB'S FREE ENERGY OF INTERACTION BETWEEN THE SOLVENT AND THE  */
/*          SOLUTE.                                                           */
/* 'GC'  : PARTIAL MOLAR GIBB'S FREE ENERGY OF CAVITY FORMATION.           */
/* 'P'   : PRESSURE.                                                          */
/* 'T'   : TEMPERATURE( DEGREES KELVIN ).                                    */
/* 'Y'   : COMPACTNESS FACTOR OF THE SOLVENT.                                */
/* 'AP'  : THERMAL EXPANSION COEFFICIENT OF THE SOLVENT.                     */
/* 'APX' : EXPERIMENTAL THERMAL EXPANSION COEFFICIENT OF THE SOLVENT.       */
/* 'V1'  : PARTIAL MOLAR VOLUME OF THE SOLVENT.                              */
/* 'V2'  : PARTIAL MOLAR VOLUME OF THE SOLUTE.                              */
/* 'M'   : MASS.                                                             */
/* 'D'   : DENSITY.                                                          */
/* 'A1'  : EFFECTIVE HARD SPHERE DIAMETER OF THE SOLVENT                    */
/* 'A2'  : EFFECTIVE HARD SPHERE DIAMETER OF THE SOLUTE.                   */
/* 'L1'  : LINEAR EXPANSION COEFFICIENT OF THE EFFECTIVE HARD SPHERE        */
/*          DIAMETER OF THE SOLVENT.                                         */
/* 'SG'  : RATIO OF THE HARD SPHERE DIAMETERS OF THE SOLUTE OVER THE       */
/*          SOLVENT.                                                          */
/* 'SG12': HARD SPHERE RADIUS OF A SPHERE WHICH EXCLUDES THE CENTERS OF    */
/*          SOLVENT MOLECULES, (A1+A2/2), WHERE 'A2' AND 'A1' ARE DEFINED    */
/*          ABOVE.                                                            */
/* 'A1S' : EFFECTIVE HARD SPHERE DIAMETER OF THE SOLVENT AT S.T.P.         */
/* 'DA1DT': THE TEMPERATURE DEPENDENCE OF 'A1'.                            */
/* 'E1K'  : MAGNITUDE OF THE FORCE POTENTIAL DUE TO THE INTERACTION          */
/*          BETWEEN TWO SOLVENT MOLECULES, DIVIDED BY THE BOLTZMAN'S        */
/*          CONSTANT 'K'.                                                     */
/* 'E2K'  : MAGNITUDE OF THE FORCE POTENTIAL DUE TO THE INTERACTION          */
/*          BETWEEN TWO SOLUTE MOLECULES, DIVIDED BY THE BOLTZMAN'S        */
/*          CONSTANT 'K'.                                                     */
/* 'E12K' : SQUARE ROOT OF THE PRODUCT OF 'E1K' AND 'E2K'.                 */
/* 'DPM1' : DIPOLE MOMENT OF THE SOLVENT.                                    */
/* 'PO2'  : POLARIZABILITY OF THE SOLUTE.                                    */
/* 'RO'   : NUMBER DENSITY OF THE SOLVENT.                                   */
/*****/

```



```

/* 'LNKH' : NATURAL LOGORITHM OF HENRY'S LAW CONSTANT. */
/* 'BT' : ISOTHERMAL COMPRESSIBILITY OF THE SOLVENT. */
/* 'BTX' : EXPERIMENTAL ISOTHERMAL COMPRESSIBILITY OF */
/* THE SOLVENT. */
/* 'DHS' : TOTAL ENTHALPY OF THE DISSOLUTION OF THE */
/* SOLUTE INTO THE SOLVENT. */
/* 'SU' : INPUT/OUTPUT ARRAY TO HOLD THE SOLUTE VALUE. */
/* 'SV' : INPUT/OUTPUT ARRAY TO HOLD THE SOLVENT VALUE. */
/* 'R' : IDEAL GAS CONSTANT. */
/* 'N' : AVOGADRO'S NUMBER. */
/* 'K' : BOLTZMAN'S CONSTANT. */
/* 'PI' : CONSTANT. */
/* 'S' : 'SYSIN' FLAG. */
/* 'I' : ARRAY SUBSCRIPT. */
/* 'SPECS' : INPUT SPECIFICATIONS VARIABLE */
/* 'OUT1' : ARRAY TO STORE THE FIRST SET OF OUTPUT DATA. */
/* 'OUT2' : ARRAY TO STORE THE SECOND SET OF OUTPUT DATA. */
/* 'TABLE' : ARRAY TO STORE THE DESIRED INPUT DATA WITH */
/* THE COLUMN HEADINGS ( T , D(H2O) , APX(H2O) , */
/* BTX(H2O) , D(BZ) , APX(BZ) , BTX(BZ) ). */
/*
/*****
DCL (HCT,HI,GI,GC,T,Y,AP,APX,V1,V2,M,D,A1,A2,L1,L2,SG,SG12,A1S,
DA1DT,E1K,E2K,E12K,DPM1,PO2,RO,LNKH,BT,BTX,DHS,DA2DT)
FLOAT DECIMAL(5),
(SU,SV) CHAR(10),
R FLOAT DECIMAL(5) INIT(1.987),
P FLOAT DECIMAL(5) INIT(0),
N FLOAT DECIMAL(5) INIT(6.0225E+23),
K FLOAT DECIMAL(5) INIT(1.38054E-16),
PI FLOAT DECIMAL(5) INIT(3.14159),
S BIT(1) INIT('0'B),
I FIXED(1), SPECS FIXED(1),
OUT1(7,6) FLOAT DECIMAL(5),
OUT2(7,6) FLOAT DECIMAL(5),
TABLE(7,22) FLOAT DECIMAL(5);

/* LOAD THE ARRAY 'TABLE' */
GET LIST(TABLE);

/* SET 'SYSIN' FLAG 'S' TO '1'B IF END OF FILE */
ON ENDFILE(SYSIN) S = '1'B;

/* OBTAIN VALUES FOR THE SOLVENT AND THE SOLUTE */
GET EDIT(SV,SU) (COL(1),A(10),A(10));

```

```
/* LOOP THROUGH THE INPUT SPECIFICATIONS WHILE THE */  
/* 'SYSIN' FLAG 'S' IS EQUAL TO '0'B */  
DO WHILE( S = '0'B );
```

```
/* SELECT THE APPROPRIATE SOLUTE 'SU' FROM THE INPUT */  
SELECT(SU);
```

```
/* WHEN THE SOLUTE IS 'HELIUM' */
```

```
WHEN('HE') DO;  
SU = 'HELIUM';  
A2 = 2.63E-08;  
E2K = 6.03;  
PO2 = .204E-24;  
END;
```

```
/* WHEN THE SOLUTE IS 'NEON' */
```

```
WHEN('NE') DO;  
SU = 'NEON';  
A2 = 2.78E-08;  
E2K = 34.9;  
PO2 = .393E-24;  
END;
```

```
/* WHEN THE SOLUTE IS 'ARGON' */
```

```
WHEN('AR') DO;  
SU = 'ARGON';  
A2 = 3.40E-08;  
E2K = 122;  
PO2 = 1.63E-24;  
END;
```

```
/* WHEN THE SOLUTE IS 'KRYPTON' */
```

```
WHEN('KR') DO;  
SU = 'KRYPTON';  
A2 = 3.60E-08;  
E2K = 171;  
PO2 = 2.46E-24;  
END;
```

```
/* WHEN THE SOLUTE IS 'XENON' */
```

```
WHEN('XE') DO;  
SU = 'XENON';  
A2 = 4.06E-08;  
E2K = 221;  
PO2 = 4.00E-24;  
END;
```

```
/* WHEN THE SOLUTE IS 'NITROGEN' */
```

```
WHEN('N2') DO;
```

```

SU = 'NITROGEN';
A2 = 3.70E-08;
E2K = 95;
PO2 = 1.74E-24;
END;
/* WHEN THE SOLUTE IS 'OXYGEN' */
WHEN('O2') DO;
SU = 'OXYGEN';
A2 = 3.46E-08;
E2K = 118;
PO2 = 1.57E-24;
END;
/* WHEN THE SOLUTE IS 'METHANE' */
WHEN('CH4') DO;
SU = 'METHANE';
A2 = 3.70E-08;
E2K = 157;
PO2 = 2.70E-24;
END;
/* WHEN THE SOLUTE IS 'S-HEXA-F' */
WHEN('SF6') DO;
SU = 'S-HEXA-F';
A2 = 5.51E-08;
E2K = 201;
PO2 = 4.48E-24;
END;

/* THE INPUT VALUE FOR SOLUTE 'SU' WAS ILLEGAL */
OTHERWISE
PUT SKIP(2) LIST('** ILLEGAL SOLUTE **',SU);

END;

/* CALCULATE DATA FOR BOTH INVESTIGATORS */
DO SPECS = 0 TO 1;

/* SELECT THE APPROPRIATE SOLVENT 'SV' FROM THE INPUT */
SELECT(SV);

/* WHEN THE SOLVENT IS 'H2O' DO CALCULATIONS FOR THE */
/* ENTIRE TEMPERATURE RANGE. */
WHEN('H2O')
DO I = 1 TO 7;
M = 18.0154;
D = TABLE(I,2);

```

```
A1S = 2.765E-08;  
DPM1 = 1.84E-18;  
APX = TABLE(I,3);  
BTX = TABLE(I,4);  
IF SPECS = 0
```

```
THEN DO;
```

```
  L1 = 0;  
  DA1DT = 0;  
  E1K = 85;  
  END;
```

```
ELSE DO;
```

```
  L1 = -.08E-03;  
  DA1DT = -.222E-11;  
  E1K = 85;  
  END;
```

```
CALL CALC;
```

```
END;
```

```
/* WHEN THE SOLVENT IS 'BZ' DO CALCULATIONS FOR THE */  
/* ENTIRE TEMPERATURE RANGE. */
```

```
WHEN('BENZENE')
```

```
DO I = 1 TO 7;
```

```
M = 78.114;
```

```
D = TABLE(I,5);
```

```
A1S = 5.26E-08;
```

```
DPM1 = 0;
```

```
APX = TABLE(I,6);
```

```
BTX = TABLE(I,7);
```

```
E1K = 531;
```

```
IF SPECS = 0
```

```
THEN DO;
```

```
  L1 = 0;  
  DA1DT = 0;  
  END;
```

```
ELSE DO;
```

```
  L1 = -.15E-03;  
  DA1DT = -.789E-11;  
  END;
```

```
CALL CALC;
```

```
END;
```

```
WHEN('N-C7H16')
```

```
DO I = 1 TO 7;
```

```
M = 100.21;
```

```
D = TABLE(I,8);
```

```
A1S = 6.25E-08;
DPM1 = 0;
APX = TABLE(I,9);
BTX = TABLE(I,10);
E1K = 573;
IF SPECS = 0
THEN DO;
  L1 = 0;
  DA1DT = 0;
  END;
ELSE DO;
  L1 = -.13E-03;
  DA1DT = -.81E-11;
  END;
CALL CALC;
END;
```

```
WHEN('CCL4')
DO I = 1 TO 7;
M = 153.82;
D = TABLE(I,11);
A1S = 5.37E-08;
DPM1 = 0;
APX = TABLE(I,12);
BTX = TABLE(I,13);
E1K = 536;
IF SPECS = 0
THEN DO;
  L1 = 0;
  DA1DT = 0;
  END;
ELSE DO;
  L1 = -.14E-03;
  DA1DT = -.75E-11;
  END;
CALL CALC;
END;
```

```
WHEN('C-HEXANE')
DO I = 1 TO 7;
M = 84.16;
D = TABLE(I,14);
A1S = 5.65E-08;
DPM1 = 0;
APX = TABLE(I,15);
```

```
BTX = TABLE(I,16);
E1K = 589;
IF SPECS = 0
THEN DO;
    L1 = 0;
    DA1DT = 0;
    END;
ELSE DO;
    L1 = -.14E-03;
    DA1DT = -.79E-11;
    END;
CALL CALC;
END;
```

```
WHEN('N-HEXANE')
DO I = 1 TO 7;
M = 86.18;
D = TABLE(I,17);
A1S = 5.92E-08;
DPM1 = 0;
APX = TABLE(I,18);
BTX = TABLE(I,19);
E1K = 517;
IF SPECS = 0
THEN DO;
    L1 = 0;
    DA1DT = 0;
    END;
ELSE DO;
    L1 = -.19E-03;
    DA1DT = -1.125E-11;
    END;
CALL CALC;
END;
```

```
WHEN('D2O')
DO I = 1 TO 7;
M = 20.028;
D = TABLE(I,20);
A1S = 2.765E-08;
DPM1 = 1.84E-18;
APX = TABLE(I,21);
BTX = TABLE(I,22);
IF SPECS = 0
THEN DO;
```

```

L1 = 0;
DA1DT = 0;
E1K = 85;
END;
ELSE DO;
L1 = -.12E-03;
DA1DT = -.33E-11;
E1K = 85;
END;
CALL CALC;
END;
/* THE INPUT VALUE FOR SOLVENT 'SV' WAS ILLEGAL */
OTHERWISE
PUT SKIP (2) LIST('** ILLEGAL SOLVENT **',SV);

END;

/* OUTPUT THE DATA STORED FOR THE SPECIFIED SOLVENT */
/* AND THE SOLUTE. */
CALL OUTPUT;

END;

/* GET THE NEXT VALUES FOR SOLVENT AND SOLUTE. */
GET EDIT (SV,SU) (COL(1),A(10),A(10));

END;

/* CALCULATIONS FOR THE OUTPUT */
CALC:PROCEDURE;
T = TABLE(I,1);
V1 = M/D;
RO = N/V1;
DA2DT=-5.44E-12;
L2 = DA2DT/A2;
A1 = A1S+DA1DT*(T-298.15);
SG = A2/A1S;
SG12 = (A1+A2)/2;
E12K = ((E1K*E2K)**0.5);
Y = (PI*(A1**3)*N)/(6*V1);
/* CHOOSE THE DESIRED 'AP' */
IF L1 = 0
THEN AP = APX;
ELSE AP = (1/T)*(1-2*(Y**3)+(Y**4)) /
(1+4*Y+4*(Y**2)-4*(Y**3)+Y**4) +

```

$$\frac{(6*L1)*(2*Y+2*(Y**2)-Y**3)}{(1+4*Y+4*(Y**2)-4*(Y**3)+Y**4)};$$

```

IF L1 = 0
THEN P = 0;
ELSE P = 82.0575*T/V1*(1+Y+(Y**2)-(Y**3))/((1-Y)**3);
HCT = (Y*R*(T**2)*(AP-3*L1)*((1-Y)**-3) *
(3*(1+2*Y)*(SG**2)+3*(1-Y)*SG+((1-Y)**2))) -
(R*N*PI*P*(A2**3)*((3*T*L2)-1))/(6*82.0575);
HI = -3.555*R*PI*RO*(SG12**3)*E12K -
1.333*R/K*PI*RO*(DPM1**2)*PO2/(SG12**3);
/* LIST CALCULATIONS ON ARRAY 'OUT1' FOR LATER PROCESSING */
CALL LIST1;
GI = HI;
IF L1 = 0
THEN P = 0;
ELSE P = P;
GC = R*T*(SG**2)*(9/2*((Y/(1-Y))**2)+3*Y/(1-Y)) *
3*Y*SG*R*T/(1-Y)-R*T*LOG((1-Y)) +
N*PI*P*(A2**3)*R/(6*82.0575);
LNKH = GI/(R*T)+GC/(R*T)+LOG((82.0575*T/V1));
/* CHOOSE THE DESIRED 'BT' */
IF L1 = 0
THEN BT = BTX;
ELSE BT = (1/P)*(1-2*(Y**3)+(Y**4)) /
(1+4*Y+4*(Y**2)-4*(Y**3)+Y**4);
V2 = BT/(AP-3*L1)*HCT/T*82.0575/R+BTX*GI*82.0575/R +
BTX*82.0575*T+N*PI*(A2**3)/6;
DHS = HI+HCT-R*T+APX*R*(T**2);
/* LIST CALCULATIONS ON ARRAY 'OUT2' FOR LATER PROCESSING */
CALL LIST2;
END;

```

```

/* PROCEDURE TO STORE THE FIRST SET OF OUTPUT CALCULATIONS */
LIST1:PROCEDURE;
OUT1(I,1) = T;
OUT1(I,2) = A1;
OUT1(I,3) = Y;
OUT1(I,4) = AP;
OUT1(I,5) = HCT;
OUT1(I,6) = HI;
END;

```

```

/* PROCEDURE TO STORE THE SECOND SET OF OUTPUT CALCULATIONS */
LIST2:PROCEDURE;
OUT2(I,1) = T;

```



```

OUT2(I,2) = DHS;
OUT2(I,3) = GC;
OUT2(I,4) = LNKH;
OUT2(I,5) = BT;
OUT2(I,6) = V2;
END;

```

```

/* PROCEDURE TO OUTPUT THE DATA STORED IN THE OUTPUT */
/* ARRAYS 'OUT1' AND 'OUT2' WITH A SPECIFIED SOLVENT */
/* AND SOLUTE AND 'L1' VALUE. */

```

```

OUTPUT:PROCEDURE;

```

```

IF L1 = 0
THEN PUT PAGE LINE (4) EDIT ('R. A. PIEROTTI'S DATA')
      (COL (6) , A) ;
ELSE PUT PAGE LINE (4) EDIT ('B. A. COSGROVE'S DATA')
      (COL (6) , A) ;
PUT LINE (8) EDIT ('SOLVENT = ', SV, ' SOLUTE = ', SU, ' L1 = ', L1)
      (COL (6) , A, A, X (12) , A, A, X (13) , A, E (12, 5)) ;
PUT SKIP (2) EDIT ('TEMP', 'A1', 'Y', 'AP', 'HCT', 'HI')
      (COL (7) , A, X (9) , A, X (14) , A, X (13) , A, X (13) , A, X (12) , A) ;
PUT SKIP (2) EDIT ('=====',
      '=====')
      (COL (6) , A, A) ;
DO I = 1 TO 7;
PUT SKIP (2) EDIT (OUT1 (I, 1) , OUT1 (I, 2) , OUT1 (I, 3) ,
      OUT1 (I, 4) , OUT1 (I, 5) , OUT1 (I, 6) )
      (COL (6) , F (6, 2) , X (3) , E (12, 5) , X (3) , E (12, 5) , X (3) ,
      E (12, 5) , X (3) , E (12, 5) , X (3) , E (12, 5)) ;
END;
PUT LINE (32) EDIT ('TEMP', 'DHS', 'GC', 'LNKH', 'BT', 'V2')
      (COL (7) , A, X (9) , A, X (12) , A, X (12) , A, X (12) , A, X (13) , A) ;
PUT SKIP (2) EDIT ('=====',
      '=====')
      (COL (6) , A, A) ;
DO I = 1 TO 7;
PUT SKIP (2) EDIT (OUT2 (I, 1) , OUT2 (I, 2) , OUT2 (I, 3) ,
      OUT2 (I, 4) , OUT2 (I, 5) , OUT2 (I, 6) )
      (COL (6) , F (6, 2) , X (3) , E (12, 5) , X (3) , E (12, 5) , X (3) ,
      E (12, 5) , X (3) , E (12, 5) , X (3) , E (12, 5)) ;
END;
END;

```